ESA/SRE(2009)6
December 2009

SPICA

Revealing the origins of planets and galaxies

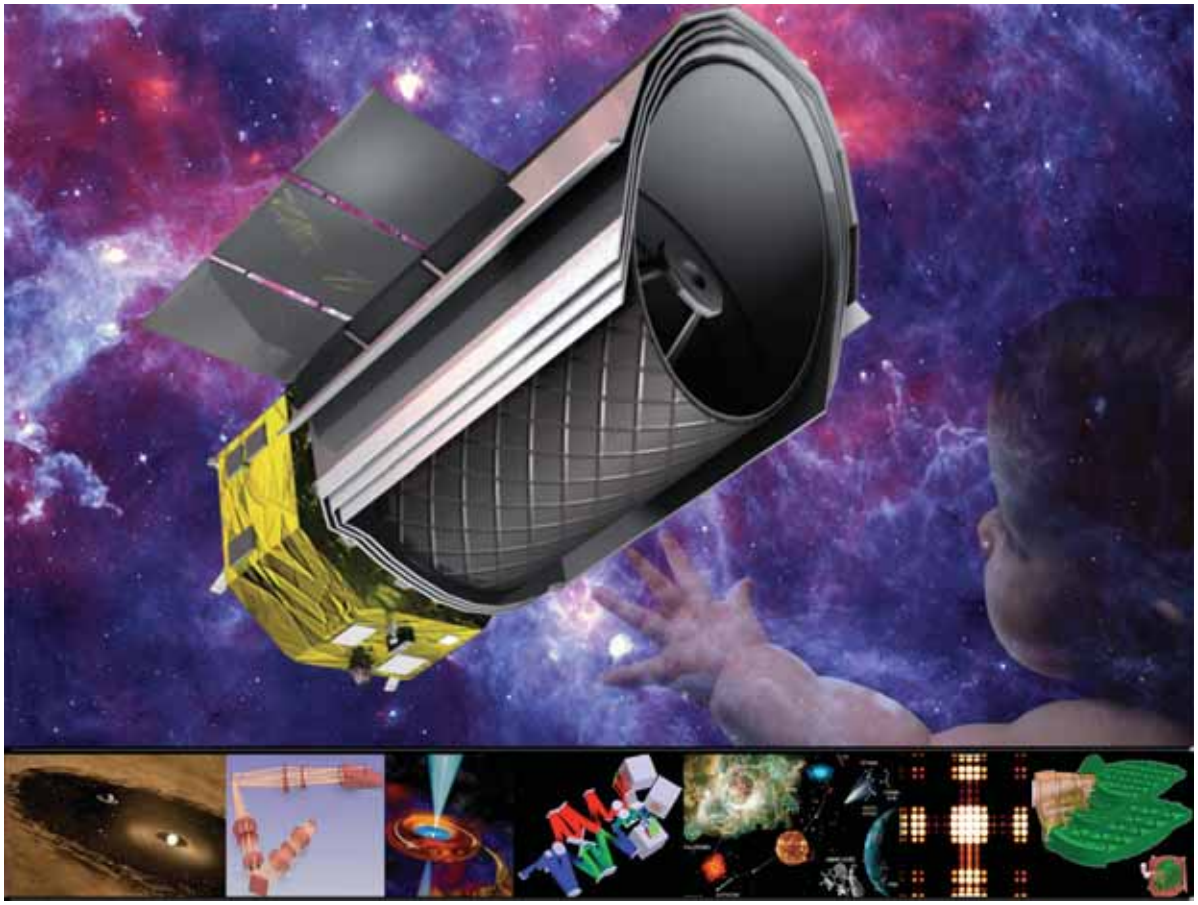

Assessment Study Report

SPICA Yellow Book
Issue 3
July 2011

European Space Agency


SPICA
JAXA
Japan Aerospace Exploration Agency
esa
ifsi
SRON
Imperial College London
LEUVEN
CSIC
INAC
Durham University
JPL
UCL
THE UNIVERSITY OF TOKYO
KOBE UNIVERSITY
Nagoya University
NAOJ
National Astronomical Observatory of Japan
茨城大学
Ibaraki University
KU
OSAKA UNIVERSITY

SPICA – SPace Infrared telescope for Cosmology and Astrophysics	
Science objectives	• Formation and evolution of planetary systems: Gas and dust in proto-planetary discs, including water, and their link to planetary formation; mineralogy of debris discs; gas exoplanets atmospheres; composition of Kuiper Belt objects. • Life cycle of dust: Physics and chemistry of gas and dust in the Milky Way and in nearby galaxies; dust mineralogy; dust processing in supernova remnants and the origin of interstellar dust in the early Universe. • Formation and evolution of galaxies: AGN/starburst connection over cosmic time and as a function of the environment; co-evolution of star formation and super-massive black holes; star-formation and mass assembly history of galaxies in relation with large scale structures; the nature of the Cosmic Infrared Background.
Wavelength range	Medium to far infrared (5–210 μm)

Page intentionally left blank

Authors

The SPICA Assessment Study Report [**science case update** (July 2011)] has been prepared with inputs from the ESA SPICA Study Team, the SPICA Telescope Science Study Team, the JAXA/ISAS SPICA Team and the SAFARI Consortium. The authors, in alphabetical order, are:

Javier Goicoechea	Centro de Astrobiología, CSIC-INTA (Spain); *SAFARI Consortium, Galactic Science Coordinator*
Kate Isaak	European Space Agency; *SPICA Study Scientist*
Peter Roelfsema	SRON (The Netherlands); *SAFARI PI*
Luigi Spinoglio	Istituto di Fisica dello Spazio Interplanetario (Italy); *SAFARI Consortium, Extragalactic Science Coordinator*
Bruce Swinyard	Rutherford Appleton Laboratory (UK); *SAFARI Consortium*

Co-authors

(Galactic): M. Audard (UNIGE, CH), S. Hasegawa (ISAS/JAXA, JP), I. Kamp (U. Groningen, NL), F. Kerschbaum (UNIVIE, AT), F. Levrier (LRA-LERMA, Fr), M. Meyer (ETHZ, CH), A. Moro-Martín (CAB/CSIC-INTA, E), S. Pezzuto (IFSI, It). M. Wyatt (Cambridge Uni., UK).

(Extragalalactic): K. Dasyra (Obs. Paris LERMA/CEA Saclay, F), D. Scott (U. British Columbia, CA), A. Franceschini (U. Padova, It), C. Gruppioni (AOBO-INAF, It), P. Perez-Gonzalez (U. Complutense de Madrid, E), F. Israel (U. Leiden, NL), J. Braine (Obs. Bordeaux, F), D. Schaerer (Obs. Geneve, CH), E. Sturm (MPE, Garching, D), E. Egami (U. Arizona, USA), A. Alonso-Herrero (CAB/CSIC-INTA, E), R. Maiolino (OARM-INAF, It), D. Rigopoulou (U. Oxford, UK), F. Pozzi (U. Bologna, It), D. Burgarella (OAMP, Marseille, F), V. Buat (OAMP, Marseille, F), E. Pointecouteau (IRAF, Toulouse, F).

Acknowledgements

The authors would like to acknowledge the essential contributions to the definition of the science objectives from: J.-C. Augereau (UJF, Fr), M. Barlow (UCL, UK), J.-P. Beaulieu (IAP, Fr), A. Belu (U. Nice, Fr), O. Berne (CAB/CSIC-INTA, E), B. Bézard (Obs. Paris, Fr), A. Boselli (LAM, Fr), V. Buat (LAM, Fr), D. Burgarella (LAM, Fr), J. Cernicharo (CAB/CSIC-INTA, E), D. Clements (Imperial College, UK), G. de Zotti (Oss. Astr. Padova, It), M. Delbo (UNS, Fr), Y. Doi (U. Tokyo, JP), S. Eales (U. Cardiff, UK), E. Egami (U. Arizona, USA), D. Elbaz (CEA, Fr), K. Enya (ISAS/JAXA, JP), A. Franceschini (U. Padova, It), H. Fraser (STRATH, UK), M. Fukagawa (Osaka U., JP), H. Gómez (Cardiff U., UK), J. Gómez-Elvira (CAB/CSIC-INTA, E), O. Groussin (LAM, Fr), C. Gruppioni (INAF, It), S. Hailey-Dunsheath (MPE, Ger), S. Hasegawa (ISAS/JAXA, JP), F. Helmich (SRON, NL), M. Honda (KAN-U, JP), Y. Itoh (Kobe U., JP), R. Ivison (U. Edinburgh, UK), H. Izumiura (NAO, JP), C. Joblin (CESR, Fr), D. Johnstone (NRC, CA), G. Joncas (ULAVAL, CA), A. Jones (IAS, Fr), I. Kamp (U. Groningen, NL), H. Kaneda (Nagoya U., JP), H. Kataza (ISAS/JAXA, JP), C. Kemper (Manchester U., UK), F. Kerschbaum (UNIVIE, AT), Y. Kitamura (ISAS/JAXA, JP), P. Lacerda (Belfast U., UK), T. Le Bertre (LERMA, Fr) F. Levrier (LRA-LERMA, Fr), D. Lutz (MPE, Ger), S. Madden (CEA, Fr), M. Magliocchetti (IFSI, It), J. Martín-Pintado (CAB/CSIC-INTA, E), H. Matsuhara (ISAS/JAXA, JP), R. Meijerinks (Sterrewacht Leiden, NL), S. Molinari (IFSI, It), R. Moreno (Obs. Paris, Fr), A. Moro-Martín (CAB/CSIC-INTA, E), P. Najarro (CAB/CSIC-INTA, E), N. Narita (NAO, JP), Y. Okamoto (Ibaraki U., JP), S. Oliver (U. Sussex, UK), T. Onaka (U. of Tokyo, JP), T. Ootsubo (ISAS/JAXA, JP), M. Page (MSSL, UK), E. Pantin (CEA, Fr), E. Pascale (U. Cardiff, UK), I. Pérez-Fournon (IAC, E), S. Pezzuto (IFSI, It), A. Poglitsch (MPE, Ger), E. Pointecouteau (U. Toulouse, Fr), C. Popescu (U. Lancaster, UK), F. Pozzi (U. Bologna,It), W. Raab (MPE, Ger), G. Raymond (Cardiff U., UK), D. Rigopoulou (Oxford U., UK), I. Roseboom (U. Sussex, UK), H. Rottgering (Leiden U., NL), F. Selsis (LAB, Fr), S. Serjeant (Open U., UK), A. Smith (U. Sussex, UK), M. Spaans (Kapteyn Astr. Inst., Neth), L. Spinoglio (IFSI, It), E. Sturm (MPE, Ger), M. Takami (Academia Sinica,Taiwan), T. Takeuchi (Nagoya U., JP), S. Takita (ISAS/JAXA, JP), M. Tamura (NAO, JP), G. Tinetti (UCL, UK), S. Tommasin (IFSI, It), J. Torres (CAB/CSIC-INTA, E), R. Tuffs (MPIK, Ger), M. Vaccari (Padova Uni., It), P. van der Werf (Leiden Obs., NL), S. Viti (UCL, UK), C. Waelkens (KUL, Be), R. Waters (UVA, NL), M. Wyatt (CAM, UK), T. Yamashita (NAO, JP).

Page intentionally left blank

Chapter 1

Scientific Objectives

1.1 Introduction

A complete understanding of the formation and evolution of galaxies, stars and planets can only be reached through the investigation of the cold and obscured parts of the Universe, where the basic processes of formation and evolution occur. Deep exploration of the cold Universe using high spatial resolution observations in the Far Infrared (FIR) and sub-mm started in 2009 with the launch of the *Herschel* Space Observatory. *Herschel* is opening this almost unexplored window through photometric surveys of star formation in our own Galaxy and of distant galaxies; however, its relatively warm telescope (between 82 and 90 K) greatly limits its sensitivity. A new much more sensitive mission reaching must therefore build on the work started by *Herschel* and gain a deeper understanding of the physics of the objects discovered there: *i.e.*, to spectroscopically identify and measure star formation rates in the obscured extra-galactic sources at different cosmic epochs and explore the physics and chemistry of planet formation. To obtain this increase in sensitivity we need a cold (< 6 K) telescope of about the same diameter as *Herschel*. The Japanese led SPace Infrared telescope for Cosmology and Astrophysics (SPICA) mission promises this in early 2020s and Europe can play a vital role in its success.

Progress in mid- and far-infrared astronomy has been slow because instruments and telescopes must be cooled to cryogenic temperatures to achieve high sensitivity and, for most of the frequency range, the observations can only be made from space. Only four small space observatories have operated in the past quarter of a century (IRAS, ISO, *Spitzer* and AKARI), offering limited spatial resolution and sensitivity. *Herschel*, with a 3.5-m $\sim$ 85-K telescope, the largest telescope ever put in space, is providing greatly increased spatial resolution with modest increases in sensitivity over the 55-210 μm band, while JWST, with a $\sim$ 6-m 45-K telescope, will provide a leap in both spatial resolution and sensitivity in the mid-IR up to 28 μm (launch $\gtrsim$2018). However, coverage of the full mid-/far-IR band with high sensitivity and spatial resolution will still be lacking and it is here that SPICA will be a breakthrough mission. SPICA will have a similar telescope to *Herschel* but cooled to < 6K, thus removing its self-emission and allowing observations limited only by the astronomical background.

SPICA offers a sensitivity up to two orders of magnitude better than *Herschel*, covering the mid-to-far-IR (the full 5-210 μm range, mostly unreachable from the ground) with imaging, spectroscopic and coronagraphic instruments (see Figure 1.1). Thanks to this substantial increase in sensitivity, SPICA will make photometric images in a few seconds that would take hours for *Herschel*, and will produce a full 5-210 μm infrared spectrum of an object in one hour that would take several thousand hours for *Herschel*. We illustrate this major increase in sensitivity in Figure 1.2 (left panel), which shows the area covered by a full spatial and spectral survey ($\sim$ 1 deg^2, e.g. the Cosmos field) in which we can detect and identify *spectroscopically* all galaxies down to a luminosity of $\sim 10^{11}$ L$_\odot$ at $z = 1$ and $\sim 10^{12}$ L$_\odot$ at $z = 2$ in 900 hours. In theory, in about twice this time, the *Herschel*-PACS spectrometer would just be able to detect a single object over its full waveband to the same sensitivity. We can immediately see that this major increase in sensitivity, combined with a wide field of view and coverage of the full 5-210 μm waveband, will revolutionise our ability to spectroscopically explore the nature of the tens of thousands of objects that *Herschel*, JWST, and SPICA will discover in photometric surveys or the regions that are too extended to be mapped with ALMA.

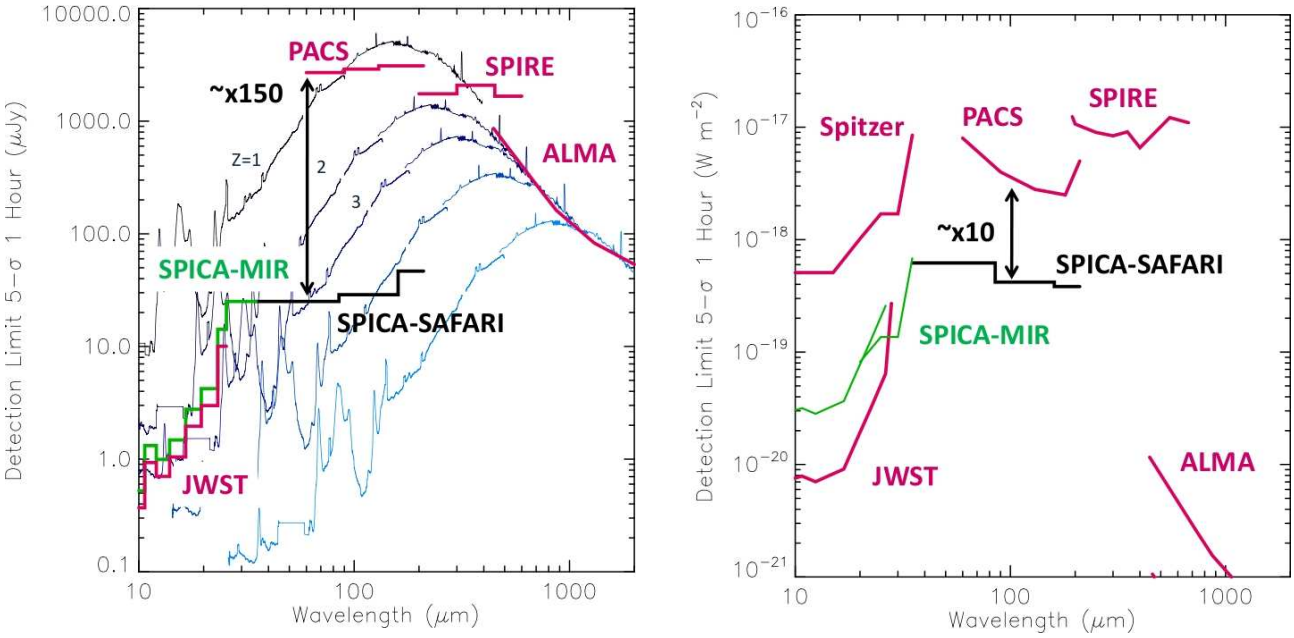

Figure 1.1: ***Left panel****: Photometric performance expected for SPICA SAFARI (black) and MCS (green), compared to Herschel, ALMA and JWST (red), for a point source (μJy, 5σ, 1 hour) using the goal sensitivity detectors on SPICA ($NEP = 2 \times 10^{-19}$ $W\,Hz^{-1/2}$). Note the $\lesssim 2$ orders of magnitude increase in photometric sensitivity compared to Herschel-PACS. The SED of the galaxy M82 as redshifted to z=1, 2, 3, 5 and 10 is shown.* ***Right panel****: Spectroscopic performance expected for SPICA (black and green) compared to other facilities (red) for unresolved line and point source ($W\,m^{-2}$, 5σ, 1 hour). For ALMA 100km s^{-1} resolution is assumed. Note that SPICA becomes more sensitive than JWST beyond 20μm.*

In the rest of this section we first place SPICA within the context of the ESA Cosmic Vision science goals before discussing the critical importance of observing in the mid- to far-IR and the diagnostic tools that are available. We then describe in detail how SPICA will shed light on the processes of planetary formation in the local Universe and the formation and evolution of galaxies in the more distant Cosmos.

1.1.1 SPICA in the Cosmic Vision

The ambition set out in the ESA Cosmic Vision (*ESA BR-247 2005*) is to seek "... the answers to profound questions about our existence and our survival in a tumultuous cosmos". To do this European scientists identified four grand themes in space science that will bring us closer to understanding how the Universe has come to look as it does and the place of our Earth within the Cosmos. Three of these themes directly require observations in the mid- to far-IR and a space-based far-IR observatory is identified as a key facility within the aegis of Cosmic Vision. We summarize those themes and show how SPICA will directly contribute to answering these fundamental questions:

Theme 1: "What are the conditions for planet formation and the emergence of life?" The Cosmic Vision calls for a mission that will "place the Solar System into the overall context of planetary formation, aiming at comparative planetology" and "Search for planets around stars other than the Sun". SPICA will have a mid-IR coronagraph that will allow imaging and spectroscopy of young massive exoplanets for the first time.

There is also the call to "Investigate star-formation areas, proto-stars and proto-planetary discs and find out what kinds of host stars, in which locations in the Galaxy, are the most favourable to the formation of planets" and "Investigate the conditions for star formation and evolution". SPICA will have a far-IR spectrometer more than an order of magnitude more sensitive than any previous facility, enabling it to probe further and into a wider range of objects and regions than ever before.

Theme 2: "How does the Solar System work?" This theme calls for the study of asteroids and comets as they are "the most primitive small bodies that can give clues to the chemical mixture and initial conditions from which the planets formed in the early solar nebula". SPICA's high sensitivity spectroscopy will allow the

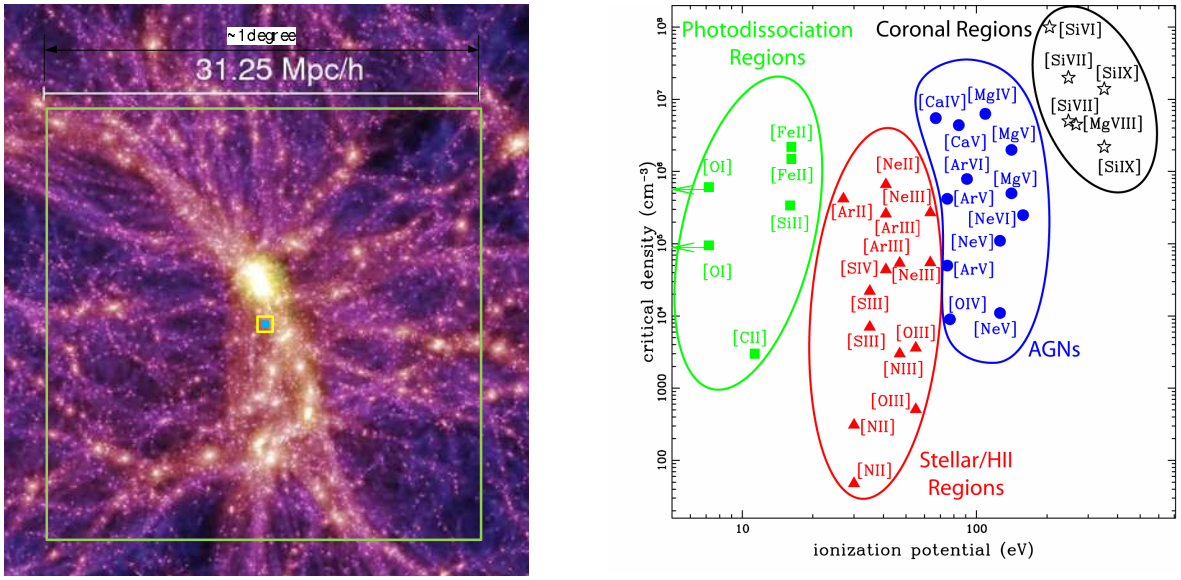

Figure 1.2: ***Left panel****: Comparison of the areas of spectral surveys with SAFARI and Herschel-PACS superimposed on a realisation of the Millennium simulation at $z \sim 1.4$ (Springel et al. 2006). In the centre are the footprints of the instantaneous spectroscopic FOV of PACS (blue) and SAFARI (yellow). The large green box shows the area covered by SAFARI in a 900 hour spectral survey ($\sim 1^\circ$) down to 5×10^{-19} W m^{-2} over the full 34-210μm band. PACS would require approximately twice this time just to cover a single pointing (blue box) to this depth over its full waveband.* ***Right panel****: A selection of the fine-structure atomic and ionic lines accessible with SPICA, plotted as a function of critical density and ionisation potential. Using ratios between lines with different ionisation or critical densities, we can trace out a wide range of different physical-excitation conditions (Spinoglio & Malkan 1992).*

chemistry of these objects to be studied by remote sensing to an unprecedented level of detail, for the first time allowing us to link our own "debris" to that seen in the formation of planetary systems around other stars.

Theme 4: "How did the Universe originate and what is it made of?" SPICA will address topics such: "…trace the subsequent co-evolution of galaxies and super-massive black holes" and to "Resolve the far infrared background into discrete sources, and the star-formation activity hidden by dust absorption". SPICA will especially be able to answer as to when and in which environment in the history of the Universe, star formation is most likely to take place and heavy elements to be created and dispersed. SPICA spectroscopy will "Trace the formation and evolution of the super-massive black holes at galactic centres – in relation to galaxy and star formation – and trace the life cycle of chemical elements through cosmic history".

In the following sections we illustrate in detail how SPICA observations are essential to answering the questions posed and we show how a European involvement in SPICA is an essential part of Europe's Cosmic Vision for the 21st century. We first set the context of why observations in the mid- to far-IR are critical to providing the observational evidence for galaxy, star and planetary formation and evolution.

1.1.2 A critical waveband

The composite spectrum in Figure 1.3 shows the importance of observations in the mid- to far-IR. Here we see the spectral energy distribution (SED) from the X-rays to the radio of a typical galaxy undergoing a modest amount of star formation, showing the different physical components at work. The bulk of the radiation is emitted both in the optical (i.e., starlight) or in the mid- to far-IR where the dust in the interstellar medium absorbs and re-radiates the starlight as grey body radiation. Superimposed on the continuum, throughout the 5-210 μm range, are atomic and ionic fine structure lines and molecular lines which control the thermal energy balance for a large variety of physical conditions. The gas cools through an extensive network of lines, which include the ionic fine-structure lines (e.g. of carbon, oxygen, neon and sulphur) and many rotational transitions of molecules (such as hydrogen, water, hydroxyl and carbon monoxide). The lines can be strong, emitting

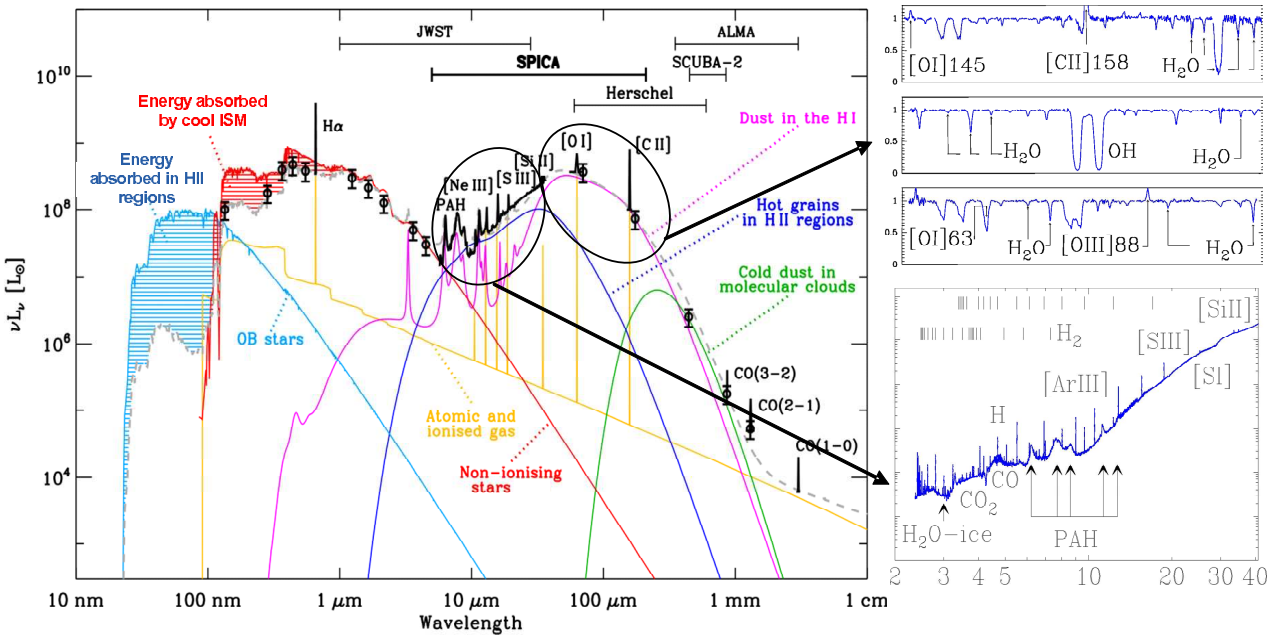

Figure 1.3: A synthetic rest-frame spectrum of a typical galaxy undergoing modest rates of star formation – similar to the Milky Way, showing the parts of the spectrum that will be covered by SPICA and contemporaneous facilities (cf. F. Galliano). The major importance and spectral richness of the mid-/far-IR region is demonstrated by the detailed spectra from ISO shown to the right of the diagram (Rosenthal et al. 2000; Goicoechea et al. 2004; Polehampton et al. 2007).

up to a percent of the total far-IR luminosity. Through the observation of combinations of lines it is possible to characterise the physical properties of many astrophysical sources, such as the nature and strength of the interstellar radiation fields, chemical abundances, local physical temperatures and gas densities. In addition to the low excitation/ionisation tracers measuring the star formation component in galaxies, the mid-IR contains important diagnostic lines that can reveal the presence of Active Galactic Nuclei (AGN), such as emission from [Ne v] and [O iv]. Figure 1.2 (right panel) shows the mid- and far-IR lines from many different species, with different ionisation potentials and excitation conditions (Spinoglio & Malkan 1992). These transitions constrain a wide range of physical conditions and phases of the ISM, from the neutral atomic ISM, through the ionised ISM as seen in photo-dissociation regions and HII regions to the highly ionised AGN and "coronal" regions.

The powerful IR line diagnostics can be used to study both star and planetary formation locally, as well as star formation and the influence of AGN at great distances. The 5-40 μm spectra contain transitions of ionised species that can distinguish AGN and starburst in the evolution of galaxies (see section 1.6.5) and, as these and other mid-IR lines are redshifted into the far-IR at increasing redshift, they can trace the star formation versus accretion history of the Universe. Similarly, the most abundant "metals", C, N and O, with ionic fine structure lines in the far-IR, allow direct and unambiguous determination of their relative abundance in distant galaxies. We refer to section 1.6.3 to give an overview of the capabilities of MIR/FIR spectroscopy for extragalactic studies. More locally, the mid- and far-IR line ratios of these species can be used as direct probes of the temperature, density and UV fields present in star formation regions, planetary nebulae, supernova remnants and proto-planetary discs. In addition to the atomic and ionic species, important molecular reservoirs of H, D, C, N and O, such as H_2, OH, H_2O, CO, HD and new molecular tracers detected by *Herschel* such as CH^+, OH^+, H_2O^+, HF and carbon clusters, have emission features throughout the mid- to far-IR, which are uniquely diagnostic of the physical conditions where they arise and, in the case of water, are critical in any discussion about how and where the conditions for life have emerged.

Dust emission and absorption dominates the continuum spectrum in the mid-/far-IR range with the most prominent features of the mid-IR continuum, being the UV-excited emission bands of Poly Aromatic Hydrocarbon molecules (PAHs) at 6.2, 7.7, 8.6 and 11.3 μm. These PAH molecules appear to be omnipresent in all phases of dust evolution both in our own Galaxy and the most distant galaxies yet seen. One of the most impor-

tant features of PAHs is that they are excited by absorption of single UV photons, making them good tracers of the UV field and so of star formation both on a galactic scale and as a function of redshift. Also present in the 5 –100 μm range are diagnostic spectral features arising from the minerals that make up the larger interstellar dust grains, as well as solid state features from the ices that condense onto them in cold environments. All these features are broad, faint and difficult to detect with the current or near future generation of facilities.

This overview of the power of the mid- and far-IR "toolbox" is of necessity brief and incomplete; in the remainder of this chapter we will give specific examples of how these tools can be used to answer some of the most vital questions about how and when planets, stars and galaxies came to form and their subsequent evolution into the Universe we see today.

1.2 Star and Planet formation and evolution

Modern astrophysics is just beginning to provide answers to some of the most basic questions about our place in the Universe: Are Solar Systems like our own common among the millions of stars in the Milky Way and, if so, what implications does this have for the occurrence of exoplanets that might give rise to life? The most straightforward method we have to start answering these questions is to compare the current knowledge of our own Solar system with observations of planetary systems. disc systems around stars other than the Sun. Observations of the most primitive bodies in the Solar System are also critical to infer the physical and chemical conditions in the early solar nebula as well as to provide clues about the water abundance, the most obvious solvent for life, its distribution, and its transfer from the outer regions to the inner terrestrial planet regions. The basic building blocks of an extra-solar system, the gas and dust, emit predominantly at mid and far infrared wavelengths, the critical domain in which to unveil the processes that transform the interstellar gas and dust into stars and planetary systems.

We are now at a threshold where we can begin to address, for the first time, crucial questions that will link our understanding of galactic star formation with the formation and evolution of galaxies, as well as address how the physics of planet formation can explain the diversity of extra-solar planetary systems we know exists as well as the curious features of our own Solar System. We discuss below how only the very sensitive observations over the entire mid infrared to far infrared (MIR and FIR) wavelength range provided by SPICA will give access to key spectral diagnostics and provide a robust and multidisciplinary approach to determine the conditions for star and planet formation. Such a comprehensive study will include the first detailed characterisation of hundreds of pristine bodies in our own Solar System, the detection of the most relevant chemical species and mineral components of hundreds of protoplanetary discs in different star forming regions at the time when planets form, the first unbiased survey of the presence of zodiacal clouds and Kuiper belts in hundreds of exoplanetary systems around all stellar-types and the first direct determination of the chemical composition of outer exoplanet atmospheres. These and other challenging science goals require more than an order of magnitude sensitivity improvement in the FIR compared to *Herschel* and higher spectral resolution than provided by JWST in the mid infrared. Additionally, direct spectroscopic coronagraphy of exoplanets and planetary discs in the critical mid infrared domain is not planned in any space telescope other than SPICA.

1.2.1 Star Formation: environment, filaments, cores and proto-stars

The power of FIR imaging-spectroscopy, with unprecedented sensitivity and large field-of-view, will help us to address crucial questions that will drastically improve our understanding of star formation, its environment and its link to galaxy evolution: **(1)** What fraction of typical giant molecular clouds is converted into stars during their lifetime and how does this depend on local conditions? ***(star formation efficiency and timescale)***; **(2)** What internal sources of energy (and cooling) drive the dynamics of molecular clouds after their formation? ***(feedback)***. It is well-known for more than two decades that: *(a)* most stars form in molecular clouds; and *(b)* the distribution of masses for these clouds indicates that most of the mass is contained in the most massive giant molecular clouds (GMCs). FIR photometric surveys of nearby clouds with *Spitzer* and *Herschel* (Evans et al. 2009a; André et al. 2010; Molinari et al. 2010) further indicate that most of the star formation within GMCs

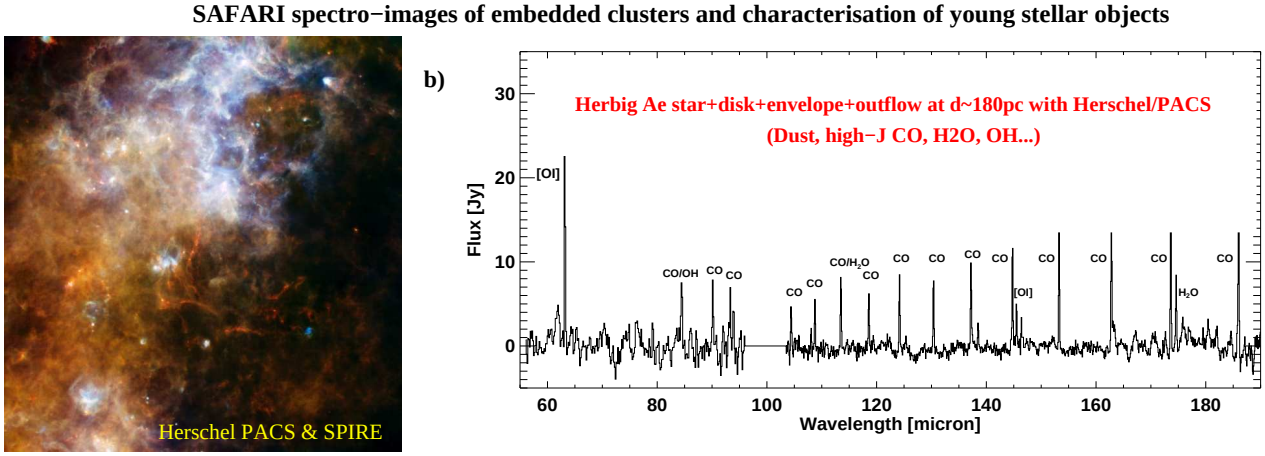

Figure 1.4: (a) Cold dust in a dark cloud near the Southern Cross revealed by Herschel photometry. An interconnected maze of filaments of different sizes and amounts of dust, with strings of newly forming stellar embryos in all phases of development are revealed in the FIR. SPICA spectrometers will observe similar cold regions in the Milky Way and also in the closest galaxies (e.g., the Local Group), allowing us to infer their physical conditions as well as their gas, ice and mineral composition. (b) FIR spectrum of circumstellar material around DK Cha, an intermediate-mass star in transition from an embedded configuration to a star plus disc stage. DK Cha was observed during ≃4 hr with Herschel/PACS spectrometers (van Kempen et al. 2010). SPICA/SAFARI will obtain simultaneous spectra for multiple objects, in a much larger FoV of ∼2′×2′, with similar spectral resolution but ∼10 times more sensitive in only ∼4 min.

occurs along dense filaments. The distribution of these core masses appears to resemble the *initial mass function* (IMF) of stars. Yet the so-called "*core mass function*" (CMF) is: (1) shifted towards higher masses by a factor of x3 and is not well sampled down to masses corresponding to the mean mass of the log-normal IMF (<0.3 $M_\odot$) or into the brown dwarf regime. Perhaps the CMF and a constant star-formation efficiency within each core (independent of mass) results in the IMF. However this seems very unlikely (Adams & Fatuzzo 1996).

Mapping GMCs across the broad instantaneous wavelength range of SAFARI at sensitivities more than an order of magnitude beyond the capabilities of *Herschel*/PACS spectrometer, we can completely sample a few appropriate molecular cloud regions for: *(a)* pre-stellar cores below the hydrogen burning limit; *(b)* short-lived (and thus rare) first hydrostatic protostellar cores – the "holy grail" of star formation; and *(c)* deeply embedded protostars down to 0.01 $M_\odot$ throughout the Class 0-I-II stages from 0.1-1 Myrs. These observations will build directly on the legacy of *Herschel*, which makes sparse photometric maps of the nearest star-forming regions (SFR) which are comprised of modest dark clouds (<10^4 $M_\odot$) containing dozens to hundreds of YSOs at most. While these regions are vital touchstones to understand star-formation at the greatest physical resolution, they are not representative of where most stars form: clusters of hundreds to thousands of stars (Lada & Lada 2003; Adams 2010). And these more massive regions are farther away from the Sun, requiring the sensitivity of SAFARI as well as its large field of view for spectral-mapping. We will target dark clouds and portions of triggered SFRs in the Milky Way (e.g., Elmegreen & Lada 1977) and in nearby galaxies such as the LMC (for which spectral mapping with *Herschel* require unrealistic amounts of time; see Sect. 1.5). Not only will this provide a rich study of potentially an important mode of SF in interacting galaxies and the early Universe (*e.g.*,, low metallicity regions) but it will also provide a range of diversity in "star forming environment".

The extended component and the "interfaces" of GMCs: Dense filaments and cores in SFRs are embedded in a more diffuse and turbulent medium that seems to be driven on larger scales (Brunt et al. 2009). These more quiescent, extended regions constitute the bulk of the mass of GMCs – as much as 90% (McKee & Ostriker 2007) – and play a critical role in their evolution. In spite of their relevance, the interfaces between the star forming cores and the environment are poorly characterized spectroscopically (owing their much lower surface brightness) and thus remain poorly understood. While *Herschel* spectral surveys towards bright star forming cores (Orion, W49, W3, Taurus, Serpens...) provide the most complete information on the physical conditions and chemical content of particular sites of star formation (hot cores, protostars or HII regions), they do not place the observations in the context of the large scale gas and dust emission of the cloud, *i.e.*, their environment.

ALMA observations of YSOs will soon help us to resolve their inner structure individually (below scales of a few tens of AU), however ALMA is not designed to map the large scale distribution of gas and dust in GMCs (with spatial scales of several parsec). However, a full picture of their physical conditions (energy budget, neutral/ionized gas filling factors, density and temperature gradients) has great relevance for Astronomy since it is the widespread gas and dust (the environment) that sets the initial conditions for star formation in diverse regions. SAFARI will map these faint extended regions both in the dust continuum and gas lines simultaneously. Ground-based single-dish submm telescopes (IRAM, JCMT or CCAT in the future) are able to map the low-energy transitions of molecules like CO, CN, C_2H, ... and the submm dust continuum emission over large spatial scales. However, they cannot access the brightest gas cooling lines of such extended regions ([Si II]34, [O I]63, [C II]158, ...) and they cannot observe the dust SED peak (essential to determine the dust temperature). SAFARI's large field-of-view will also help us to trace the action of parsec-scale molecular outflows as they impact the ambient inter-clump medium and the role of UV radiation at large scales. As an example, Figure 1.4a shows the large-scale distribution of cold dust in a dark cloud revealed by *Herschel*. In order to answer the questions posed above, **a coordinated spectral survey with SAFARI of several clouds that can not be accessed spectroscopically with *Herschel*, both locally and in nearby galaxies is vital**.

1.2.2 Protoplanetary and debris discs

All planets are thought to form in the accretion discs that develop during the collapse and infall of massive dusty and molecular cocoons ($\gtrsim 10\,000$ AU) where stars are born. However, we still have a very incomplete understanding of the physical and chemical conditions in such discs, how they evolve when dusty bodies grow and collide, their mineral content, how they clear as a function of time and, ultimately, how planets as diverse as the Earth or hot-Jupiters form around different types of stars and at different places of the galaxy.

Primordial **protoplanetary discs** are very optically thick in dust, with high radial midplane optical depths in the visual ($\tau_V >> 1$). Such young discs evolve over a timescale of a few million years (Haisch et al. 2006; Fedele et al. 2010); during that period, their IR excess decreases as a function of age and also their gas accretion rate as measured by different gas diagnostics (Hα emission line, UV excess, etc.). This is the critical intermediate stage when planetary formation is believed to take place, with dust particles colliding and growing to form larger bodies reducing the disc opacity. Spitzer has shown that their outer regions (beyond $\sim 10-20$ AU) can remain intact for longer, and thus residual gas can exist in the disc and play an important role in its evolution. However, statistical surveys of direct disc gas tracers for 10-20 AU are only starting to emerge from *Herschel* observations. Some discs have large inner dust holes on scales of several 10 AU which could be due to the formation of planets. Spitzer has provided us with a large sample of such discs based on their photometric SEDs; these discs are often referred to as "**transitional discs**" (Kim et al. 2009; Sargent et al. 2009; Evans et al. 2009b). Several of these transitional discs are shown to have CO gas present inside the dust gaps (Goto et al. 2006; Pontoppidan et al. 2008). Discs with ages above $\gtrsim 10$ Myr are practically devoid of gas (Duvert et al. 2000; Fedele et al. 2010) and the dust in these older discs is generally not primordial but continuously generated "debris" from planetesimals and rocky body collisions. The smallest dust grains have, at this stage, either been dispersed or have coagulated into larger grains and the disc becomes very optically thin ($\tau_V << 1$). **Debris discs** are thus more massive (and usually younger) analogs of our own asteroid (hot inner disc, $T_d \simeq 200$ K) and Kuiper belts (cool outer disc, $T_d \simeq 60$ K) so their study is vital to place the Solar System in a broader context.

The gas content in planet forming discs

The physical and chemical conditions in young protoplanetary discs set the boundary conditions for planet formation, and an understanding of the formation and evolution of such discs will finally link star formation and planetary science. Although the dust is relatively easily detected by photometric observations in the far infrared range, very little is known about the gas phase. It is evident that too little gas is left at ages $\gtrsim 10$ Myr (Meyer et al. 2008) to form giant planets; this is an age when the majority of at least the giant, gaseous planets (e.g., Jupiters and "hot Jupiters") must have formed according to current accretion formation models (Pollack et al. 1996a; Mordasini et al. 2008). The very fact that these planets are largely gaseous means they

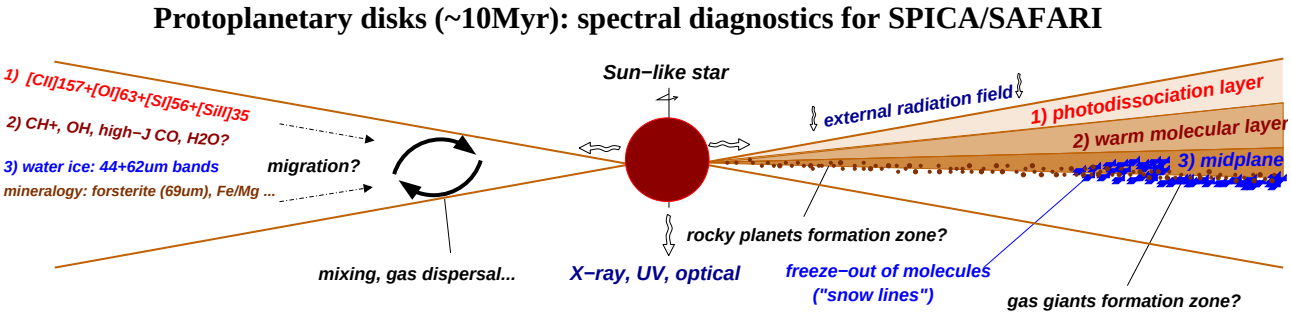

Figure 1.5: Diagram showing where FIR radiation arises from a protoplanetary disc (at the time when planets assemble) and why the FIR (i.e., SAFARI) and the millimetre (e.g., ALMA) are essential to understanding the full picture of planetary formation and the primordial chemistry that leads to the emergence of life.

must be formed before the gaseous disc dissipated, making the study of the gas in discs essential to understand how and where they formed. For instance, the recently detected massive "hot Jupiters" orbiting close to the parent star are very unlikely to have formed in situ, but rather they must have migrated inwards from outer disc regions beyond the *snow line*. Likewise it seems clear that Neptune and Uranus must have formed in a region closer to the Sun and migrated outwards. The mechanism for either of these scenarios is not certain.

According to our current theories, gas giant planets form in discs either via accretion of gas onto rocky/icy cores of a few earth masses (Lissauer 1993; Pollack et al. 1996b; Kornet et al. 2002) or by gravitational instability in the disc that triggers the formation of overdense clumps that afterwards compress to form giant planets (Boss 2003). In the latter scenario, gas giants form quickly and the gas may dissipate early ($\lesssim 10$ Myr), whereas longer gas disc lifetimes ($\gtrsim 10$ Myr) may leave enough time for building a rock/ice core and facilitate the subsequent accretion of large amounts of gas. Therefore, observations of the amount of gas in transitional discs around a large sample of stars can discriminate between the two most accepted planet forming theories. The residual gas content in the innermost regions (< 2 AU for a Sun-like star but much larger for more massive stars) at the time terrestrial rocky protoplanets assemble will also determine their final mass, chemical content and orbit eccentricity, and therefore its possible habitability (Agnor & Ward 2002).

Protoplanetary disc models predict a "flared" disc structure (see Figure 1.5) which allows the disc to capture a significant portion of the stellar UV and X-ray radiation even at large radii (Qi et al. 2006), boosting the MIR/FIR dust thermal emission and the MIR/FIR lines emission from gas phase ions, atoms and molecules. Theoretical models of protoplanetary discs recognise the importance of these X-UV irradiated surface layers, which support active photochemistry and are responsible for most of the MIR/FIR line emission. State-of-the-art 2D and 3D disc models are nowadays able to simulate the disc dynamics, thermodynamics, chemistry and radiative transfer (Ilgner et al. 2004; Gorti & Hollenbach 2004; Aikawa et al. 2002; Willacy et al. 2006; Gorti & Hollenbach 2008; Woitke et al. 2009a; Cernicharo et al. 2009; Kamp et al. 2010) and they guide us in the interpretation of the observed disc emission (generally spatially unresolved). In particular, the FIR fine structure lines of the most abundant elements (O, C, S, Si...) together with FIR rotational line emission of H_2O, OH, CH^+, high-J CO, ... are predicted to be the strongest gas coolants (i.e., the brightest lines) of the warm disc, especially close to the star. In particular the FIR [Si II] 34 μm, [O I] 63 μm, [S I] 56 μm and [C II] 158 μm fine structure lines are likely the most intense lines emitted in the disc, and thus the best diagnostic of their gas content (Gorti & Hollenbach 2004). **By detecting these FIR lines we can directly probe a wide range of physical and chemical conditions (e.g., those associated with the X–ray and UV-illuminated disc regions) that are very difficult, if not impossible, to trace at other wavelengths** (*e.g.*, by ALMA).

SPICA studies of the gas dispersal and of the chemical complexity in protoplanetary discs:
In order to shed some light on the gas dispersal time scales, and thus on the formation of gaseous Jovian-type planets, high sensitivity infrared to sub-mm spectroscopic observations over large statistical stellar samples tracking all relevant disc evolutionary stages and stellar types are clearly needed. Until recently, studies of the gas content are biased to young and massive protoplanetary discs (probably not the most representative)

through observations with ground-based (sub)mm interferometers and optical/near-IR telescopes. Sub-mm observations allow one to trace the outer cooler disc extending over a few hundred AU where most molecular species start to freeze-out onto dust grains (e.g., Dutrey et al. 2007; Öberg et al. 2011).

In terms of chemistry, the protoplanetary disc is the major reservoir of key species with prebiotical relevance, such as oxygen, ammonia (NH_3), methane (CH_4) or water (H_2O) to be found later in (exo)planets, asteroids and comets. But how the presence and distribution of these species relates to the formation of planets, and most particularly, rocky planets with substantial amounts of water present within the so called habitable zone, remains open to speculation without a substantial increase in observational evidence. Water is an obvious ingredient for life, and thus it is very important that we understand how water transfers from protostellar clouds and primordial protoplanetary discs to more evolved asteroids, comets and planets like our own. Ultimately one has to understand how the water we see today in our oceans was delivered to the Earth.

Recently the very inner regions of protoplanetary discs have been probed by means of optical/IR observations (Najita et al. 2007). Spitzer and ground-based telescopes have just started to show the potential diagnostic power of MIR/FIR spectroscopy in a few "template" discs. This has allowed the exploration of the gas content and composition at intermediate radii (1 – 30 AU), i.e., the crucial region for the formation of planets. MIR detections toward young discs include atomic lines such as [Ne II], [Fe II], etc. (Lahuis et al. 2007; Güdel et al. 2010), molecules like H_2, H_2O, OH, HCN, C_2H_2 and CO_2 (Carr & Najita 2008; Salyk et al. 2008; Pontoppidan et al. 2010), and complex organics like PAHs (Geers et al. 2006; Habart et al. 2006).

Molecular hydrogen (H_2) is the most abundant gas species in a primordial protoplanetary disc ($\sim$90% of the initial mass). Electronically-excited FUV H_2 emission from the very inner disc (<1 AU) has been detected towards several TT Tauri stars (Ingleby et al. 2009). However, due to the relatively poor line sensitivity that can be achieved with even the largest ground-based mid infrared telescopes (a few 10^{-17} W m^{-2}), pure rotational H_2 lines from the outer planet-forming regions have been detected only towards a few protoplanetary discs so far (*e.g.,* Bitner et al. 2008). SPICA's mid infrared high resolution spectrometer (MCS/HRS) will be able to detect the brightest H_2 line (the v=0-0 S(1) line at $\sim 17\,\mu$m) and several water vapour excited lines around $\sim 13\,\mu$m with < 10 km s^{-1} resolution respectively, and with much higher sensitivities than those achieved from the ground and with an order of magnitude higher spectral resolution than JWST/MIRI (see some lower spectral resolution H_2O detections with VISIR/VLT in Pontoppidan et al. 2010). Such a high spectral resolution will be enough to resolve the gas Keplerian rotation. In this way, one can use molecular spectroscopy and resolved emission-line profiles to map out the temperature, density, and composition of gas in the inner disc of a large sample of young stellar objects. This is just barely possible now from the largest ground-based telescopes studying the nearest and brightest targets. SPICA/MCS/HRS will open up the study to objects more typical of those that could represent analogues of our forming Solar System.

In the FIR, *Herschel* is showing that the [O I]63 μm line is the strongest line detected so far in discs and with the highest detection rate (*e.g.,* Meeus et al. 2010; Sturm et al. 2010a; Thi et al. 2010). In addition, high-J CO rotational lines, CH^+, OH and water lines are detected towards a few of discs. Despite very deep searches, ground–state water lines in the submm domain are only detected towards a single disc, TW Hya (Hogerheijde et al. 2011) suggesting that most of the water vapour is either warm (detectable in the MIR/FIR) or that the bulk of cold water freezes-out as ice grain mantles (again, only detectable in the MIR/FIR). *Herschel* can only detect discs with strong FIR lines (above a few 10^{-18} W m^{-2}); these are generally the younger discs and/or most likely outliers in terms of their disc properties. In fact, *Herschel*/PACS is predicted to detect just the tip of the iceberg (see Figure 1.6a), while SPICA/SAFARI will provide a more unbiased view of disc properties (Woitke et al. 2010a). SAFARI will be able to detect gas lines with sensitivities of a few times 10^{-19} W m^{-2}. Using a large unbiased grid of parametrized thermo-chemical disc models, DENT, the detection probability with SAFARI for disc models with pure photospheric irradiation amounts to $\sim$ 80 % down to disc masses of 10^{-5} M$_\odot$. The exciting prospect of detecting small amounts of gas in a statistically significant sample of discs, e.g., toward the 6 closest ($\lesssim$140 pc) young stellar clusters with ages of $\simeq 1 - 30$ Myr, Taurus, Upper Sco, TW Hya, Tuc Hor, Beta Pic and Eta Cha, will provide a crucial test on the lifetime of gas and its dissipation timescales in planet forming discs and therefore on the exoplanet formation theory itself.

Nevertheless, the angular resolution of SPICA ($\sim 1''$ at the H_2 17 μm line and $\sim 5''$ at the [O I]63 μm line) can not compete with the resolution of telescopes with much larger collecting area (*e.g.,* ALMA) and thus

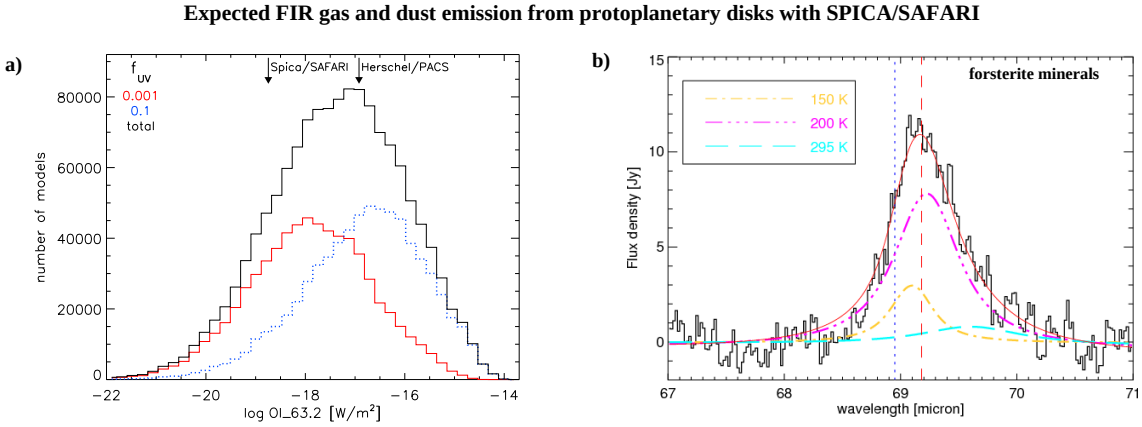

Figure 1.6: ***(a)*** *Dependence of the [O I]63 μm line flux on the stellar UV excess f_{UV}. The black histogram counts protoplanetary disc models that result in certain [O I]63 μm line fluxes at distance 140 pc (the closest SFRs). The red histogram represents the low f_{UV} = 0.001 models, and the blue dotted histogram the high f_{UV} = 0.1 models. The difference between high- and low-UV excess causes a difference of about 1–1.5 orders of magnitude in line flux.The arrows show the detection limits (3σ, 0.5h) of SPICA/SAFARI and HERSCHEL/PACS (Woitke et al. 2010b). First gas line detections confirm that Herschel is only detecting the "tip of the iceberg".* ***(b)*** *Forsterite grains emission at 69 μm (histogram) towards the protoplanetary disc around the pre-main-sequence star HD 100546. The contributions of the different grain temperatures are indicated. The dotted vertical line locates the peak position of 70 K pure forsterite (Sturm et al. 2010b).*

most protoplanetary discs will be spatially unresolved (a young disc like TW Hya, at a distance of ∼ 50 pc, has a size of ∼ 10″ on the sky). However, SAFARI has access to the critical FIR domain that can not be observed with ALMA or JWST, thus enabling the detection of unique diagnostics of the disc (dust, ice, atomic and light hydrides molecular features). **SAFARI will permit us to**: (1) Take advantage of the broadband coverage of SAFARI-FTS to obtain **unbiased FIR spectral line surveys**, *e.g.*, surveying the entire high-J CO rotational line ladder (J_{up}=13-79 !) as a key tracer of gas temperature and excitation and (2) Carry out **deep searches of gas towards large samples of discs** (including more evolved debris discs) by e.g., searching for the bright [O I]63 μm and [C II]158 μm lines. Even if the line emission can not be fully spatially resolved, SPICA observations will allow us to detect the presence of both water vapour and water ice as well as the basic building blocks of the X-ray/UV illuminated-disc chemistry (C^+, CO, CH^+, O, OH, Si^+, S, HD, ...) for the first time in hundreds of discs and, together with sophisticated thermo-chemical disc models, relate their presence with the main parameters of each planetary system (stellar mass, temperature, age ...).

Planetesimals, dust and mineralogy in debris discs

Dust is a key building block of rocky planets and the cores of giant gas planets. Dust appears to be present at all stages of planetary system formation with the mass ratio of gas to dust, the amount of dust present, its temperature and its distribution evolving rapidly through the process of planetary formation (Tanaka et al. 2005; Su et al. 2005). The processing and evolution of dust from protoplanetary discs to evolved solar systems like ours is key to understanding the formation and mineralogy of rocky, Earth-like, planets. For instance, it appears that in discs around intermediate mass, pre-main sequence stars, the dust in the inner regions of the disc (≤ 2 AU) can be more evolved. That is, it shows signatures of grain growth and crystallisation (see Figure 1.6b) whereas the dust in the outer region is often seen to be pristine and similar to the interstellar dust (Natta et al. 2006). This implies a strong radial dependence of the dust processing whereby the inner regions are dominated by the stellar radiation field, leading to grain heating and crystallisation, and by higher densities, leading to coagulation, whilst the outer regions remain largely unprocessed and carry the signature of the pre-stellar nebula from which the star formed. And yet in our own Solar System we see crystalline silicates present in comets that clearly originate from regions far from the zones where this processing must have occurred. Only with detailed mapping of the MIR/FIR mineral and ice band emission/absorption of our own and distant circumstellar material, will we be able to understand the evolutionary track that leads to this

situation. Observations using **SPICA spectrometers will allow us to carry out mineral and ice studies** (started with ISO and followed by Spitzer and AKARI) with unprecedented sensitivity and angular resolution.

The final stage of planetary system formation, the formation of small planetesimals that sweep up much of the disc's material, together with the formation of larger planetary bodies via collisions of planetesimals, often appears to result in an almost gas-free, "second generation" dusty disc, the debris disc. The dust in these discs is produced by mutual collisions of planetesimals in the final stages of planetary formation and the "heavy bombardment" phase (>300 Myr) evidenced in the impact craters seen in all rocky Solar System planets. Debris discs can survive over billions of years. This points towards the presence of large reservoirs of colliding asteroids and evaporating comet-like bodies. Moreover, since colliding planetesimals need to be present to replenish the dust grains in the disc, **detecting a debris disc is a strong signature of an emerging planetary system and is indicative of the presence of analogous asteroid and Kuiper belts** (Wyatt 2008), or of regions where the formation of Earth-like or Pluto-like planets is ongoing (Kenyon & Bromley 2008). Indeed, the very recent direct detection of exoplanets towards several stars that host bright debris discs (Kalas et al. 2008; Marois et al. 2008; Lagrange et al. 2009) have quantitatively confirmed that studies of debris discs are critical to advance in our understanding of the formation and diversity of extra-solar planetary systems.

The dust emission in circumstellar discs produces an "excess" of FIR continuum emission that becomes apparent and reaches its maximum in the SAFARI wavelength range; because the dust in a large fraction of debris discs is cold (Carpenter et al. 2009), many of these discs will not be seen at the shorter wavelength mid infrared range covered by JWST (see Figure 1.7a). The exact wavelength location of the disc dust emission peak depends on the grains temperature, size distribution and composition. Around ~ 300 debris discs have been photometrically discovered so far with ISO and Spitzer. The **most recent FIR photometric census suggests that about 10–15% of lower-mass, Sun-like stars, are surrounded by debris discs**, at least down the limiting fluxes observables with Spitzer (Bryden et al. 2006; Meyer et al. 2008). Spitzer discovered very few debris disc detections around stars later than K2, likely due to an observational bias because these discs would have been too cold and faint to be detected. Below we will see that there is a large discovery space of discs around solar-type and cool stars yet to be explored.

The study of debris discs is an emerging field that is currently limited by the available FIR sensitivity which makes it impossible to **(1) perform large statistical surveys that reach low levels of dust over meaningful survey volumes**; **(2) probe more distant discs and/or less massive dusty discs around all types of stars including young M dwarfs and cooler substellar objects**. As an example, the sensitivity required to detect the dust disc over stellar luminosity ratio (L_{dust}/L_{star}) in a planetary system analogous to the Kuiper Belt disc ($L_{dust}/L_{star} \simeq 10^{-7}$) or Asteroid Belt ($L_{dust}/L_{star} \simeq 10^{-8}$) in our Solar System remains below the far infrared capabilities provided by IRAS, ISO, AKARI, *Spitzer* and *Herschel*. Besides, recent estimates place the Solar System in the faintest 10% of all Kuiper belts (Greaves & Wyatt 2010), meaning that with much higher sensitivity we would we able to detect dusty discs around a much larger fraction of stars. Note that the flux of a Kuiper Belt disc with a mass of ~ 0.1 M_{earth} at 30 pc corresponds to ~ 4 mJy at 70 μm (Meyer et al. 2008).

SAFARI offers two powerful methods to detect and characterise the dust emission from debris discs **(1)** fast and ultra sensitive photometric searches in the 48 μm, 85 μm and 160 μm bands simultaneously reaching a few hundred μJy sensitivity for 5σ in 1 min and **(2)** very sensitive spectral characterisation at modest spectral resolution ($R \sim 100$) over the full 34 – 210 μm waveband with ~ 1 mJy level sensitivity for 5σ in 1 hour. Figure 1.7b shows the minimum detectable fractional luminosities (L_{dust}/L_{star}) for debris discs at different distances as observed with Spitzer-MIPS at 24 μm and 70 μm, *Herschel*-PACS at 70 μm, 100 μm and 160 μm, and SPICA/SAFARI at 48 μm, 85 μm and 160 μm. Note that in this estimation the sensitivity is driven by confusion with the FIR background at long wavelengts but it assumes that we can separate the photospheric and the dust disc emission down to very low fractions. For solar-type stars, we see that **Herschel will not detect dust at the Kuiper or asteroid belt levels**, and debris disc detections with Spitzer have generally been limited to $\sim 100\times$ and $1000\times$ the luminosity of the dust in the Kuiper and asteroid belts, respectively. Figure 1.7b indicates that **SPICA/SAFARI sensitivity is equivalent to the detection of dust at the level of the asteroid and Kuiper belts for solar-type stars at $d < 20$ pc and $d < 140$ pc, respectively**. The number of solar-type stars within these volumes of space are approximately 400 and 1.4×10^5, respectively, the latter being much larger than the ~ 300 debris discs detected by Spitzer around all stellar types. This warrants that there is a

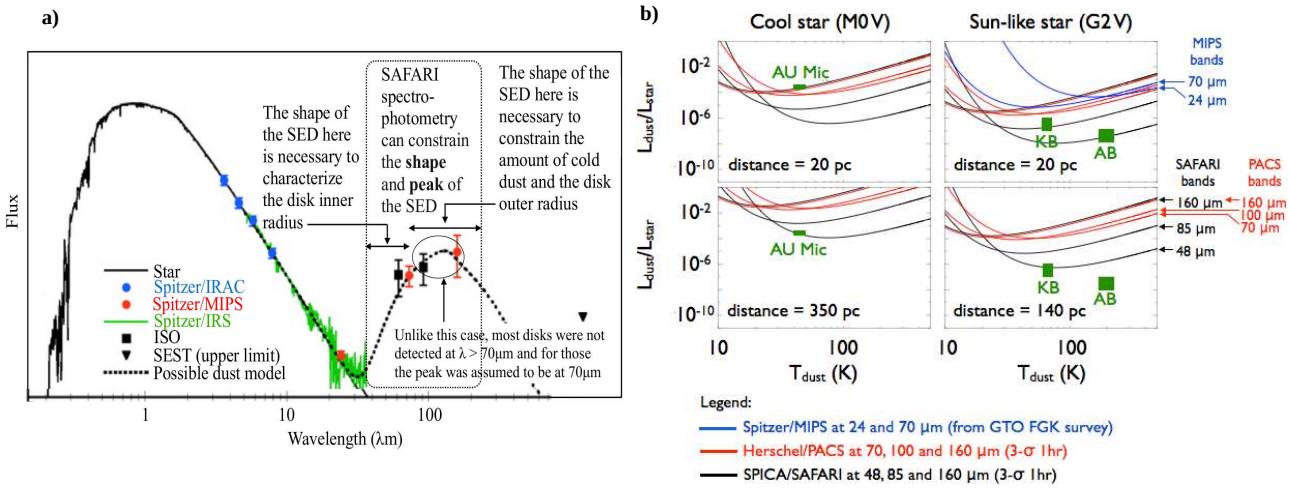

Figure 1.7: ***(a)*** *SED of HD105 star. The lack of excess emission at MIR wavelengths is due to the depletion of dust at distances <35 AU from the central star. The FIR wavelengths covered by SAFARI are thus critical (adapted from Meyer et al. 2008).* ***(b)*** *Minimum detectable fractional luminosities for discs at different distances around stars of different types: cool M0 V (left) and solar G2 V (right) – with characteristic values for the KB and AB shown as black squares. The different colours correspond to different FIR instruments (3σ-1hr): Spitzer-MIPS at 70 μm (blue); Herschel-PACS at 70 and 100 μm (red); and SPICA/SAFARI at 48 and 85 μm (black) (Adapted from Moro-Martín 2009).*

large discovery space that only SAFARI can probe, potentially being able to search for dust discs at the level of that of the Kuiper belt that may indicate the presence of hitherto undetected planetary systems. By increasing the number of debris disc detections, SAFARI will improve significantly the statistics on the frequencies and properties of debris discs as a function of stellar type, age and environment. In particular, **SAFARI will be the first instrument to detect low mass debris discs out to** ∼ 140 **pc (Fig. 1.7b)**. This is the distance to the closest star forming regions, meaning that **SAFARI will be particularly adept at studying discs during the brief epoch at** $\gtrsim$ **10 Myr when the transition from protoplanetary to debris disc occurs**, a transition which is as yet poorly understood but which is of prime importance due to its curtailment and direct link with planet formation and migration.

SAFARI will be so sensitive that it will be perfectly adapted to detect the faintest, coldest and maybe the most profuse planet forming systems in the Galaxy, those around cool stars and brown dwarfs (BDs) (Teixeira et al. 2009). About ∼77% of stars in the local neighbourhood are cool M-stars and there is observational evidence that at least 3% harbor planets (with "super-earths" being more common than giants). However, the detection of the faint FIR excesses around cool stars and brown dwarfs is a great challenge for current instrumentation, with disc fluxes around mJy or less. In fact, Spitzer surveys around M-type stars resulted in non-detections and concluded that the excess ratio for these discs is at least 4× smaller than for discs around solar-type stars (Gautier et al. 2007). Therefore, the frequency and properties of debris discs around M-type stars remains unknown. Figure 1.7b shows that SAFARI will be able to detect discs with L_{dust}/L_{star} 300× fainter than that around AU-Mic within 20 pc (AU Mic is at 9.9 pc). There are ∼ 1300 M-type stars (with stellar masses between 0.3–0.8 $M_{\odot}$) within 20 pc, warranting an important discovery space that only SAFARI can probe. In fact, **most of the new debris discs discovered by the *Herschel* are found around stars colder than K2**, indicating of the potential of this region of parameter space. SAFARI will open new frontiers in planetary studies: What kind of planetary systems could form around such cool stars? Will they be habitable? SAFARI will routinely observe them and increase our knowledge of how these enigmatic objects are formed.

Debris discs are also expected to persist on the post-main sequence after stellar mass loss and onto the white dwarf phase. Indirect evidence for such discs comes from the metal-rich atmospheres of some white dwarfs (*e.g.*, Farihi et al. 2010), but the disc of debris that is supposed to be feeding this enrichment has yet to be detected, presumably because the low stellar luminosity means the debris is also be faint. The sensitivity of SAFARI is essential for detecting these discs (Bonsor & Wyatt 2010).

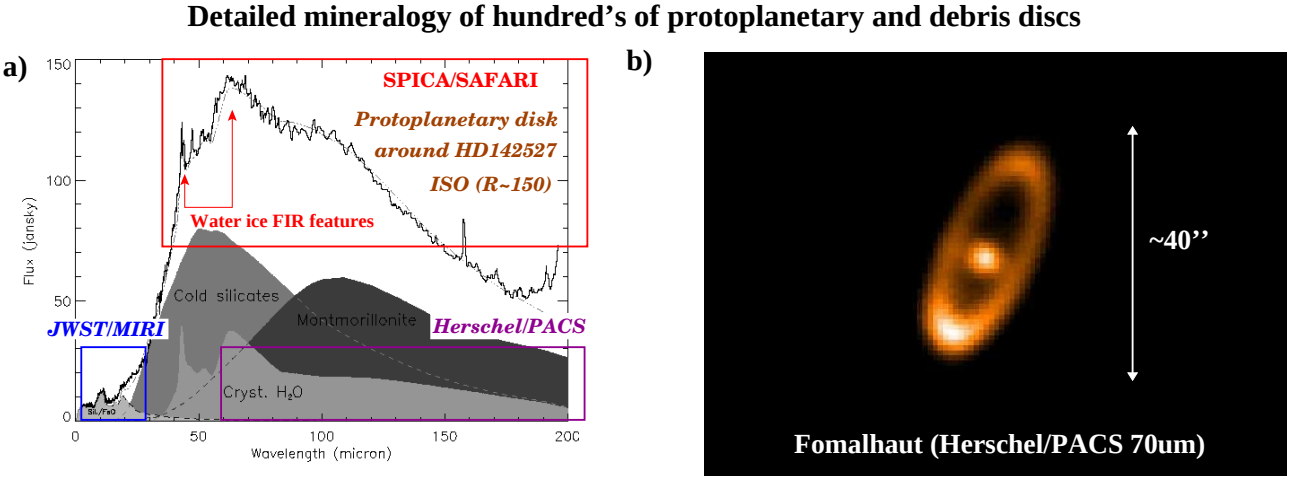

Figure 1.8: ***(a)*** *ISO spectrum of the disc around HD142527 (Malfait et al. 1999). Note that amorphous water ice only shows bands at ~ 44 μm in the FIR (Moore & Hudson 1992). Such features can not be accessed with Herschel or JWST. SPICA will take the equivalent spectra of objects at flux levels less than ~ 10 mJy per minute.* ***(b)*** *Image of Formalhaut debris disc at 70 μm with Herschel/PACS (PSF≃6″; Acke et al., in prep). SAFARI's large FOV and smaller PSF at shorter wavelengths (~ 4″ at the ~44 μm water-ice feature) will provide very detailed spectroscopic images of nearby discs.*

Spectrophotometric characterisation of circumstellar discs (mineralogy):
Despite the poorer angular resolution of SPICA compared to the future facilities (*e.g.*, ALMA in the submm), much will be learnt by going beyond photometric detections and carrying out extensive MIR/FIR spectroscopy studies of the strongest dust/ice features in a large sample of protoplanetary and debris discs. SAFARI will provide the continuous FIR spectral energy distribution (SED) and be able to detect both the dust continuum emission and the brightest grain/ice bands as well as the brightest lines from any gas residual present in the disc. The ability of FIR spectroscopy to determine the mineral makeup of dusty discs around young stars is illustrated by the ISO spectrum of HD142527 shown in Figure 1.8a. SPICA will be hundreds of times more sensitive than ISO and so will see not only the young and massive opaque protoplanetary discs like this, but will be able to trace the mineralogy of dust within discs at all stages of planetary system formation. SPICA will not only determine the detailed mineralogy of discs, but will also trace the variation grain size distribution and temperature, which are both expected to evolve with disc age leading to a variation in the disc SED. Models suggest that there is little predicted evolution of the mid infrared SED with disc age and a possible ambiguity in the mid infrared intensity between age and disc structure which is removed with observations in the far infrared (Tanaka et al. 2005). A key step forward needed to cope with all model complexities (Dullemond et al. 2001) and to fully characterise the nature of dusty discs will be to use SAFARI's spectro-photometric mode (R~100) to obtain full far infrared SEDs in order to accurately determine the emission peak, slope, and dust spectral features (see Figure 1.6b), and so be able to constrain grain sizes and opacities, critical ingredients to determine the disc mass. The same issues also apply to the characterisation (*e.g.*, composition and size distribution) of dust in debris discs (see *e.g.*, Spitzer's MIR spectroscopy of IRAS-dicovered discs in Chen et al. 2006), as well as in Solar System objects (see Sect. 1.2.3). In summary, SPICA/MCS and SAFARI spectroscopy will allow us to compare the mineralogy seen in extrasolar systems with that in our own system.

Water Ice in discs: Below temperatures of ~ 100 K water vapour freezes-out onto dust grains and the main form of water in the cold circumstellar disc midplane and at large disc radii will be ice. The physical location of the point at which water freezes out determines the position of the so called "*snow line*", i.e., the water ice sublimation front, which separates the inner disc region of terrestrial, rocky, planet formation from that of the outer giant planets (Nagasawa et al. 2007; Woitke et al. 2009a,b). Grains covered by water icy mantles can play a significant role in planetary formation, enabling the formation of planetesimals and the core of gas giants protoplanets beyond the *snow line*. Observations of the Solar System's asteroid belt suggest that our *snow line* occurred near a disc radius of ~ 2.7 AU (Lecar et al. 2006). In the outer reaches of our own Solar System, i.e.,

beyond the snow line, most of the satellites and small bodies contain a significant fraction of water ice; in the case of comets this fraction is as high as 80% and the presence of water in the upper atmospheres of the four gas giants is thought to be highly influenced by cometary impacts such as that of Shoemaker-Levy 9 on Jupiter. It is possible that it is during the later phases of planetary formation that the atmospheres, and indeed the oceans, of the rocky planets were formed from water ice contained in the comets and asteroids that bombarded the inner Solar System. For more distant exoplanetary systems, very little is known as (1) we first need to detect the presence of water-ice and infer its abundance in a large sample of protoplanetary systems (spanning a broad range of host star types and ages) and (2) even for the closest discs, the exact location of the *snow line* is very hard to resolve spatially with current instrumentation.

In the far infrared there is a powerful tool for the detection of water ice and determination of the amorphous/crystalline nature, namely the transverse optical mode at $\sim 44\,\mu$m both from crystalline and amorphous water ice and the longitudinal acoustic mode at $\sim 62\,\mu$m arising only from crystalline water ice (Warren 1984; Moore & Hudson 1992; Maldoni et al. 1999). In contrast to the MIR $\sim 6.1\,\mu$m water ice feature (that has a stronger band strength and that SPICA MIR spectrometers will observe with sub arcsec angular resolution), the difference between the amorphous and crystalline phase is best defined in the FIR (see Figure 1.8a) and, again unlike the MIR features (*stretching, bending or twisting of intramolecular bonds*), the FIR ice bands (*broad features due to intermolecular lattice vibrations*) are not confused with other solid state features of less abundant species. In optically thin discs it is extremely difficult to use MIR absorption to trace water ice and the material is too cold to emit in the NIR/MIR bands. Hence, these strong FIR features are robust probes of **(1)** the presence/absence of water ice, even in cold or heavily obscured or cold regions without a MIR background, and **(2)** the amorphous/crystalline state which provides clues on the formation history of water ice. Note that JWST and even *Herschel* cannot access most of these FIR ice bands (see Moore & Hudson 1994, for more examples).

First observed in emission towards the Frosty Leo Nebula (Omont et al. 1990), water ice has been detected in young protoplanetary discs in a few bright sources either in the FIR using the ISO-LWS (Dartois et al. 1998; Malfait et al. 1999) or MIR (Pontoppidan et al. 2005; Terada et al. 2007). The FIR features were also observed using ISO-LWS in comets within our own Solar System (Lellouch et al. 1998). Since the bands change shape i.e., they narrow for crystalline ice and the peak shifts in wavelength with the temperature, relatively high spectral resolution is needed to extract all the available information from the ice band profiles. In its highest resolution mode SAFARI provides $R \sim 4500$ at $\sim 44\,\mu$m which is appropriate for very detailed ice spectroscopy studies. Indeed **SPICA is the only planned mission that will allow water ice to be observed in protoplanetary and debris discs** and fully explore its impact on planetary formation and evolution and the emergence of habitable planets. In many cases, the MIR ice features from other species (e.g., water ice at $\sim 6.1\,\mu$m, but also methanol, carbon dioxide, formaldehyde and methane ice) will be studied also with SPICA/SCI and MSC. In combination with SAFARI observations, such complete MIR/FIR ice spectra will help to determine ice abundances and structures (amorphous vs. crystalline) accurately constrain disc models, and determine for how long ice mantles survive under the irradiation of different stellar UV fields (Grigorieva et al. 2007).

Spatially resolved debris discs (resolving the snow line in discs?): Images of the few spatially resolved debris discs, either seen in reflection or directly in the FIR or sub-mm, can show gaps and ring-like structures indicating the presence of planets which "shepherd" the dust. This has been most readily observed so far using HST (*e.g.,* Kalas et al. 2005) and ground based near-IR scattered emission and thermal MIR emission (e.g., Subaru, Gemini; Fukagawa et al. 2006; Fujiwara et al. 2006) and sub-mm and mm telescopes (JCMT, CSO and IRAM). ALMA will undoubtedly add a great deal to the subject by detecting the optically thin sub-mm continuum emission of the cold dust, but will not be very efficient in mapping the very extended emission of the closest discs which can extend to a few arcmin in size. *Spitzer* and *Herschel* have revealed that the size of some disc systems, such the Vega debris disc, is surprisingly larger in the FIR (e.g., at the emission peak) than in the sub-mm (see the *Herschel*'s view of Formalhaut disc in Fig. 1.8b). Obviously this is telling us something about the disc nature and it is clear that only through multi-wavelength spatially resolved observations we can fully understand the complete picture of the formation and evolution of these discs. SPICA's improved sensitivity over *Herschel* will allow to detect the extended emission of the debris discs, increasing significantly the number of discs that can be spatially resolved. Particularly interesting will be the study of the new class of debris

discs detected by *Herschel* that show excess emission at 160 μm and little or no excess at shorter wavelengths, corresponding to $T_{dust} < 30$ K (Eiroa et al. 2011). SPICA's unprecedented sensitivity will undoubtedly shed light on these objects that currently represent a challenge in terms of their collisional and dynamical regime.

Herschel is starting to increase significantly the number of spatially resolved debris discs in photometry; these discs will be ideal targets for mineralogy and compositional gradient studies with SPICA spectrometers, allowing us to obtain high resolution spectroscopy of the inner and the outer discs (to be compared to the compositional gradients found in our own Solar System). In the case of discs around A-type stars like Vega and Formalhaut, the spatial resolution of SPICA at the 44 μm feature will likely be sufficient to spatially resolve the distribution of water ice, i.e. the *snow line*, because in these systems the snow line is pushed away to $\sim$ 22 to 44 AU or even larger radii (Ida & Lin 2005; Grigorieva et al. 2007; Kennedy & Kenyon 2008).

SAFARI will be so sensitive that it will not only be able to produce fully sampled spectroscopic images of the $\sim$ 44 μm and $\sim$ 62 μm water ice bands, but also of any "secondary" or "residual" gas (e.g., by detecting [O I], [C II], H_2O or OH lines) produced by the photoevaporation of ice grain mantles, outgassing of comets or collisional evaporation. Very recent *Herschel* detections confirm the presence of gas in a few debris discs. Roberge et al. (2006) showed that the composition of the residual gas in β Pic is carbon rich, where a detection of the [C II] line has been confirmed by *Herschel*/PACS (see also Kamp et al. 2003).

Additionally, the MIR coronagraph (SCI) will cover the $\sim 5 - 27$ μm range, providing high stellar suppression within a small inner working angle (IWA $\simeq 1''$). Images of protoplanetary and debris discs with SCI will reveal their morphology in great detail (*e.g.*, detecting structures associated with the formation of planets like gaps or clumps) and also will allow us to carry out low-resolution MIR spectroscopy of PAHs and dust features that can be used to constrain the process of grain growth and sedimentation in discs (*e.g.*, Sauter & Wolf 2011). All in all, the study of discs with SPICA will shed light on the diversity of planetary systems, the link between circumstellar discs and planets and the link between extra-solar planetary systems and our own.

1.2.3 The inner and outer Solar System "our own debris disc"

The observation of circumstellar discs around distant stars at different evolutionary stages provide clues on how our planetary system was formed, from which materials, and how they were processed. However, in order to understand the observed diversity of extra-solar planetary systems, we also need to explain how our own Solar System emerged. Clearly both approaches complement each other and represent intimately and increasingly interconnected research fields. The study of the Solar System extends from the traditional investigation of the planets and their rings and moons, to the most recent characterisation of the different populations of primitive leftovers of their construction (comets, asteroids, Kuiper belt bodies, etc.). Finally, investigations of how life came to exist on Earth are fundamental and becoming of great general interest.

Our current view of the Solar System's early evolution is based on the "Nice Model" (Gomes et al. 2005). This model argues that, after a relatively slow evolution, the orbits of Saturn and Jupiter crossed their mutual 2:1 mean motion resonance about 700 Myr after formation, which caused a violent destabilisation of the orbits of planetesimals throughout the disc. This event populated the Kuiper belt (> 40 AU) with different families of leftover bodies and delivered pristine, icy planetesimals to the inner Solar System. This model agrees with the geochemical evidence (e.g., in the Moon) of a very peaked cratering rate at that time, and is generally known as the late heavy bombardment period (or LHB). Because there is also evidence of planet migration and planetesimal belts in extra-solar systems, a natural question arises: Are LHB-type events common in other planetary systems? From a broader astrobiological point of view, those primitive bodies coming from the outer Solar System (with little or no chemical processing) could have delivered significant amounts of volatiles and chemical species to the inner rocky planets (e.g., water and organic matter) that are relevant for the habitability of such planets. The study of the enigmatic nature of the outer Solar System is very challenging because **(1)** at such large distances from the Sun, rocky and icy bodies are cold, below $\simeq$ 60 K, therefore their thermal emission peak occurs at FIR wavelengths that cannot be observed from the ground and **(2)** the FIR fluxes are very weak (a few mJy and below). As we shall describe hereafter, the very sensitive instruments on board SPICA, together with their broadband spectroscopic capabilities, will provide a new perspective of the Solar System's outermost belts, the regions that hide a record of the earliest phases of the solar nebula.

Studying the Kuiper Belt object by object

Kuiper Belt Objects (KBOs) refer to the physico-chemically unaltered population of bodies beyond Neptune's orbit. Since the discovery of the first KBO (Jewitt & Luu 1993), more than 1200 objects have been detected so far in the outer Solar System ($> 30 - 40$ AU), including planetary-sized objects such as Eris (Bertoldi et al. 2006). Several thousands of KBOs are expected to exist, especially at high ecliptic latitudes. Unlike asteroids in the inner Solar System, KBOs must have formed relatively slowly and they are thought to be composed of pristine, almost unprocessed chemical material. The detailed study of their physical parameters (temperature, size distribution and albedo) and chemical characteristics (mineral/ice content) is thus fundamental to consistently link the history of our system with that of distant extra-solar systems. Unfortunately, most of the KBO attributes and chemical composition are almost unknown. Together with the inner asteroid belt, these remnant planetesimal belts are analogues of the cold debris discs observed as FIR photometric excess towards more distant stars. In this sense, the outer Solar System provides the closest "template" to study the composition, processing and transport of minerals, ices and organic matter by **studying debris disc bodies "one by one"**.

Spitzer-MIPS has detected a few KBOs photometrically at 24 and 70 μm by observing from minutes to hours per target. Measurements of the FIR thermal emission of KBOs (where the bulk of the KBOs' energy is radiated) reveal the thermal properties of the near-surface layers (Stansberry et al. 2006). Complementary observations in the visible are needed to establish the position accurately, determine the objects albedo, and, in combination with the FIR observations, determine the object size and mass. About ~ 30 KBOs have known albedos; low albedo values (such as those in comets) are presumed to be darkened by the presence of organic matter while high albedos are thought to be associated with ice mantles. Surprisingly, all inner and cold KBOs targets detected in the Spitzer sample ($\sim$20) have much higher albedos (Brucker et al. 2009) than previously assumed (Jewitt & Luu 1993). The underestimation of the KBO albedos leads to a significant overestimation of their mass. This is an unexpected result, and it is clear that future FIR studies on the size and mass distribution of the outer Solar System will need to provide a much more robust confirmation by observing a large sample of thousands of KBOs. *Herschel* FIR and submm cameras are observing the largest trans-Neptunian objects (with sizes from $\gtrsim$100 to 1000 km; see Fig. 1.9a), confirming low heat conductivities at temperatures far from the Sun (Müller et al. 2010). Dwarf planets like Orcus, Makemake and Haumea (KBOs with sizes of $\sim$1000 km) show thermal emission peaks at FIR wavelengths (Lim et al. 2010) and such observation constrain surface composition models. As an example, the interpretation of Haumea's FIR photometric data suggests that its surface is covered by loose regolith with poor thermal conductivity (Lellouch et al. 2010).

SAFARI photometry – FIR detection of all known KBOs: While *Herschel* requires ~ 300 hr to detect photometrically $\sim 10\%$ of the currently known KBOs (those with diameters larger than > 250 km at rate of ~ 1 per hr), SAFARI will detect almost all known KBOs (those with diameters > 100 km) in only ~ 50 hr at a rate of 1 object per minute. SAFARI's ultra-deep FIR photometric surveys will provide the crucial observational input to determine their sizes and albedos. SAFARI will also detect bodies as small as ~ 10 km diameter, thus including the new KBOs to be discovered from now to the launch of SPICA, the number which is expected to increase by a factor ~ 2, to ~ 2500 by the early 2020s. Future deep wide-angle optical surveys such as the Large Synoptic Survey Telescope (LSST in $\sim$2016) will be able to detect hundreds of new KBOs (and record their coordinates and orbits). This will help us to constrain their size distribution and build appropriate target lists for future space missions such as SPICA. However, LSST and other large optical telescopes will measure the KBO's reflected light and therefore it will only give some clues on their chemical composition from the observed colors. By operating at FIR wavelengths (e.g., not accessible to JWST), SAFARI will be able to detect their intrinsic thermal emission, thus providing a powerful tool to constrain KBO models. **The ability to constrain sizes, albedos and surface conditions in different families of KBOs, and relate them with their chemical composition and impact history in the Solar System is a unique driver for SAFARI**. Figure 1.9 shows the diameters (in km) of a population of known KBOs as a function of their heliocentric distance, and the detection limit predictions for the different photometric bands of *Herschel*-PACS and SAFARI showing the large number of KBOs that could be detected photometrically in the FIR in short time exposures by SAFARI.

SAFARI spectroscopy: What are the most primitive objects in the Solar System made of? Neither Spitzer nor *Herschel* have the required sensitivity to detect spectral features from KBOs in the FIR as the expected flux

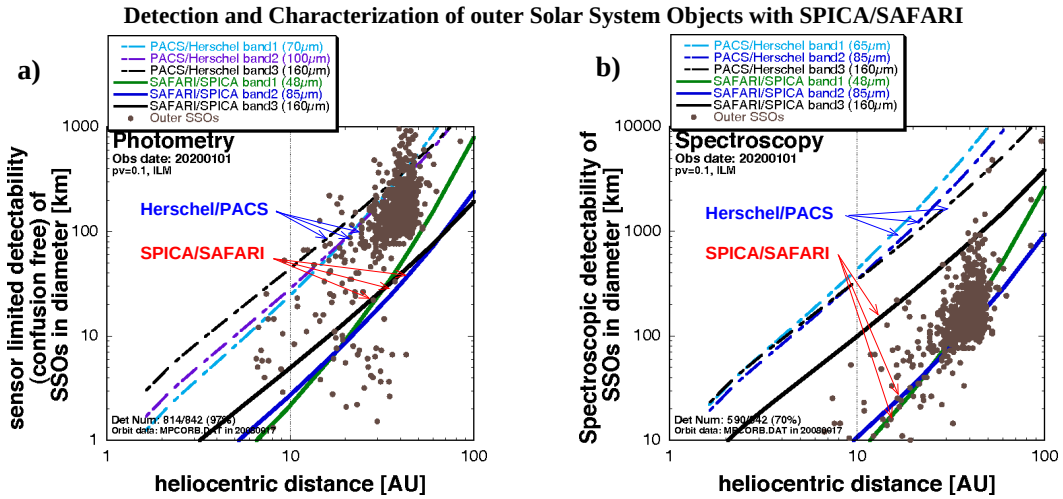

Figure 1.9: ***(a)*** *Diameters (in km) of known outer Solar System objects (SSOs), that emit at FIR wavelengths, as a function of their heliocentric distance. The coloured curves display detectability estimations for the different FIR photometric bands of Herschel-PACS (dashed) and SPICA/SAFARI (continuous). Predictions take into account that SSOs are moving objects so that they can be detected below the FIR confusion limit by pair-subtracting within a reasonable time interval. An iso-thermal latitude model (ILM) is assumed.* ***(b)*** *Same but for low-resolution spectroscopy, which will allow us to detect the mineral/ice content of the most primitive SSOs for the first time (updated from Hasegawa 2000).*

at 70 μm is below a few mJy and below a few μJy at 24 μm (Brucker et al. 2009). SAFARI will be the first FIR spectrometer to cover simultaneously the $\sim 34 - 210$ μm spectrum of KBOs with the required sensitivity, thus opening the outer Solar System studies to FIR spectroscopy. SAFARI low-resolution spectra ($R \sim 100$) will be a **new powerful tool** to constrain KBOs thermal models, because it does not just add a few photometric measurements, but fully samples the peak and shape of the thermal emission. Even more importantly, with spectroscopy we will be able investigate the presence of the main minerals and ices in a statistically significant sample of targets. The broad wavelength range and high sensitivity of SAFARI will allow us to detect both the water ice features at ~ 44 and ~ 62 μm and the broadband FIR emission from Mg-rich crystalline silicates (e.g., forsterite, clino-enstatite and diopside; Bowey et al. 2002) and other Fe-rich minerals. As a result, **we will be able to identify mineral features observed by SPICA MCS and SAFARI in extrasolar discs (see Sect. 1.2.2) with real physical objects in the outer Solar System**. SAFARI promises even more ambitious discoveries such as the detection of the possible tenuous gas atmospheres of some KBOs, by looking for water vapour and FIR lines of elements such as atomic sulphur or oxygen in their FTS spectra.

The inner Solar System, its size distribution and its chemical composition:

SPICA will not only characterise the composition of the cold and outer KBOs, but also of the different families of inner, hotter centaurs, comets and asteroids, thus probing the primary/secondary dust processing in the Solar System. The similarity between interstellar and cometary ices (Ehrenfreund et al. 1997; Crovisier et al. 1997; Bockelée-Morvan et al. 2000) may not directly prove that comets accrete unprocessed material, but rather suggest that similar chemical processes were at work in the early Solar Nebula and in interstellar clouds (Cernicharo & Crovisier 2005). However, abundant water, ammonia and methanol ice mantles in Solar System objects could well be the seeds of more complex biogenic molecules, such as the aminoacids, that do form when interstellar ice analogues are irradiated with UV radiation (Muñoz Caro et al. 2002). Some of the amino acids identified in the laboratory are also found in meteorites which suggests that prebiotic molecules could have been delivered to the early Earth by cometary dust, meteorites or interplanetary dust particles. Spectroscopic studies with SPICA in the critical MIR/FIR domain will clearly advance our understanding of the chemical complexity in planetary systems by direct searches of the “ingredients for life”.

In summary, SPICA will provide for the first time the means to quantify the composition of hundreds of Solar System objects. Sensitive FIR photometric and spectroscopic observations will give the first unambigu-

ous determination of their size distribution (and thus mass) and composition providing critical observational evidence for models of Solar System formation.

1.3 Exoplanet characterisation in the infrared: new frontiers

The mid infrared region (from ~ 3 to ~ 30 μm) is especially important in the study of planetary atmospheres as it spans both the peak of thermal emission from the majority of exoplanets (EPs) so far discovered, and is particularly rich in molecular features that can uniquely identify the composition of planetary atmospheres and trace the fingerprints of primitive biological activity. Extra-solar systems may include a variety of planets even richer than the selection we have in our own Solar System: gas-giants, icy bodies as well as less massive rocky planets with their oceans, moons and rings. In the coming decades many space and ground based facilities are planned that are designed to search for EPs on all scales from massive, young "hot Jupiters", through large rocky "super-Earths". Few of the planned facilities, however, will have the ability to characterise the atmospheres which they discover through the application of infrared spectroscopy.

Two different observational approaches can be used to characterise both *outer* and *inner* EPs: direct detection and transit techniques respectively. ***Direct detection***, which refers to observations where the star and the planet can be spatially separated on the sky with coronagraphs. Due to the limited size of current telescopes, this technique is only able to image EPs at large orbital distances (~ 50 – 100 AU). Besides, the huge contrast between the host star and the planet flux (e.g., the Sun is 10^9 times brighter than the Earth in the visible) makes the direct detection of an Earth-like planet at ~ 1 AU a distant goal for future instrumentation. Fortunately, EPs orbiting very close to the host star ($\lesssim 0.05$ AU) and with a favourable inclination (almost edge-on systems) can be indirectly studied via the ***transit technique*** by which the dimming of the starlight as the EP transits the star is followed, ***primary transits*** when the EP passes in front of the star and ***secondary transits*** when the EP disappears behind the star (Seager & Sasselov 2000). Because of the precise timing of a transit event, this technique allows high-contrast observations if very sensitive, low background and stable observing conditions are available (i.e., from space). **Although not specifically designed for EP research, transit observations with Hubble and Spitzer have revolutionised and redefined the field of EP characterisation over the past 5 years** (Barman 2007; Beaulieu et al. 2008; Deming et al. 2006, 2007; Marley et al. 2007; Demory et al. 2007; Gillon et al. 2007; Harrington et al. 2007; Knutson et al. 2007; Richardson et al. 2006, 2007; Machalek et al. 2008; Swain et al. 2008b,a; Tinetti et al. 2007). Collectively, this work has conclusively established that the detailed characterisation of EP atmospheres is feasible and today we can discuss the observational signatures including weather and atmospheric chemistry (e.g., Selsis et al. 2002; Tinetti & Beaulieu 2009).

The observation of EPs at IR wavelengths offers several advantages compared to traditional studies in the visible domain. First, the star-to-planet flux contrast is much lower than in the visible ($\sim 10^3$ for a typical "hot Jupiter" around a Sun-like star) and second, transiting planets around stars much cooler than the Sun have to be observed in the IR where their emission peaks. Spitzer has measured EP photometric transits out to 24 μm demonstrating that the light-curve is simpler ("box-like") than in the visible domain due to the negligible role of stellar limb-darkening effects. This allows a robust and precise determination of the EP radius as a function of wavelength and provides further strong constraints to the atmospheric properties. SPICA will achieve a precision similar or better than that reachable with Spitzer instruments, enabling us to detect the atmospheric features of hot-Jupiters and Neptunes. Besides, transit observations with the Spitzer-IRS MIR spectrometer have been used to extract the absolute intrinsic spectrum of HD209458b hot Jupiter around a Sun-like star – with the resultant spectrum in physical units (e.g., in μJy) as opposed to relative contrast measurements (Swain et al. 2008a) (see Figure 1.10). Infrared observations have allowed to characterise temperature-pressure profiles, chemistry and circulation patterns of a select subset of massive, close-in hot Jupiters along with several less massive EPs: the hot Saturn HD14926b and the cooler Neptune-mass planet GJ 436b.

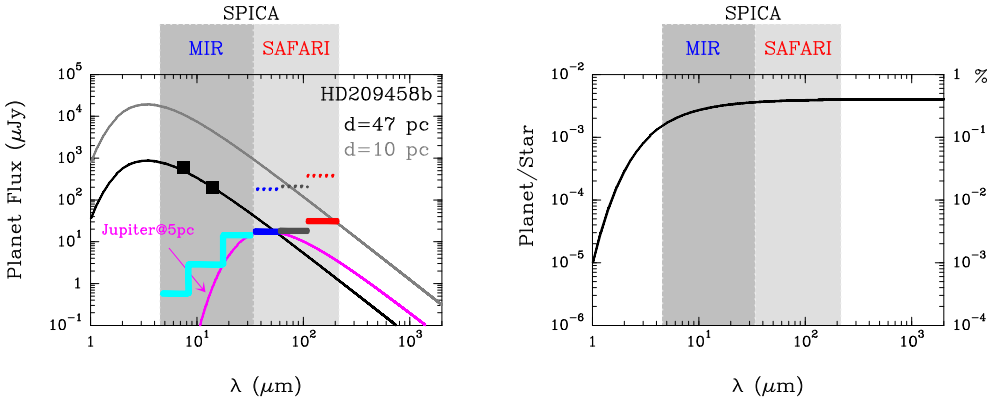

Figure 1.10: ***Left panel****: Fit to HD 209458b "hot Jupiter" ($T_{\rm eff} \simeq 1000$ K) MIR fluxes inferred from a secondary transit with Spitzer (Swain et al. 2008a) around a G0 star ($d \sim 47$ pc, in black) and interpolation to $d = 10$ pc (gray). The emission of a cooler Jupiter-like planet at 5 pc is shown in magenta (reflected emission neglected). The thick lines are the 5σ-1hr photometric sensitivities of SPICA MIR instruments (cyan) and SAFARI (blue, magenta and red). Confusion with the FIR extragalactic background does not apply to temporal variations of a signal from a known source (with coordinates). Dashed lines show sensitivities in spectrophotometric mode ($R \simeq 20$). SPICA will observe similar inner "hot Jupiter" transits routinely and will potentially extract their IR spectrum (rich in H_2O, O_3, CH_4, NH_3 and HD features as in Solar System planets).* ***Right panel****: Increasing planet-to-star contrast at long wavelengths (SPICA White Paper on EPs).*

1.3.1 Mid-infrared coronagraphy: "Direct" imaging and spectroscopy of EPs

High–contrast "direct" observations with coronographs are needed to study outer and cooler planets. The projected coronagraph on SPICA (SCI) is a unique instrument that provides several advantages over JWST coronagraphs. First, the monolithic mirror of SPICA will be better optimised for coronagraphy than the segmented mirror of JWST due to its much simpler and clean PSF. The segmented geometry of JWST also requires complex Lyot stops for the suppression of the light diffracted by each mirror segment, reducing the throughput and requiring a high degree of alignment stability. Secondly, the SPICA telescope itself will be actively cooled down to ∼6 K (compared to passive cooling down to 45 K for JWST); it is, therefore, further optimised for MIR/FIR astronomy. From the scientific point of view, **the main difference from JWST is the possibility of undertaking "direct" spectroscopy with SPICA/SCI in the critical MIR domain** (using a grism/prism providing $R \sim 20 - 200$) in addition to imaging. This spectral capability in a continuous wavelength domain rich in chemical signatures ($\sim 3.5 - 27$ μm) represents a unique science possibility of SPICA (Abe et al. 2007) compared to JWST, which will just have quadrant phase and Lyot photometric coronagraphs in the MIR and will provide lower contrast than SCI.

The most significant atmospheric features expected in the SPICA MIR spectra of EPs can be summarised as follows: (1) The $\sim 4 - 5$ μm "emission bump" due to an opacity window in EGPs and cooler objects with temperatures between 100 and 1000 K; (2) Molecular vibration bands of H_2O ($\sim 6 - 8$ μm), CH_4 (~ 7.7 μm) , O_3 (~ 9.6 μm), silicate clouds (~ 10 μm), NH_3 (~ 10.7 μm), CO_2 (~ 15 μm) and many other trace species. If detected, the relative abundance of all these species could be compared among different EPs and with Solar System planets and bodies. Note that giant planets like Saturn in the Solar System show strong NH_3, PH_3 and H_2O features around ∼5 μm (de Graauw et al. 1997). SPICA will also have access to the PAHs features; (3) He-H_2 and H_2-H_2 collision induced absorption band features as tracer of the He/H relative abundance; (4) Features from deuterated molecular species to distinguish cool brown dwarfs from "real" EP (e.g., CH_3D at ∼8.6 μm) and non-equilibrium species (e.g., PH_3 at ∼8.9 and ∼10.1 μm).

As we have seen earlier, exo-giant-planets (EGPs) are thought to form beyond the "snow line". Indeed, several of them are known from Doppler shift measurements or direct imaging in the visible (Wetherill & Stewart 1989; Kalas et al. 2008; Marois et al. 2008) and more will be detected in the near future (with large optical telescopes equipped with coronagraphs, JWST and SPICA itself). This key population of outer and young EGPs can not be studied through transit experiments but will be targets for SCI direct characterisation. In fact, in the next decade **SPICA/SCI will be the only instrument available to characterise outer and cool EPs**

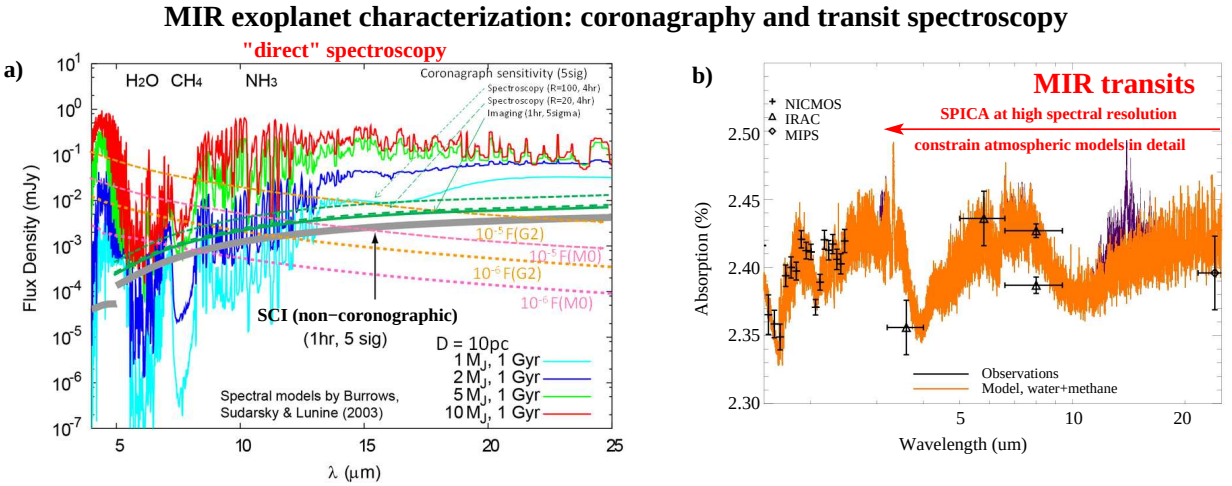

Figure 1.11: ***(a)*** *Simulated spectra for a range of exoplanet masses at an age of 1 Gyr and a distance of 10 pc (from Burrows et al. 2003). SPICA/SCI is the only planned coronagraph that will carry out MIR "direct" spectroscopy of outer (>10 AU) and young EPs.* ***(b)*** *Hubble and Spitzer primary transit of HD 189733b hot Jupiter (photometry) and H_2O and CH_4 models (by G. Tinetti). Transit observations with SPICA/MCS will characterise the atmospheric composition.*

through direct spectroscopy in the MIR. Therefore, SPICA will add greatly to EP research (and much earlier than the future Terrestrial Planet Finder type missions; TPF) by imaging young EPs directly and by recording their MIR spectra, thus constraining their temperature and atmospheric composition. The SCI simpler binary mask type approach will achieve a contrast of $\sim 10^{-5}$ ($\sim 10^{-4}$ raw contrast plus PSF substraction methods) at the equivalent to ~ 9 AU ($\sim$ Saturn's orbit) at $\sim 5\,\mu$m for a star at 10 pc (IWA$\sim 1''$). At this wavelength we probe the younger end of the planet age range ($\sim$100 Myr to 1 Gyr) as older planets are fainter (see Figure 1.11a). We expect that a rather complete list of more than 60 EP targets for direct spectroscopy will be available by SPICA launch as a consequence of ongoing ground-based projects with 8-10m telescopes (Subaru-HiCIAO, VLT-SPHERE, Gemini-GPI, etc.). A target field identified by the SPICA teams is the Ursa Major group. SCI is expected to produce an "spectral atlas" of several outer EPs ($\sim$ 1-4 hr integration per EP), therefore completing the discovery and characterisation space of other telescopes and methods. According to their expected flux at long wavelengths ($\lambda > 5\,\mu$m), the main targets for SCI spectroscopy will be $\sim 5\,M_{Jup}$ planets around solar-type stars and lower mass planets, $\sim 2\,M_{Jup}$, around M dwarfs. In photometric mode, SCI will perform imaging surveys integrating a few minutes per target (both young M stars: $\sim$300 Myr, < 50 pc; and FGK stars: $\sim$1 Gyr, < 25 pc). Last but not least, SPICA/SCI would be sensitive not only to the exoplanets themselves, but also to circumplanetary dust which can be even brighter than the exoplanets theirselves (*e.g.*, Kennedy & Wyatt 2011).

1.3.2 Mid-IR "transit" photometry and spectroscopy of exoplanets

Together with SCI, the SPICA MIR Camera and Spectrometer (MCS) will cover the mid infrared range with low, medium, and high spectral resolution (out to $R \sim 30\,000$). Following the unexpected but successful observations of "hot-Jupiters" EPs made by Spitzer in the MIR, these instruments will be used **to study primary and secondary transits of EPs orbiting very close to the star**. SPICA's spectrometers will be used to perform (1) multi-wavelength transit photometry of hot Jupiters routinely and (2) carry out "transmission" and "occultation" spectroscopy of an appropriate sample of bright EPs. Hot-Jupiters in particular, are bright and the possibility to carry out detailed atmospheric spectroscopy will allow us to study exo-atmospheres in great detail. This will help to develop the techniques and models that will be needed to interpret the spectra of habitable exo-Earths in the future. We estimate that the $\sim 24\,\mu$m thermal emission of gas giant planets similar to HD 209458b could be extracted from secondary transit observations around stars as far as ~ 150 pc (a few hundred star targets) as the contrast requirement is relatively modest ($\sim 0.1\%$). We anticipate that several giant EPs, with a great diversity of mass, semi-major axis, eccentricities, etc. will be available to SPICA for detailed mid infrared characterisation by $\sim$2020. Another example, a super-Earth ($2 - 3R_{earth}$; $T_p \sim 300$ K) orbiting around the habitable zone

of a cool M8 star ($T \sim 2500$ K) will produce an intrinsic flux of $\sim 25\,\mu$Jy at MIR wavelengths, roughly a few times higher than the projected 1σ-1min photometric sensitivity of SPICA's MIR instruments (but very hard to achieve even with ground-based MIR instruments on "Extremely Large Telescope"-type observatories). These photometric flux levels are accessible for SPICA secondary transit studies with a contrast of $\sim 0.1\%$.

In summary, SPICA will be an important intermediate milestone in exoplanet research, both in science achievements (direct spectroscopy of outer EPs for the first time in the MIR, atmospheric characterisation of transiting EPs at long wavelengths...) and in the required technological developments for future longer-term missions (e.g., coronagraphic techniques, cryogenic systems...). Besides, the operational wavelength domain of TPF or DARWIN-type missions is also the 5-30 μm range that SPICA will exploit in depth, both in "direct spectroscopy" and in "transit spectroscopy" by observing tens of gas giant exoplanets.

1.4 The life cycle of gas and dust in the Milky way and beyond

SPICA will provide an unprecedented window into key aspects of the dust life-cycle both in the Milky Way and in nearby galaxies: from the dust formation in evolved stars, its evolution in the ISM, its processing in supernova-generated shock waves and massive stars (winds, HII regions, etc.), to its final incorporation into star forming cores and protoplanetary discs. Dust grains are a key player in determining the energy budget of the interstellar and circumstellar media because of their fundamental role in reprocessing stellar UV/visible photons into IR to sub-mm radiation, and in heating the gas via photo-electron emission from small grains and PAHs. **SPICA will be the first space telescope since ISO (launched in 1995) covering in spectroscopy the uninterrupted MIR/FIR domain where PAH and astro-mineralogy studies can be carried out**. ISO caused a revolution in the field of astromineralogy (*e.g.*, Waters et al. 1996; Tielens et al. 1998; Henning 2003) and showed that the critical keys to unlock our understanding of the dust evolutionary cycle are MIR/FIR spectroscopy and the FIR dust SEDs. The former gives direct access to the poorly known ice and grain composition and its evolution along the dust life-cycle, and the latter enables us to determine the dust temperature uniquely.

In addition to dust, other very important gas-phase species that are hard, often impossible, to detect from the ground have their spectral signatures in the MIR/FIR: ions, atoms, light molecules and heavier organic species. Their associated MIR/FIR spectral features provide means to derive physical conditions in environments that are difficult to probe at other wavelengths (in UV/X-ray illuminated PDR/XDRs, shocked regions, galactic nuclei, etc.). They provide clues on the elemental abundances (C, O, S, Si, Fe ...) and also provide deep insights into the gas/dust chemical interplay: ice formation/evaporation, grain growth and metal depletion (Okada et al. 2008). In this context, **SAFARI will provide FIR spectroscopic images of the regions that are too obscured for JWST to examine in the MIR or too warm/extended to be efficiently traced by ALMA**. Thanks to its superb sensitivity, SPICA will extend our knowledge of the physics and chemistry of the gas and dust in our galaxy (e.g., acquired with *Herschel*) to similar detailed studies in nearby galaxies (see next Sections). In the following we list several fields where we anticipate that SPICA will play a unique role. This is not an exhaustive list, and probably does not do justice to the great discovery space available to SPICA (see Sec. 1.8):

Chemical complexity: Spectral observations from UV to cm wavelengths reveal a high degree of chemical complexity in our Galaxy that was until recently not expected. Such complexity is demonstrated by the diversity of detected species, that range from simple light hydrides, molecules carrying heavy metals, alcohols (methanol, ethanol,...), and a collection of many organic families (acetylenic chains, methane or benzene; Cernicharo et al. 2001) that lack permanent electric dipole (i.e., do not have radio spectrum to be observed with ALMA) but show MIR/FIR vibrational features. Either in the gas phase or as ice mantles, those species can be precursors of more complex molecules (sugars, amino acids, etc. Muñoz Caro et al. 2002). Therefore, SPICA MIR/FIR spectrometers will open new windows to probe the chemical complexity in the universe by observing: (1) MIR vibrational bands of PAHs and other organic molecules; (2) FIR rotational lines of light hydrides (H_2, HD, H_2O, OH, CH^+...) and (3) Solid-state bands from different minerals and ice mantles. None of these can be observed with ALMA (thus missing a significant fraction of the chemical species that build up the chemical complexity of the Universe!). Finally, JWST/MIRI will struggle to detect warm diffuse dust but will not see the cold dust at all as emits at longer FIR wavelengths (*i.e.*, SAFARI territory).

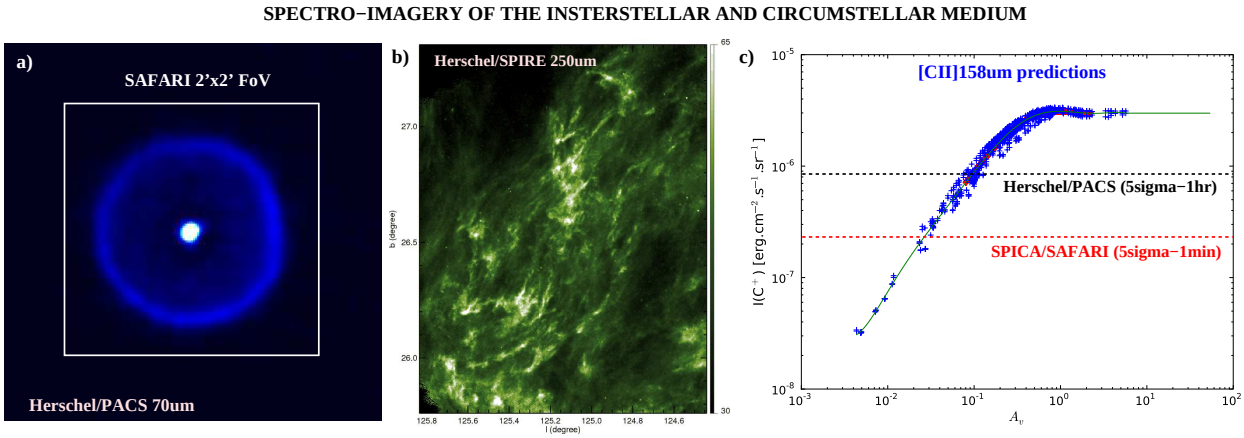

Figure 1.12: ***(a)*** *Herschel/PACS 70μm image of U Ant detached shell (Kerschbaum et al. 2010). Circumstellar envelopes and shells around evolved stars can have sizes of several arcmin. SAFARI large FoV and much improved sensitivity in spectroscopic modes will allow us to probe the outermost curcumstellar regions and their faint interaction with the ISM.* ***(b)*** *Herschel/SPIRE 250 μm image of the Polaris Flare, a high latitude diffuse cloud (Miville-Deschênes et al. 2010). The intensity scale corresponds to 30-65 MJy sr^{-1}. SAFARI will be able to obtain deeper images of very faint and diffuse clouds in the Galactic Poles and in the Galactic halo (at 48, 85 and 160 μm simultaneously). Operating in SED mode (R∼100) SAFARI will be more sensitive than Herschel photometers, reaching a few MJy sr^{-1} (5σ) in 10s exposures.* ***(c)*** *Using narrow band filters, SAFARI will image relatively large areas of diffuse clouds (with $A_V < 1$) in key gas tracers of the structure and physics of the ISM phases (e.g., [C II]158 μm and [N II]122 μm; MHD/PDR simulations from F. Levrier).*

Diffuse ISM: The structure of the diffuse ISM provides the initial conditions for the formation of molecular clouds. The physics that governs the large– and small–scale structure of diffuse clouds is complex (magnetic fields, turbulence, cooling, etc.). For the first time, *Herschel* is providing large scale photometric images of high Galactic latitude diffuse clouds that unambiguously reveal the filamentary and clumpy structure of the diffuse ISM down to spatial resolutions of ∼0.01 pc (see Fig. 1.12b; Miville-Deschênes et al. 2010). While *Herschel* photometers detect the broadband dust continuum emission, the sensitivity of the spectrometers is clearly not enough to map the brightest gas lines. In particular, the [C II]158 μm line is the dominant cooling line of the neutral ISM, and interest for this line has very much increased recently as it may well be an good tracer of warm H_2, the so-called "dark gas", a component of the ISM dense enough for hydrogen to be mostly molecular, but not dense enough for carbon to be in the form of CO. Studing the neutral and ionized phases of the diffuse ISM over very large scales through simultaneous observations of [C II]158 μm and [N II]121 μm lines will only be possible with SAFARI using narrow-band filters (see Fig. 1.12c and Levrier et al. 2009). The combination of much larger field-of-view and sensitivity (*i.e.*, much faster mapping speed) compared to *Herschel* will allow us to "image" these critical gas diagnostics in very particular and faint regions of our galaxy that are not accessible to *Herschel* nor to future FIR stratospheric telescopes: **(1)** The Northern and Southern Galactic Poles: diffuse clouds structure (photometry) and gas cooling in some fields (spectroscopy); **(2)** Gas and dust in the Milky Way's *halo* and the high-velocity hydrogen clouds (e.g., Wolfire et al. 1995) and relation with extragalactic halo studies: gas fountains driven by SNe explosions, stripped gas from nearby galaxies, etc; **(3)** Spectroscopy of GMCs outskirts (faint PDRs).

Evolved stars (dust factories): The principal objects injecting dust into the ambient ISM in our Galaxy are the evolved stars, mainly red giants and AGB stars that predominantly emit at MIR/FIR wavelengths. So far, the study of evolved stars has been limited to the the closest and thus brightest ones. SPICA will allow to cover a much greater volume in our galaxy, and to observe extragalactic evolved stars in quite some detail. SAFARI will be specially adapted to study the inner parts of their circumstellar envelopes (CSE), and to study the mass-loss history and mineralogy of a large sample of targets in very different environments including the closest galaxies. SAFARI observations will include **(1)** spectroscopic images of spatially resolved CSEs, **(2)** their faint interaction with the ISM ("wakes" and "tails"), **(3)** detailed spectroscopic studies of unresolved CSEs, and **(4)** point source observations of unresolved AGB populations in nearby galaxies of the Local Group.

1) For nearby objects, SAFARI will provide spectroscopic images of faint but very extended "detached" shells around evolved stars (see Figure 1.12a) revealing their physical and chemical structure in great detail (for a prototype shell like TT Cyg, Kerschbaum et al. 2010, ∼5″ corresponds to only a few hundred years of expansion). **(2)** Following pioneering work using Spitzer (Ueta et al. 2006) and Akari (Ueta et al. 2010) the interaction of AGB-winds with the sourrounding ISM became evident as a common phenomenon from *Herschel* imaging that provides valuable clues on both the stellar wind and the local ISM. GALEX discovered a 2-degree long turbulent wake arising from the motion of Mira, a prototypical mass losing red giant, through the ISM. The UV emission detected by GALEX probably comes from H_2 molecules excited by ∼30 eV electrons formed in shocked gas (Martin et al. 2007). Very recent FIR observations with *Herschel/PACS* reveal broken dusty arcs and filaments that indeed probe the complex interaction of Mira's wind and the ISM (Mayer et al. 2011). The injection in the ISM of circumstellar matter enriched by the stellar nucleosynthesis takes place in such complex environments. Hence, the spectro-imaging capability of SAFARI will allow us to detect emission lines associated with the mixing of circumstellar and interstellar gas, and to study in different targets the processes controlling this injection. As these targets can be characterized by their distances, proper motions, mass loss rates, etc., many geometrical and physical conditions can already be constrained, which makes these sources particularly appropriate for describing the physical processes at work in ISM (instabilities, shock chemistry, photodissociation, dust destruction, etc.). Whereas *Herschel* can only image the brightest ones (not differentiating continuum from line emission) the spectroscopic imaging capabilities of SAFARI will be a unique feature. **3)** The broad wavelength coverage of SPICA/MCS and SAFARI, especially when compared with *Herschel*-PACS, will allow us to probe many critical gas and solid state features and also to unambiguously determine dust temperatures and masses using both the MIR and FIR ranges (*e.g.,* Arimatsu et al. 2011). Moreover SAFARIs high sensitivity makes also very low mass loss rate stars ($\leq 10^{-8}$ $M_\odot\,yr^{-1}$) accessible, an by this the onset of mass loss at the RGB/AGB transition **4)** Further out, photometric measurements will constrain the mass-loss rates in AGB stars out to the Large Magellanic Cloud (LMC; $d \sim 50$ kpc) in modest integration times. For example, the expected flux at 48 μm (where SAFARI is limited by sensitivity and not by confusion) of evolved stars like IRC+10216 or R Cas at the distance of the LMC is ∼70 and ∼1.3 mJy respectively, while old (faint) detached shells like TT Cyg will have fluxes of ∼400 μJy, requiring an integration time of a few seconds with SAFARI. Even in the *Herschel* era we see only the tip of the mass loss iceberg in our own and in the Local Group galaxies, making it impossible to use them as a stellar evolution laboratory (different star forming histories, metallicities, etc).

Supernova remnants (dust processing): Stars much more massive than our Sun end their lives with a violent explosion where massive flows are blown outward and shock waves propagate through the surrounding medium. When supernova (SN) remnants encounter molecular clouds, they drive slower shock waves that compress and heat the molecular material and result in strong MIR/FIR line emission (Neufeld et al. 2007). At the same time, dust grains are processed (eroded, fragmented, amorphised ...), their physical state changes, and large quantities of refractory elements are sputtered back to the gas phase (Si, Fe, Mg, etc.). Dust grains may condense after the shock passage, and therefore SNe may contribute to the formation of dust. In fact, high-z galaxies seem to contain dust that may mainly have formed in SNe ejecta, because the galaxies may be too young for a significant contribution of AGB stars' dust. Thus, dust condensation must be efficient, requiring about 1 $M_\odot$ of dust per SNe. The efficiency of SN dust formation is still debated. With Spitzer mid-IR studies typically detected less than 10^{-3} $M_\odot$ of newly formed dust within the first three years of the outburst. Unexpectedly, *Herschel* has detected SN 1987A (Matsuura et al. 2011) and its dust mass is estimated as 0.5-0.7 $M_\odot$. This young supernova remnant has just started to be affected by shock destruction of dust. By the time of the SPICA launch, the dust mass may have deceased. The flux from SN 1987A detected by *Herschel* was about 70 mJy at 100 micron. The high sensitivity of SAFARI potentially enables it to detect SNe and SNRs within 2 Mpc (*i.e.* to just beyond the Galaxies in the Local Group). SPICA spectroscopic imaging will allow us to infer the physical conditions prevailing in the shocked gas while directly tracing the dust emission to the faint levels required to measure SN dust production, and even its composition.

1.5 Local Universe: Detailed studies of the ISM

1.5.1 The role of Local Group observations

The Local Group contains a wide variety of galaxies, all within 1 Mpc, allowing observations to be carried out with unprecedented sensitivity and resolution to measure all of the major cooling lines of the ISM at a scale smaller than that of molecular or atomic clouds. The Large and Small Magellanic clouds (LMC and SMC) are barely further than the other side of our own Galaxy and allow the study of the ISM and star formation at the same scale as in the Milky Way, **but in an environment inaccessible within our Galaxy because of the very different gravitational potential and lower metallicity** (much lower in the case of the SMC). A programme carefully structured to study the effects of, e.g., metallicity and irradiation would start with the Magellanic Clouds, observing the entire systems at the scale of individual cloud complexes.

The Andromeda galaxy provides a reference, similar to the Milky Way, of a large evolved spiral, while Messier 33 represents a first step towards chemically younger (less processing of gas into stars and hydrogen into ”metals” in the stars) yet still spiral galaxies. The Local Group is rich enough that the above galaxies are far from being the only targets – WLM, IC10, NGC 55, Leo A, NGC 3109, Sextans A, GR8, NGC 6822 and DDO210 provide an even greater variety of conditions, including still lower metallicity environments. These can be used to assess the role of metallicity versus other factors (mass, morphology, age) in the physics of the gas. **By fully mapping these galaxies, feasible only with SAFARI thanks to its high mapping speed, we can, for example, compare the emission from the gas in colliding streams of HI with that of the molecular clouds that are suspected to form in these streams.** By mapping large regions at high spatial resolution, we will be able to detect rare and/or transient phenomena, such as phase changes (e.g. atomic to molecular) which have not been detectable up to now, and obtain a measure of the length scale on which the changes occur. These changes would be identified by anomalous line ratios from SAFARI.

Typical [CII]158μm line strengths in galaxies like M33 or the Magellanic clouds are of order 10^{-4} erg s^{-1} cm^2 sr^{-1} or about 5×10^{-16} W m^2 in a SAFARI beam, yielding a signal-to-noise ratio of 10000 in one hour of observation. To obtain a S/N ratio of 500 in [CII], such that lines 100 times weaker could be mapped at the same time, then requires about 10 seconds per field of $2' \times 2'$, or about 2.5 hours per deg^2. A detection threshold 100 times below the [CII] line intensity has never been reached in extragalactic objects so many new lines will be discovered and mapped in great detail in these nearby objects. Among the lines that would be mapped with high S/N are [OI]63μm, [NII]122μm, [OIII]88μm, [OIII]52μm, [OI]145μm, $H_2O\lambda$179μm, [NIII]57μm, HDλ112μm, OHλ119μm, [SiII]35μm and probably other lines, including the CO ladder for J > 13.

At this mapping speed and excellent S/N ratio, the LMC would require about 55 hours, the SMC about 15, M 31 (our Milky-Way like reference) and M 33 about 6 and 4 hours respectively, 2.5 hours each for NGC 6822 and IC 10, and less than 10 hours for the other Local Group Dwarf Galaxies. Thus, less than 100 hours of SAFARI time would be required to fully map the far-IR emission at high spectral and spatial resolution throughout the Local Group. In the time estimate we have allowed for observing times twice as high per field for the low metallicity galaxies SMC, NGC 6822, NGC 3109, and IC 10 and four times as high for the very low metallicity objects WLM, NGC 55, Leo A, Sextans A, GR8, and DDO210 in comparison with the LMC, M 31, and M 33. **With *Herschel*, the same observations would require 100 years, instead of 100 hours**, to reach the same sensitivity and cover the same spectral region!

1.5.2 The metallicity on the ISM

The ISM is the repository of the metals ejected by dying stars, as well as the site for the birth of the next generation. Stellar winds and SN explosions continually raise the metallicity of the ISM, where it is recycled by the formation of new stars. Metallicity and star formation history are thus intimately tied together.

Late-type spiral galaxies have metallicity gradients ranging roughly from twice solar in the centre to less than half solar in the outer regions, presumably reflecting star formation gradients. Late-type dwarf galaxies have metallicities from just below solar to less than a tenth solar, but it is not clear whether this is caused by relatively little star formation in the past or by preferential removal of metals from the shallow central

gravitational wells by the stellar winds and SN explosions that release them. Despite a superficial resemblance, these galaxies differ from low-metallicity galaxies in the early Universe; they are the products of a long galactic evolution just as the spirals are.

In metal-poor ISM environments, the physics of both gas and dust, as well as their spectral fingerprints, differ markedly from those of gas-rich starburst galaxies or even the Solar Neighborhood. In metal-poor environments, the heating and cooling of the ISM no longer operates the same way as in the Galactic ISM. **The presence of fewer heavy elements alters the gas-phase chemistry (due to the lower atomic and molecular abundances with respect to hydrogen), lowers the dust-to-gas-ratio, and changes the grain surface chemistry (affecting the formation of H_2)**, while the erosion of large dust particles affects the nature and size distribution of the dust. Lower dust content decreases extinction and UV photons travel further, altering radiation-dependent rate coefficients (dissociation, ionisation). The CO abundance is drastically reduced, but the self-shielded H_2 stays largely unaffected (Shetty et al. 2011), and CO is no longer a useful gas column density tracer. Depending on the dynamics of the grain-size distribution, the photo-electric heating efficiency of the medium is also modified. Low dust-to-gas ratios allow UV radiation to penetrate deep into molecular cloud layers, producing abundant ionised carbon (C^+). Although we observe these effects in a qualitative way, we know very little about their actual quantitative expression, and surprises occur when details are studied. For instance, under low-metallicity conditions, C^+ emission ([CII]) is *both strengthened and weakened* with respect to CO and the far-IR continuum. Low levels of extinction cause very long UV mean free paths enhancing photo-electric gas heating *efficiencies* and hence [CII] cooling and line intensity, whereas low PAH abundances simultaneously decrease photo-electric gas heating *rates* limiting the increase in [CII] intensity (Israel & Maloney 2011). Thus, in the low-metallicity ISM, [CII]/CO and [CII]/FIR ratios are an order of magnitude higher than in the Milky Way, but otherwise all very similar, independent of actual (low) metallicity.

Determining the physics and life-cycles of gas and dust is an essential part of any study of the evolution of late-type galaxies. It is critically incomplete without the dimension of metallicity. Large numbers of actively star-forming dwarf galaxies with (low) metallicities covering a range of more than an order of magnitude are known in the Local Universe. They provide ideal laboratories in which to study the interplay between star formation and ISM physics. Recent surveys with ISO and *Spitzer* have observed the dust and mid-IR line properties of less than ∼75 dwarf galaxies: however, only a handful of the most metal-poor (1/20 of solar) were detected (Madden et al. 2006; Engelbracht et al. 2006). Extensions to far-IR dust emission, as well as spectroscopic surveys of the major far-IR cooling lines, are being obtained with *Herschel*: in particular, detecting the [C II]158μm line in the low metallicity galaxies is a major breakthrough. However, the sensitivity of the *Herschel* instruments limits these spectral surveys to measure only the strongest lines from the brightest regions in these galaxies.

We need the molecular and atomic fine structure diagnostic lines in both the mid- and far-IR, especially those of C, N, and O, to detect and measure the properties of the more *extended diffuse gas and dust* in the brightest dwarf galaxies, as well as those of both *the dense and diffuse ISM* components in all those still unexplored systems. These lines are fully covered by SAFARI, and the gain in sensitivity and overall scan speed of two orders of magnitude of SAFARI will finally bring mid-/far-IR spectroscopy of the entire population within our reach. While it is not clear to what extent local metal-poor systems can be used as proxies for high redshift galaxies, a certain chemical similarity seems to be present. Most of the high-redshift surveys have targeted the more massive galaxies, but recent spectroscopic surveys of the low-mass population at $z \sim 1$ (Davies et al. 2009) are putting dwarf galaxies into a clearer perspective in galaxy evolution. A SAFARI survey of such targets would be the next step in understanding the evolution of metals in the gas and dust, and how these properties affect the star formation density as a function of redshift.

1.6 Galaxy evolution

1.6.1 Major recent discoveries and open questions

Studies of galaxy evolution in a cosmological context have greatly progressed in the recent past, observationally establishing several results predicted from theory such as the relation of black hole and galaxy masses (e.g., Fabian 1999). Optical studies of the local massive galaxy population show that most, if not all, galaxy spheroids host massive relic black-holes (Richstone et al. 1998) which, in turn, suggests that all massive galaxies pass through a material-accreting, active galactic nucleus (AGN) phase. **The observed correlations between the masses of black holes at the centres of massive local galaxies and key properties of the host galaxies**, such as their luminosities, dynamical masses, and velocity dispersions of their spheroids (e.g., Magorrian et al. 1998; Ferrarese & Merritt 2000; Ferrarese & Ford 2005; Shankar et al. 2009) **are astonishing, given the vastly different scales that they involve.** The enormous difference between the Schwarzschild radius of a supermassive black hole (SMBH) and the characteristic radius of the stellar population in its host galaxy suggest that these relations are **likely due to the coeval formation of the black hole and the bulge**. The origin of these correlations cannot be fully explained by observations of local galaxies, and so both activities must be seeded at earlier epochs.

Given that highly accreting black holes are often hosted by dusty galaxies, the latter are ideal for studies of the coeval growth of black holes and galaxies. To test this suspected coevolution **from a statistical point of view, we need to compare four quantities as a function of look-back time: the host-galaxy masses and star-formation rates vs the black hole masses and accretion rates. To date, this comparison has been mainly performed for the rates of star-formation vs black hole accretion.** The evolution of the two processes with time can be seen in Figure 1.13b. Global accretion power, measured using X-rays (Hasinger et al. 2005) and the star formation power, measured by Hα and rest-frame UV observations (Shim et al. 2009), were both ∼20 times higher at z=1-1.5 than today. That both peak at around $z \sim$ 1-3 strongly supports the co-evolution of SMBHs and the star formation rate (SFR, e.g., Marconi et al. 2004; Merloni et al. 2004, Gruppioni et al. 2011, MNRAS, submitted). To understand and unravel the relationship between the black hole growth and bulge formation we need to track back the evolution of black hole growth and star formation over cosmic time, and determine whether there is a causal link between the growth of the central black hole and its host spheroid. If there is such a link, how and when is it established, and which, if either, process drives or regulates the other? To further study this link, we will need to compare the origin and shape of the galaxy mass and luminosity functions with those of black hole mass functions in large samples that include obscured sources.

In addition to finding out that AGN are often optically obscured by dust, both locally (e.g. Goulding & Alexander 2009) and at high-z (Hernán-Caballero et al. 2009), we know from Galactic and extragalactic studies that the processes of **star formation and early stellar evolution are typically deeply enshrouded in dust.** Therefore, galaxies pass through the most active periods of their lives obscured at optical wavelengths. A direct manifestation of this came from the important discovery of a dusty population of galaxies that emit a significant fraction of their bolometric luminosity in the far-IR/submillimetre (sub-mm) because of the strong starbursts that they are undergoing. IR and sub-mm surveys indicated that luminous and ultra-luminous infrared galaxies ([U]LIRGs) are rare in the local Universe, but become much more common (factor of $\sim$ 1000) at high-redshift. Evidence for this first came from the identification of the so-called sub-mm galaxies (SMGs) (Smail et al. 1997; Hughes et al. 1998), and was subsequently confirmed with *Spitzer* (e.g. Le Floc'h et al. 2005; Pérez-González et al. 2005; Caputi et al. 2007) and *Herschel* (i.e. Gruppioni et al. 2010; Eales et al. 2010b). *Spitzer* led to **the discovery of thousands of IR-bright galaxies** in the MIR images of various survey fields (Papovich et al. 2004; Rigby et al. 2004; Fadda et al. 2004; Le Floc'h et al. 2004; Houck et al. 2005; Huang et al. 2009), in addition to the **hundreds of submm** (e.g., Smail et al. 1997; Hughes et al. 1998; Barger et al. 1998; Scott et al. 2002; Borys et al. 2003; Webb et al. 2003; Coppin et al. 2006) **and mm galaxies** (e.g., Greve et al. 2004; Laurent et al. 2005; Scott et al. 2008; Perera et al. 2008; Weiß et al. 2009; Austermann et al. 2010) and the **thousands of NIR-band selected high-z objects** (e.g. Caputi et al. 2005; Daddi et al. 2005a; Papovich et al. 2006) that we know today. However, these galaxies **are often thought of or treated as physically disconnected populations**, given the different selection techniques used to find them. **Sampling the peak of their IR SEDs**, and observing new FIR-

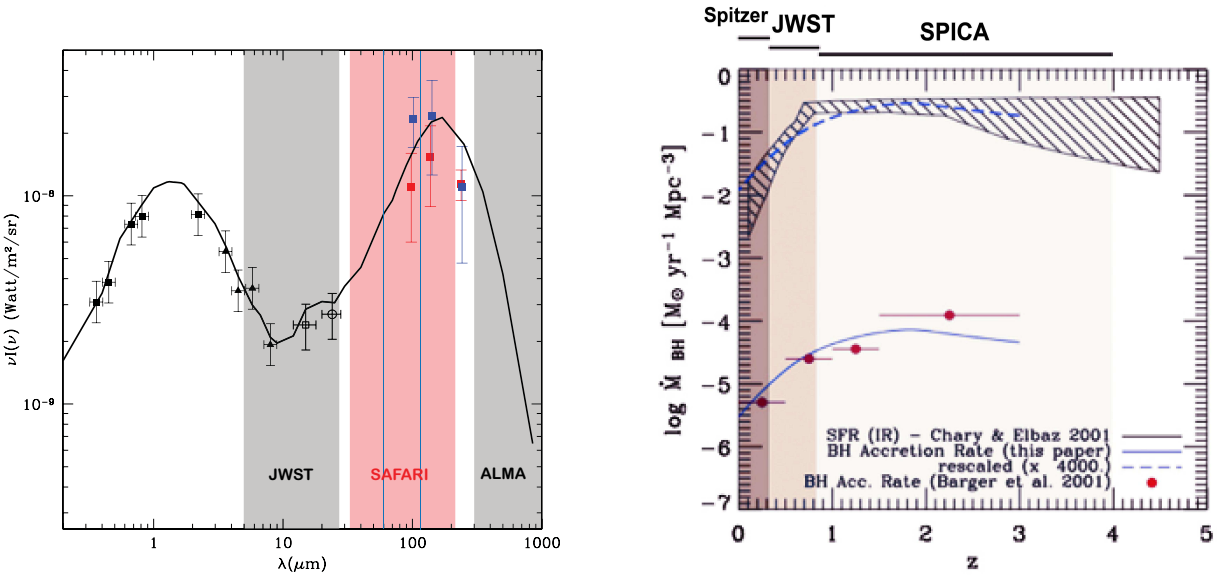

Figure 1.13: ***(a) Left panel****: Constraints placed on the cosmic infrared background (CIRB) by Spitzer show that the mid-/far-IR peak is comparable to the optical peak. The CIRB peak measures the light reprocessed by dust over cosmic time, whilst the COB measures the light directly emitted by stars and unobscured AGN; a significant piece of the integrated light of the Universe is missed if we neglect the IR. The solid line traces the CIRB spectrum predicted by the galaxy evolution model of Franceschini et al. (2010). The data points can also be found in this paper.* ***(b) Right Panel****: A composite plot of the evolution of the star formation rate (SFR) density and black hole accretion rate (BHAR), adapted from Marconi et al. (2004).The BHAR is competed from X-ray data. In color, we show the redshift range for which each IR telescope can provide BH mass estimates using the MIR fine structure lines (see Section 1.6.4).*

selected galaxy samples that bridge IR and submm-selected sources **will enable us to obtain a more coherent picture of high-*z* galaxies.** *Herschel* has certainly contributed to resolving these issues, but its sensitivity only enables the connection to be made for the brightest sources rather than the more typical galaxies which will be studied in detail with *SPICA*-SAFARI.

The integrated luminosity of the (U)LIRG population accounts for the majority of the cosmic infrared background (CIRB, Dole et al. 2006; Devlin et al. 2009; Berta et al. 2010, Berta et al 2011, submitted), the infrared component of the extragalactic background light. Yet this population is insignificant in the optical. Shown in Figure 1.13a is a plot of the extragalactic background light from optical to millimetre wavelengths. The two peaks in the energy density – the peak in the CIRB which includes reprocessed light emitted by dust, and the peak in the optical (the cosmic optical background, COB), which is made up of contributions from stellar processes – are of approximately equal height, **further underscoring the importance of galaxy evolution studies in the IR.**

Locally, the galaxies with IR luminosities exceeding 10^{12} $L_{\odot}$ are predominantly associated with mergers of comparable mass spirals instead (Dasyra et al. 2006). **At high *z*, high IR luminosities can be achieved both via galaxy mergers and accretion of cold gas via cooling flows** (Powell et al. 2011). Recent studies of the global infrared continuum and molecular gas properties of galaxies in the local and high redshift Universe suggest that, independent of resdhift, mergers and non- or weakly-interacting star-forming galaxies follow two separate Kennicutt-Schmidt relations ($\Sigma_{\rm SFR} \propto \Sigma_{\rm H_2}^{N}$), with similar exponents N $\simeq$ 1.1–1.2, but different normalizations (Genzel et al. 2010; Daddi et al. 2010; Graciá-Carpio et al. 2011). **The properties that regulate the two different star formation efficiencies of the gas are not yet understood.** The two modes (merger-driven versus cold-accretion) of star formation could be also identified in the correlation between the star formation rate and the stellar mass of galaxies, found to exist for both local Universe and high-*z* galaxies (e.g. Elbaz et al. 2007; Noeske et al. 2007; Santini et al. 2009). The normalization of this star-formation rate vs stellar mass correlation changes with z. The average specific star formation rate (sSFR=SFR $M_{\star}$) increases by a factor of $\sim$ 20 from $z \sim 0$ to 2.5 (Daddi et al. 2007), revealing a more intense star formation process in the past. It is

unclear whether the sSFR continues to increase between 2.5< z <7 (e.g. Schaerer & de Barros 2010) or not (Stark et al. 2009; Labbé et al. 2010). A constant sSFR for galaxies at $z > 2.5$ poses serious difficulties to current galaxy-formation models that favour baryonic cold accretion as the dominant mode of star formation in the early Universe (Bouché et al. 2010; Dutton et al. 2010; Weinmann et al. 2011), and which are otherwise supported by some observations (Dekel et al. 2009; Bournaud et al. 2011).

Another important discovery of modern astrophysics that has changed our perspective of galaxy evolution is that the naive picture of hierarchical galaxy formation is often inconsistent with observations. This can be summarised using simple key words such as the "downsizing" or "bimodality" of galaxies (Cowie et al. 1996). "Downsizing" evidence has been found, for example, in the assembly of the stellar populations of massive galaxies, which was very efficient at z>2 (e.g., Fontana et al. 2006; Pérez-González et al. 2008; Marchesini et al. 2009), and the production of metals, which also indicates that the most massive galaxies formed early and fast in the history of the Universe (Thomas et al. 2005), i.e., with high SFRs. This contradiction reflects a major limitation of our theoretical framework for the behaviour of baryons within dark matter halos, that only observations of large galaxy samples, beating the effects of cosmic variance, will enable us to address. Probing the range between z~1 and z~4 and analyzing the galaxies with high SFRs at those redshifts is particularly important. In this sense, *Spitzer* and *Herschel* have helped in characterizing ULIRGs at z=2–3, but the bulk of the star formation at these redshifts is thought to take place in LIRGs (Pérez-González et al. 2005; Reddy et al. 2008; Rodighiero et al. 2010), and z=3–4 is still a largely unexplored territory for IR surveys, although we know stellar mass functions evolved significantly at those epochs (Pérez-González et al. 2008; Marchesini et al. 2009).

1.6.2 Major goals of SAFARI

In the framework of galaxy formation and evolution, several key questions remain open when attempting to reconcile observational data with models. SAFARI is designed to help us:

- Provide, for the first time, a complete census of the star formation history of galaxies over the last 90% of the age of the Universe, by measuring dust-obscured star formation down to the limits at which galaxies become optically thin, and redshifted ultra-violet light becomes a robust tracer of star formation.
- Investigate how and when normal, quiescent galaxies such as our own form, and how they are related to (U)LIRGs.
- Address what drives the evolution of the massive, dusty distant galaxy population, and what physical processes are responsible for making the mass (and luminosity) function(s) of galaxies differ considerably from that of dark-matter halos.
- Resolve the individual sources that make up the cosmic infrared background. Herschel-PACS has directly resolved only 58 and 74% of the CIRB at 100 μm-160 μm wavelengths respectively, mostly limited by the confusion, dominating the performance of *Herschel* long-ward of 100μm.
- Unveil the population of heavily obscured active nuclei responsible for the missing half of the cosmic X-ray background (CXB) at its peak around 30 keV.
- Estimate the growth rate of these obscured black holes and derive the history of black hole accretion through cosmic time up to z~4–5.
- For the first time from the IR assess the masses of black holes in obscured systems and create black hole mass functions up to z~4.
- Study the bimodality of star formation at intermediate and high-z, and investigate whether it is accompanied by a similar bimodality of black hole growth.

- Test whether environment or feedback effects can significantly alter the interplay between the AGN and star-formation phases.
- Determine the warm molecular mass content of intermediate and high *z* galaxies, as probed by either H_2 and high-J CO lines and study the origin of its excitation.
- Compare the warm-to-cold H_2 gas fraction in galaxies with redshift, and assess the role of H_2 as a major cooling mechanism for the first galaxies.

In Sections 1.6.3 and 1.6.4 we describe the best observational technique to address the above questions and we describe the specific role of the SAFARI spectrometer. In Sections 1.6.5 and 1.6.6 we further elaborate on specific scientific questions that SAFARI will address through spectroscopic and photometric surveys, respectively. In Section 1.7 we place SPICA/SAFARI in context with the other IR/submm large facilities and, finally, in Section 1.8 we describe goals that will be uniquely achieved by SAFARI.

1.6.3 The observational key: mid-/far-IR imaging spectroscopy

Two key requirements need to be met to address these questions: first, we need access to the mid-/far-IR to overcome the obscuring effects of dust and to fingerprint and track both star formation and AGN activity through cosmic time. Second, we need an imaging capability combined with a spectroscopic capability to undertake the large-scale surveys required to locate and study these dusty sources during their evolution. These two requirements translate into high sensitivity, large instantaneous spectral coverage and spectroscopic imaging capabilities. SPICA provides all of these. In the remainder of this section we demonstrate how these instrumental features will address the science questions posed above.

A wide field imaging capability with broad instantaneous spectral coverage provides the key to surveying large areas of the sky, so tracing, in an unbiased way, galaxy evolution in large numbers of objects. Substantial areas and numbers of objects (several thousands) are even more needed for investigating the evolution of galaxies as a function of environment. By the time SPICA is launched, the deep cosmological surveys undertaken in the past by ISO, AKARI and *Spitzer* and those currently being done with *Herschel* (e.g. Berta et al. 2010; Gruppioni et al. 2010; Eales et al. 2010b; Clements et al. 2010; Oliver et al. 2010; Vaccari et al. 2010) will have produced catalogues containing the fluxes of many tens of thousands of faint MIR/FIR/submm sources. Photometric surveys can be used to determine source counts and to establish the contribution to the extragalactic background of the observed populations at the given wavelength. However, to derive source luminosities, a reliable estimate of the source redshift is required, and this is most reliably obtained from spectral lines. IR-selection of AGN is a powerful way to identify heavily obscured nuclei missed in even the deepest X-ray surveys (Lacy et al. 2004; Stern et al. 2005; Alonso-Herrero et al. 2006; Donley et al. 2007, 2008). However, photometric data alone do not allow us to unambiguously differentiate between AGN and star formation activity. Moreover, IR-selected AGN candidates still require spectroscopic confirmation; as seen in the *Spitzer* FLS survey (Lacy et al. 2004) the simple mid-IR colour criteria used for the *Spitzer* IRAC Shallow Survey select over 90% of the spectroscopically identified type 1 AGN, but only 40% of the more numerous type 2 AGN (Stern et al. 2005).

Substantial progress in studying galaxy evolution therefore can only be achieved by using direct **mid- to far-IR spectroscopic surveys,** which will provide measured (rather than estimated) redshifts and also unambiguously **characterise the detected sources**, by measuring the AGN and starburst contributions to their bolometric luminosities over a wide range of cosmological epochs. The essential difference between the photometric surveys that *Herschel* is performing and those that could be tackled by the SAFARI far-IR imaging spectrometer is the capability of obtaining *unbiased spectroscopic data* **in a rest-frame spectral range that has been shown** *in the local Universe to be highly unaffected by extinction and* **to contain strong unambiguous signatures of both AGN emission and star formation**.

Hot and young stars and black hole accretion discs show strong differences in the shape of their primary ionising continuum. However the far-UV continuum, dominating the total bolometric output luminosity in both processes, is in general not observable directly, due to absorption by HI and, at longer wavelengths, by dust. In

both stabursts and AGN a fraction (10-20%) of the ionising continuum is absorbed by gas and then re-radiated as line emission. Detecting the exact fraction of the ionising radiation absorbed by the gas surrounding the powering sources is in fact not as efficient for probing the energy production mechanism as using emission line ratios: it is the emission lines from the photoionised gas that are the best tracers and discriminators of accretion and star formation processes (see, e.g., Osterbrock & Ferland 2006). In order to overcome heavy extinction, emission lines in the mid- to far-IR should be used to probe obscured regions. Mid-/far-IR imaging spectroscopy is therefore able to track galaxy evolution throughout cosmic times in an unbiased way by minimizing dust extinction.

The rest-frame mid-IR waveband contains several emission lines and spectral features (Figure 1.14a) which measure the contributions from AGN and star formation to the overall energy budget. These features do not suffer the heavy extinction that affects the UV, optical and even the near-IR lines, and therefore provide an almost unique insight into highly obscured regions (Spinoglio & Malkan 1992). ISO demonstrated that the ratios of emission lines tracing the hard UV field found in the narrow line region of AGN (e.g., [Ne v], [O iv], [Ne vi]) to those tracing stellar HII regions (e.g., [S iii], [Ne ii]) versus the strength of the PAH emission features – indicators of star formation – define a diagram which separates star-forming from AGN-dominated galaxies (e.g., Genzel et al. 1998, Figure 1.15a). *Spitzer* observations have further extended these results (Armus et al. 2007; Smith et al. 2007; Tommasin et al. 2008, 2010). They have further enabled the calibration of the (luminosity-corrected) line widths to the masses of black holes (, Dasyra et al. 2011, ApJ, submitted, Figure 1.15c) and the calibration of the bolometric infrared luminosity to the luminosities of lines that can be used as star-formation tracers, e.g., the [Ne ii]12.8μm, [S iii]34μm, and [Si ii]35μm lines, several PAH features (e.g., 7.7μm, 8.6μm, 11.25μm) and the H_2 pure rotational lines (Wu et al. 2010, Spinoglio et al. 2011, ApJ submitted).

Pioneering spectroscopy of a handful of nearby star-forming galaxies and AGN with ISO-LWS (Fischer et al. 1999; Braine & Hughes 1999) has demonstrated the importance and diagnostic power of the rest-frame far-IR. Shown in Figure 1.14b are ten different spectra that have been observed: from strong atomic/ionic fine-structure line emission originated in photon dominated regions (PDR) and HII regions, to spectra showing strong molecular and even atomic absorption lines. ISO observations show, for example, that far-IR fine structure lines (e.g. the line ratio diagram of [C ii]/[O i] vs. [O iii]/[O i]) can be used to separate starburst and AGN (Spinoglio et al. 2003). It has been seen in Arp220, Mrk231 and NGC1068 that molecular emission lines can be used to probe the spatial extent and the geometry of the far-IR continuum in the centres of galaxies (González-Alfonso et al. 2004, 2008; Spinoglio et al. 2005). The high excitation lines of OH and H_2O provide constraints on dust opacity models. Within this context, recently PACS spectra have shown that blueshifted OH and H_2O absorption lines can reveal massive molecular outflows, likely tracing AGN feedback onto the host galaxy (Fischer et al. 2010). High-J lines of CO can be used to detect the XDR in the circumnuclear region of AGN, as recently shown by Herschel (van der Werf et al. 2010); these can trace the physical conditions of the molecular gas in the circum-nuclear region. *Herschel*-PACS is observing 55-210μm spectra of a few local galaxies and confirm the diagnostic power of the far-IR molecular and atomic lines, thus locally calibrating the future SPICA observations of distant galaxies.

1.6.4 The role of SPICA-SAFARI

The SAFARI instrument onboard SPICA will survey the Universe in a most efficient way for studies of galaxy formation and evolution with a 3.2m class telescope in space. **With its broad instantaneous spectral coverage and high sensitivity, it will cover the 34 – 210 μm band in a few thousandths of the time that *Herschel*-PACS takes to obtain a deep spectrum of comparable resolution.** SAFARI will detect key mid- and far-IR lines from distant galaxies and use the mid-/far-IR diagnostics that have been revealed and calibrated by *Spitzer* and *Herschel* in the local Universe. At a redshift of $z \sim 1$ the rest-frame 11 – 35 μm range, very rich in ionic fine structure lines as well as H_2 rotational lines (see Figure 1.14a,b), moves to 22 – 70 μm (and starts being observable with SAFARI). By $z \sim 2$, it moves out to 33 – 105 μm, which is entirely covered by SAFARI, and it will still be in the SAFARI spectral range out to a $z \sim 6$.

The wide SAFARI FOV of $2' \times 2'$ will make it possible for the first time to collect *blind* spectroscopic surveys (Figure 1.16a), **wide and deep enough to measure the underlying physical processes driving galaxy**

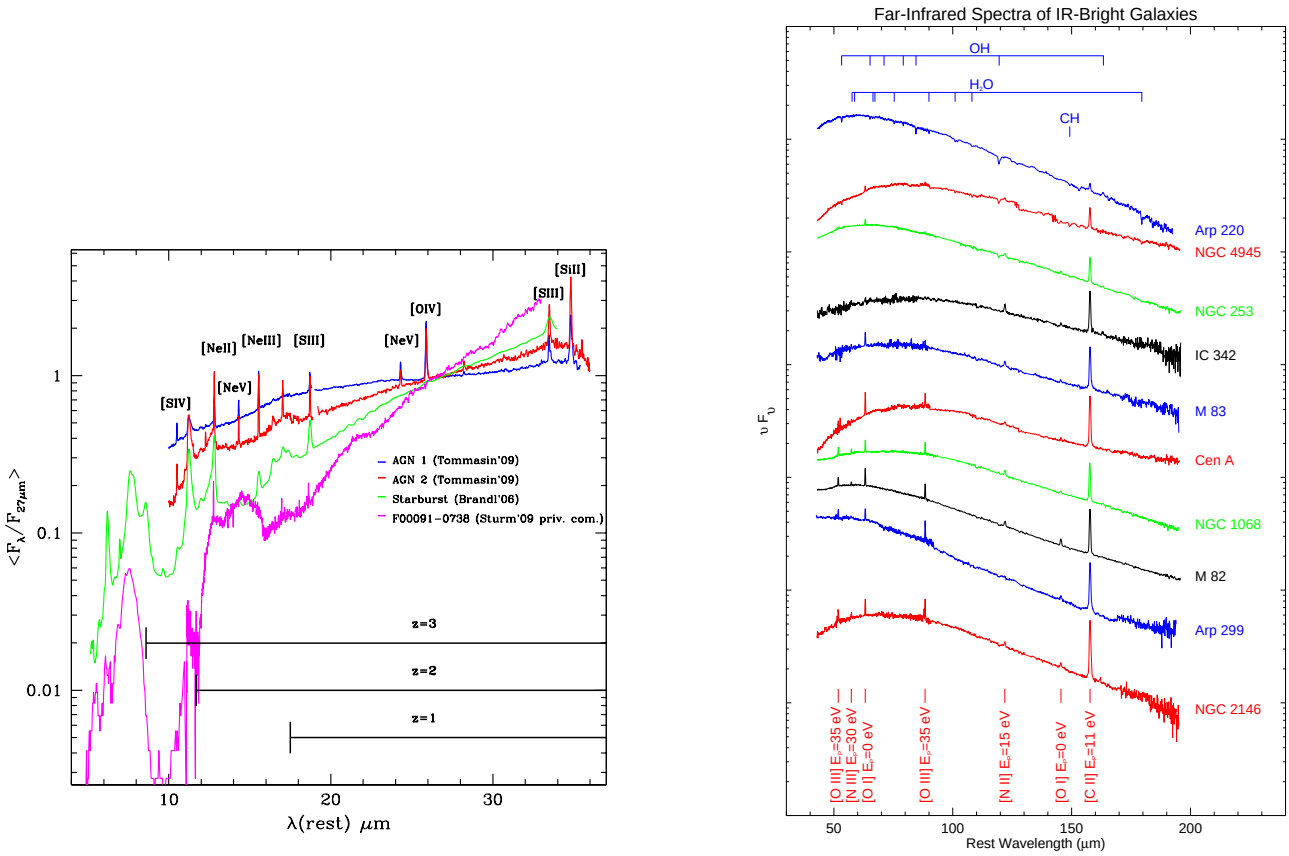

Figure 1.14: ***(a) Left panel****: An illustration of mid-IR spectra, and their lines and features that can be seen in Seyfert type-1/type-2 AGN (Tommasin et al. 2010), a starburst galaxy (Brandl et al. 2006) and a heavily obscured ULIRG (Sturm, priv. comm.). The strongest of these lines will be detectable with SAFARI in a single 1-hr observation. Superposed onto the plot is the fraction of the waveband that will be accessible to SAFARI at* $z \sim 1$, $z \sim 2$ *and* $z \sim 3$*. The spectra have been normalised at* ~ 27 μm*.* ***(b) Right panel****: The full ISO-LWS spectra of ten local galaxies, illustrating the range of emission line strengths observed. The spectra have been offset vertically and plotted as a sequence (bottom-to-top) of increasing obscuration (Fischer et al. 1999).*

evolution out to $z \sim 4$ and, in the most luminous/lensed objects, to even higher redshift. By comparing blind surveys with those targeted around known, high-z objects, we will be able to determine the role of environment on galaxy evolution. We will see in the following sections that SAFARI will detect the brightest mid-IR lines to $z \sim 2$ in *intermediate luminosity* objects in a 1 hour integration (see also Figure 1.16b). This should be compared with Herschel-PACS, which only has the sensitivity to detect the very brightest mid-IR (and far-IR) lines in several hours of integration *per line* on the most luminous objects at $z \sim 1$. Photometrically, SAFARI will have the sensitivity to undertake very deep large-area, confusion-limited surveys at e.g., 70 μm (see Figure **??**), detecting all galaxies with $L_{IR} \geq 10^{11}$ L$_\odot$ at a redshift of $z = 2$, all those with $L_{IR} \geq 5 \times 10^{11}$ L$_\odot$ at a redshift of $z = 3$ and the most luminous IR galaxies ($L_{IR} \geq 10^{12}$ L$_\odot$) out to $z = 4$, as well as the Milky Way-type populations ($L_{IR} \sim 10^{10}$ L$_\odot$) out to $z \sim 1$.

1.6.5 Spectroscopic cosmological surveys with SAFARI

Requirements and predictions

While *Herschel* is spectroscopically identifying only local galaxies and AGN or rare, extremely bright and lensed galaxies at high z (Sturm et al. 2010c; Ivison et al. 2010), the spectroscopic capabilities of SAFARI will allow us to perform, for the first time and in a very efficient way, deep spectroscopic surveys up to high redshifts (z~4).

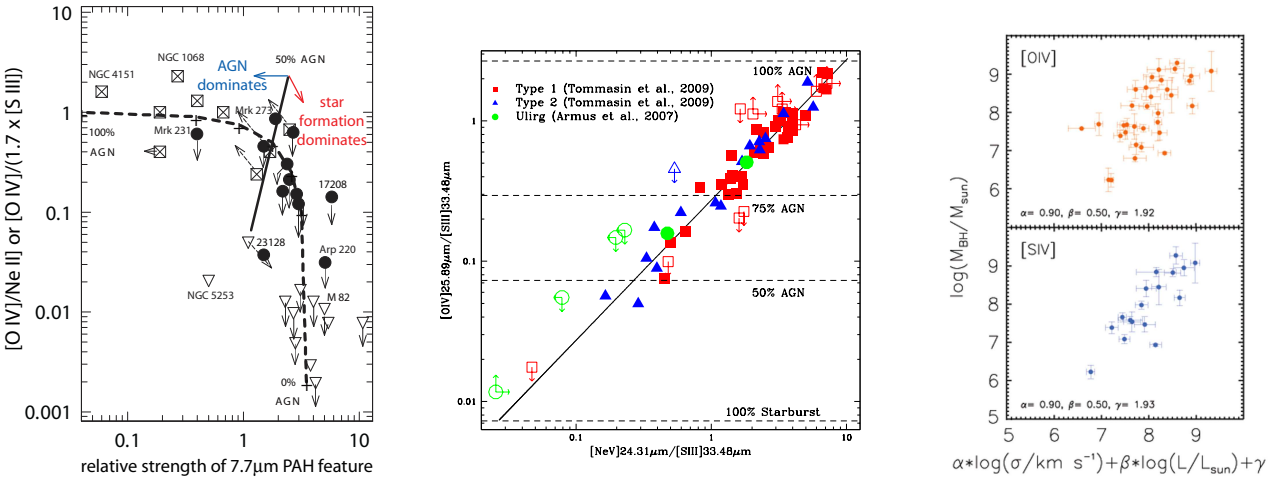

Figure 1.15: ***(a) Left panel****: An example of how the combination of mid-IR line/feature emission can be used to determine the relative importance of AGN- and starburst-activity in IR-luminous galaxies in the local Universe (Genzel et al. 1998).* ***(b) Middle panel****: Line ratio diagram of [OIV]26μm/[SIII]33.5μm vs [NeV]24.3μm/[SIII]33.5μm for local Seyfert and ULIRGs. Data for the Seyfert galaxies are from Tommasin et al. (2008, 2010) and for the ULIRGs from Armus et al. (2007). Open symbols represent upper or lower limits. This diagram is able to quantify the percentage of AGN and starburst emission in the mid-IR continuum luminosity (Tommasin et al. 2010), as can be seen from the horizontal dashed lines.* ***(c) Right panel****: Calibration of the luminosity-corrected velocity dispersions of MIR fine-structure lines to the known black-hole masses in local AGNs (Dasyra et al. 2011, ApJ, submitted). A similar calibration has also been presented for [NeV].*

To demonstrate that high redshift galaxies can indeed be detected with SAFARI, we have predicted the line intensities as a function of redshift (in the range z=0.1–5) for local galaxies evolved back in cosmic time. We have chosen three local template objects with measured mid- and far-IR spectra: NGC1068, the prototypical Seyfert 2, a Hidden Broad Line Region (HBLR) galaxy containing both an AGN and a strong starburst; NGC6240, a bright starburst with an obscured AGN (Iwasawa & Comastri 1998); and M82, the prototypical starburst galaxy. The infrared line intensities have been taken from Alexander et al. (2000) and Spinoglio et al. (2005) for NGC1068, Lutz et al. (2003) for NGC6240 and Förster Schreiber et al. (2001) and Colbert et al. (1999) for M82. To predict the line intensities as a function of redshift, we assumed that they scale with the bolometric luminosity, adopting a luminosity evolution of the form $L_\nu \propto (z+1)^2$, consistent with the *Spitzer* results at least up to redshift z=2 (Pérez-González et al. 2005). Figure 1.16b shows the predicted intensities of a selection of fine-structure emission lines that trace AGN, stellar ionisation and PDR regimes. These have been plotted as a function of redshift for the three templates. It is clear from the figure that the *Herschel*-PACS spectrometer will be able to observe only the brightest object (NGC6240) up to $z \sim 2$ in the brightest line ([O I]63μm). In contrast, the SAFARI *goal* sensitivity (5σ-1hr of $2-4\times10^{-19}$ W m^{-2}, depending on λ, at $R \sim 2000$) will enable us to detect, simultaneously – *in a single observation* – tracers of both AGN and star formation activity and to determine redshifts even in low luminosity objects out to $z \sim 1-2$ for most lines, and even higher redshifts for the brightest lines. Line diagnostic diagrams, such as the one shown in Figure 1.15a (using the [O IV]25.9μm, [Ne V]24.3μm and [S III]33.5μm lines) can readily separate AGN-dominated and starburst-dominated galaxies. Critically, these redshifted mid-IR lines *all fall* into the SAFARI waveband at redshifts of $z \geq 0.4$.

With the aim of demonstrating the feasibility of large-scale spectroscopic cosmological surveys in the far-IR with SAFARI, we have estimated the number of galaxies at different redshifts that can be detected in one single field of view of $2' \times 2'$ (Spinoglio et al 2011, ApJ, submitted). To do this, we used the following method: we identified the best available star formation and AGN activity spectroscopic tracers in the rest frame mid- to far-IR. We have computed the correlations between the line and the continuum far-IR luminosity using samples of galaxies in the Local Universe for which we have reliable and complete spectroscopic mid- to far-IR data; we have used three different galaxy evolution models linked to the galaxy counts and luminosity functions observed in the various IR bands by the latest and current missions (*Spitzer*, AKARI and *Herschel*) to predict the total

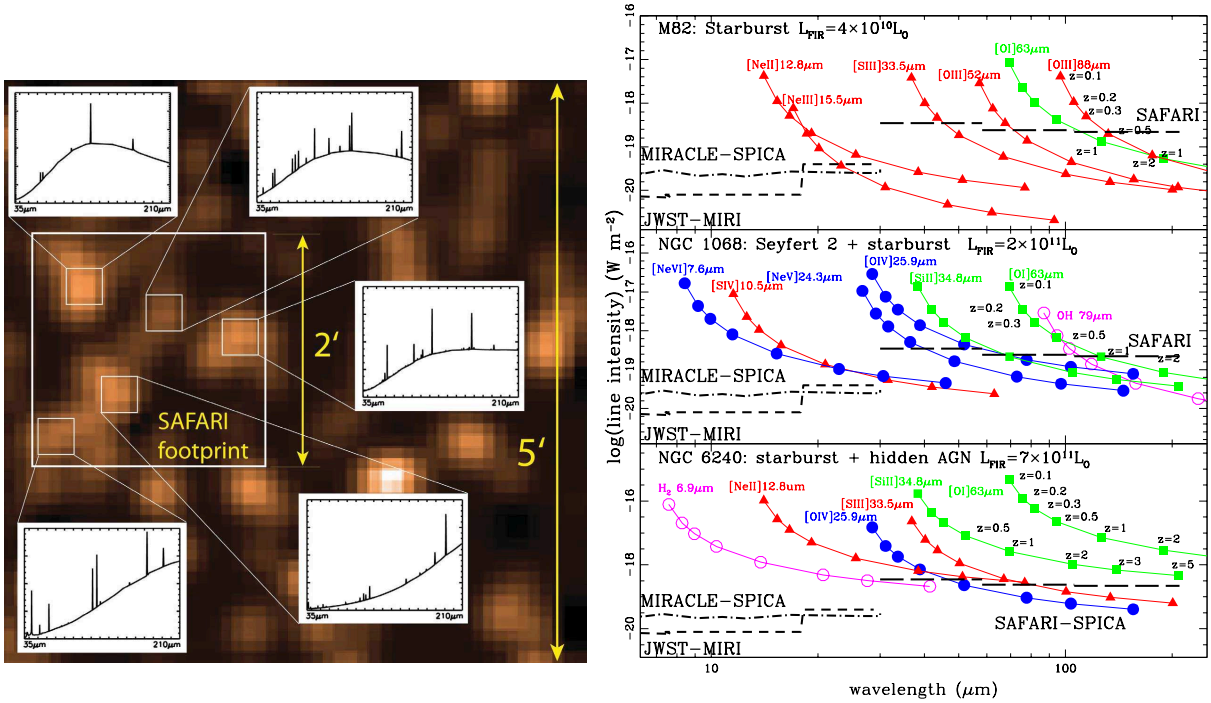

Figure 1.16: ***(a) Left panel****: A 5′ × 5′ region taken from an off-source part of a 250 μm ESA SPIRE publicity image, with the 2′ × 2′ FOV of SAFARI outlined (credit: ESA and the SPIRE consortium). With its spectral imaging capability, SAFARI will be able to obtain spectral information covering the full 34 – 210 μm range, in multiple sources, simultaneously – in a single pointing;* ***(b) Right panel****: Line predictions and their observability with SPICA. A few selected diagnostic lines are shown as a function of redshift for the three template objects M82, NGC1068 and NGC6240 (from top to bottom). Luminosity evolution of the form $L_\nu \propto (z+1)^2$ has been assumed. Line intensities are given in W m^{-2}. The long dashed lines give the 5σ, 1 hour sensitivities of SPICA-SAFARI. For comparison, the expected sensitivities of the SPICA-MIRACLE and MIRI spectrometers are indicated with dash-dotted lined and short dashed lines.*

far-IR luminosity functions up to z∼4. Finally, we have transformed the continuum luminosity functions (in the range of z=0–4) into line luminosity functions for the chosen spectroscopic tracers. Given the sensitivity and the field of view of the SAFARI spectrometer, we were able to derive the number of sources detectable in each infrared line as a function of redshift. Considering an effective diameter of the SPICA telescope of $D_{tel} = 3.0$ m and an NEP of 2×10^{-19}W/ $\sqrt{\text{Hz}}$ for the SAFARI detectors, the 5 σ, 1 hour detection limits for an unresolved line at R ∼ 2000 are predicted to be: 4.16, 2.58, 1.89 and 2.48 $\times 10^{-19}$Wm^{-2} for the four planned spectral bands centred at 48, 85, 135 and 160μm, respectively.

Three different and independent galaxy evolution models (Gruppioni et al 2011, MNRAS, in press, Franceschini et al. 2010; Valiante et al. 2009) predict about 6–12 sources (depending on the model) to be spectroscopically detected in more than one line at a 5σ level in a 2′ × 2′ SAFARI field of view, at redshifts reaching $z \simeq 3$ (Spinoglio et al 2011, ApJ, submitted). These estimates confirm that in a deep SAFARI survey of 450 hours covering 0.5 deg^2 (1800 arcmin^2), with 1 hour integration per field of view, we will detect thousand of sources in the key mid-/far-IR tracers that will identify the energy sources powering the detected galaxies. We report in Table 1.1 the number of sources detectable in such a survey in the infrared lines and features. The brightest lines for any model are those mainly excited in starburst galaxies, namely [OI]63μm and [SiII]35μm. However the [OIII]88μm line is also bright, followed by the [OIV]26μm line, which are typical of AGN dominated galaxies, while being contaminated by HII region emission. On the other hand, the [NeV] lines, which are exclusively produced in AGN, are relatively weaker. To detect them at high-z, deep surveys will be needed. An analysis of the results of Table 1.1 shows that 1800–3150 sources can be detected simultaneously in four lines at 5σ, depending on the adopted model. This number increases to 2250–3600 and 2700–5400 sources in three and two lines, respectively. If we allow 3σ detections, the number of detected sources increases by a factor two on average.

Table 1.1: **Simulated spectroscopic survey: number of galaxies detectable in a 0.5 deg^2 survey in mid- and far-IR lines and features at 5σ (3σ) in a total observing time of 450 hr**

#	Line/Model	Gruppioni et al (2011)	Franceschini et al (2010)	Valiante et al (2009)
1.	PAH(11.25μm)	170 (375)	715 (1277)	1491 (3747)
2.	[NeII] 12.81 μm	162 (397)	228 (507)	42.3 (201)
3.	[NeV] 14.32 μm	....	60.7 (207)	....
4.	[NeIII] 15.55 μm	121 (245)	113 (423)	179 (507)
5.	[SIII] 18.71 μm	67.0 (152)	55.8 (177)	6.3 (26.5)
6.	[NeV] 24.32 μm	143 (318)	37.8 (177)	....
7.	[OIV] 25.89 μm	638 (1208)	232 (631)	933 (1961)
8.	[SIII] 33.48 μm	850 (2061)	1753 (3307)	1104 (2553)
9.	[SiII] 34.81 μm	2224 (4159)	2713 (4738)	3037 (5836)
10.	[OIII] 51.81 μm	1929 (3962)	2983 (5076)	3883 (8100)
11.	[NIII] 57.32 μm	625 (1461)	567 (1613)	973 (2351)
12.	[OI] 63.18 μm	5422 (8496)	5611 (8905)	8896 (14679)
13.	[OIII] 88.35 μm	3028 (5062)	4274 (6682)	5121 (9490)

We have assumed a redshift-independent relation between line and continuum luminosity: if, however, the lines evolve more strongly with redshift than the continuum, then the number of sources that will be detected by SAFARI in blind surveys would increase significantly, particularly at high redshift.

Science cases

We now present examples of specific science questions that SAFARI will enable us to address.

Querying for the obscured AGN missing from the X-ray background

The combination of IR and X-ray survey data has indicated that the number density of accreting black holes is significantly lower than that of highly star-forming galaxies throughout cosmic history (Marconi et al. 2004; Merloni et al. 2010). This result can pinpoint a missing population of obscured AGN if black holes and galaxies coevolve. Indeed, **the most extreme population of obscured AGN is missed by the deepest current-generation X-ray surveys, even in hard X-ray bands**, as it is composed of Compton-thick sources. For example, the prototype Compton-thick AGN, NGC 1068, would be missed above $z = 0.5$ even in 2 Ms with *Chandra*. The fraction of unidentified AGN responsible for the cosmic X-ray background at 30 keV is substantial (Comastri et al. 1995; Gilli et al. 2001, 2007b,a; Treister et al. 2009). Observations at mid-IR wavelengths often provide the only means to reliably identify such AGN. A key AGN signature at those wavelengths is the emission of fine structure lines from ions of high ionization potential. **The [Ne v]14.3μm line, for example, is a reliable tracer of gas clouds photoionized by an AGN, since it is emitted from an ion of 97 eV**. [Ne v] was detected in NGC6240 (Armus et al. 2006), which has a buried active nucleus as seen by *Chandra* in the X-rays (Komossa et al. 2003) even though its mid-IR continuum resembles those of starburst galaxies. The [O iv]25.89 μm line can also be used for the same purpose, even though a small contribution to its luminosity can come from star-forming complexes. **In addition to a tracer of AGN activity, a tracer of high column density can be used for the efficient identification of obscured AGN in the mid-IR**. This role can be played by **the broad 9.7 μm silicate absorption feature**, typically seen in absorption in type 2 AGN (Shi et al. 2006). Georgantopoulos et al. (2011) found that ~2/3 of the local AGN selected at 12μm that are optically thick (τ>1) at 9.7 μm are Compton thick. *Spitzer* spectroscopic surveys have used this feature to identify sizeable samples of obscured AGN at $z < 3$ (e.g., Weedman et al. 2006; Georgantopoulos et al. 2011). Using the above tracers, SAFARI will characterize AGN and starburst populations at high-z, through mid-IR rest frame spectroscopy.

Accretion history of the Universe and black hole masses in obscured environments

Fine structure lines from ions of high ionization potential can be used not only to reveal previously unknown AGN populations (Goulding & Alexander 2009), but also to quantify various properties of the black holes driving their activity. The luminosities of such lines (e.g., [O IV]) correlate with the AGN X-ray luminosity, indicating that they **are good tracers of the rate of accretion onto the black hole** (Meléndez et al. 2008; Rigby et al. 2009). Althought the [O IV] emission line is also detected in a large number of star-forming galaxies, it is only when the AGN bolometric contribution is below 5% that star-formation activity would dominate the [O IV] emission (Pereira-Santaella et al. 2010). The construction of luminosity functions from such high ionization lines (Tommasin et al. 2010) can be used as a means of studying the accretion rate history of the Universe that is an alternative to X-rays. **The widths of the same lines** depend on the kinematics of the clouds that they probe, determined by either the gravitational potential out to a radius that the AGN luminosity dictates, or by AGN feedback effects. They **can be used to weigh the masses of black holes** (Dasyra et al. 2008, 2011, ApJ, submitted, Figure 1.15), permitting the creation of black hole mass functions that include obscured AGN with SAFARI **out to redshift of 4 using the [O IV] 25.89μm line**.

AGN feedback: outflows of molecular gas in warm and cold phases

Mass outflows driven by stars and active galactic nuclei are a key element in many current models of galaxy evolution. They may produce the observed black hole-galaxy mass relation and regulate and quench both star formation in the host galaxy and black hole accretion ("negative mechanical feedback"; e.g. Veilleux et al. 2005, for a review). This would create a population of red gas-poor ellipticals, thereby explaining the bimodal colour distribution observed in large galaxy surveys (e.g., Kauffmann et al. 2003). **Finding observational evidence of such feedback processes in action is one of the main challenges of current extragalactic astronomy**. The first systematic and conclusive evidence **for outflows of** *molecular* **gas, i.e. the gas component from which stars are formed**, has recently been found with the *Herschel* PACS spectrometer. The massive molecular outflows reveal themselves as P Cygni profiles of the far-IR lines of OH and water (Fischer et al. 2010; Sturm et al. 2011). The detection of broad wings in the CO(J=1-0) line (with velocities of several hundreds km/sec), spatially resolved on the kiloparsec scale (Feruglio et al. 2010), confirmed the PACS result for the brightest local ULIRG Mrk231. Moreover, extended wings (of $\pm$ 400km s^{-1}) in multiple molecular lines have been detected with CARMA in NGC 1266 (Alatalo et al. 2011), recently classified as an AGN from optical spectroscopy (Moustakas & Kennicutt 2006), making this galaxy another candidate for AGN feedback. Beside the systematic search of outflows in complete samples of galaxies and AGN through far-IR lines of water and OH, SAFARI will be able to detect asymmetric H_2 line profile wings, characteristic of outflows in AGN. *Spitzer* high-resolution spectroscopic observations have demonstrated the feasibility of such studies, confirming that feedback can significantly affect the H_2 gas in its warm phase (Dasyra et al. 2011b, in preparation). When compared to CO observations, the SAFARI data will allow us to study the the relative role of feedback on gas in the cold vs warm phase.

Molecular content evolution of the Universe

Molecular hydrogen (H_2) is the most abundant molecule in the Universe and plays a fundamental role in many astrophysical contexts (e.g. Dalgarno 2000) It is found in all regions where the shielding of the ultraviolet (UV) photons, responsible for its photo-dissociation, is sufficiently large (i.e. where $A_V \geq 0.01$ mag). **H_2 makes up the bulk of the mass of the dense gas in galaxies and could represent a significant fraction of the total baryonic mass of the Universe**. It is key in our understanding of the interstellar medium. **Its formation on grains initiates the chemistry of the interstellar gas**. Its emission lines provide insight into the conditions of its excitation in photodissociation regions (PDRs), in X-ray dissociation regions (XDRs), or in regions with strong shocks. Lines from other cooling transitions, including those of the HD molecule, are also in the spectral range covered by SAFARI, although these are expected to be weaker than H_2 lines (Mizusawa et al. 2005).

Detection of the pure rotational lines of H_2 will be feasible for various z ranges in deep SAFARI surveys. Based on detections of H_2 in nearby galaxies, we find that the power emitted in the two H_2 lines S(0) (28.2μm)

and S(1) is typically around 20–25% of that found in the mid-IR lines of [Si II] or [S III]. For disc galaxies (Roussel et al. 2007), this corresponds to about 3-3.5×10^{-4} of the total infrared power. Large molecular H_2 reservoirs in high-*z* galaxies are expected because of the correlation found between H_2 and PAH emission in local galaxies (Rigopoulou et al. 2002; Roussel et al. 2007). **To date, H_2 has only been detected in stacked spectra of** $z \sim 1$ **galaxies** (Dasyra et al. 2009). PAHs are ubiquitous in high-*z* galaxies (Valiante et al. 2007; Sajina et al. 2008; Pope et al. 2008; Huang et al. 2009; Dasyra et al. 2009), and if the PAH-H_2 correlation holds at higher redshifts, we could see up to 7 sources per SAFARI field of view in the S(1) line, out to $z < 3$. *Spitzer* observations of distant radio galaxies (Egami et al. 2006; Ogle et al. 2007), have also unveiled a class of objects termed "H_2 luminous galaxies" whose spectra are dominated by H_2 rotational lines. The lack of detection of PAH emission and hydrogen recombination lines, ruling out UV fluorescence as a possible excitation mechanism, indicates that H_2 is produced by shocks which deposit huge amounts of kinetic energy into the ISM. These H_2 luminous galaxies may represent a population at high redshifts where interactions and mergers are more common. Theoretical work (Mizusawa et al. 2005) predicts that in these galaxies the S(1) (17μm), S(2) (12.3μm) and S(3) (9.6μm) should have luminosities in excess of 10^{35} erg s^{-1} and thus within the reach of deep SAFARI surveys. **The role of the H_2 emission as a contributor to the cooling of astrophysical media is even more significant in the Early Universe. The first generation of stars form by the gravitational collapse of primordial clouds** induced by H_2 line cooling (e.g. Saslaw & Zipoy 1967). Therefore, very high-*z* objects should be bright in the mid-IR H_2 lines. We further elaborate on this science case in Section 1.8.

The diagnostic power of the PAHs for studying star formation evolution

The ability of the **UV-excited PAH bands** to **trace star formation** has been demonstrated for local galaxies (Soifer et al. 2002; Peeters et al. 2004). The ratio of the different PAH band fluxes has been related to star formation activity for a wide variety of galaxies (Galliano et al. 2005, 2008), while the ratio of PAH emission strength to the underlying continuum has been used to disentangle star-forming and AGN contributions (Brandl et al. 2006). *Spitzer* IRS spectra (Sajina et al. 2008; Menéndez-Delmestre et al. 2009; Siana et al. 2009; Dasyra et al. 2009; Fadda et al. 2010) to $z > 2$, including sources as faint as $S(24\,\mu\text{m}) \sim 100\,\mu$Jy. The detection of PAHs out to $z \sim 2.5$ suggest similar dust properties, and thus that significant enrichment of the ISM has already taken place by $z \sim 2.5$ (e.g., Swinbank et al. 2004). This result raises questions. When did the bulk of dust production and evolution occur? Was dust mainly provided from AGB stars or also from other sources, such as supernovae or AGN winds (Maiolino 2007)?

Moreover, IRS spectra have shown that **the equivalent widths of PAHs in *z*>1 galaxies can be elevated**, or even unmatched, when compared to those in their local analogues (Rigby et al. 2008; Dasyra et al. 2009). Both *Spitzer* spectra (Farrah et al. 2008; Menéndez-Delmestre et al. 2009) and ground-based submillimetre spectra (Hailey-Dunsheath et al. 2008) have further demonstrated that **the emission from ULIRGs at** $z \sim 1-2$ **is markedly different from that observed in local ULIRGs, instead resembling that seen in lower luminosity starburst galaxies**. This result can be understood if the high-redshift ULIRGs represent vigorous star formation extended over a few kiloparsecs, rather than the sub-kpc bursts that power local ULIRGs, and may be a consequence of the higher gas mass fractions present at these earlier epochs (Tacconi et al. 2010).

The increased sensitivity provided by SAFARI will allow studies to encompass large samples at high redshift. **A wide-field, spectrophotometric survey with SPICA over an area of 1/4 the size of the COSMOS field (0.5 deg^2) would yield spectra of** ~ 5000 **high-*z* galaxies in 500 hours. This is a factor of 10 more than the total number of high-*z* galaxies observed with *Spitzer* IRS, over the whole 5-years mission lifetime** and a significant increase on those that will be observed by JWST.

Metallicity evolution of the Universe

Beside the rest-frame fine-structure mid-IR lines, useful for studying dust enshrouded AGN- and starburst-dominated galaxies, the oxygen lines of [O III]52μm, [O III]88μm and the nitrogen [N III]57μm line can be used to measure the metallicity of the gas in galaxies (Nagao et al. 2011). The importance of low metallicity at high redshift is highlighted in recent studies of gamma ray burst hosts (Chen et al. 2009), Lyman-Break

galaxies (Maiolino et al. 2008) and damped Ly-α systems (Pettini et al. 2003, 2008), which all bear the tell-tale hallmarks of low redshift, low metallicity dwarf galaxies. SAFARI can detect these (nearly reddening free) lines out to z~1.4 even in galaxies with modest SFR (Nagao et al. 2011) and, therefore, will enable us to trace the metallicity evolution of galaxies through the cosmic epochs in an unbiased way.

Spectroscopy of faint galaxy populations through gravitational lensing

The strong gravitational lensing of distant Universe galaxies by intervening galaxy clusters has been exploited at many wavelengths in order to push the luminosities and redshifts out to the farthest limits. In the IR/sub-mm, lensing clusters act as transparent lenses, and cluster surveys at these wavelengths have been particularly powerful at pushing below the confusion limits of sub-mm surveys (e.g., those with SCUBA on JCMT) to constrain the faint end of the source counts (Smail et al. 1997; Blain et al. 1999) and opening up the study of not only some of the most distant objects, but also of those that are less extreme at slightly more modest redshifts (Knudsen et al. 2006).

With *Herschel*, observations of gravitationally lensed galaxies are generating exciting results. In addition to cluster-lensed galaxies (Egami et al. 2010; Rex et al. 2010), galaxy-lensed sources are also playing an important role with *Herschel* because wide-field surveys like *Herschel*-ATLAS (Eales et al. 2010a) is efficient in finding such systems (Negrello et al. 2010). Note that the apparent brightness of these lensed *Herschel* sources are quite high, with peak flux densities above 100mJy, allowing a variety of follow-up observations. Among the gravitationally lensed galaxies studied so far, the most spectacular is the cluster-lensed $z = 2.3$ galaxy discovered through the APEX/LABOCA observations of the cluster MACSJ2135-0201 ($z = 0.3$) Swinbank et al. (2010). This galaxy is so bright (430mJy at 350μm) that even *Herschel*/SPIRE spectroscopy was able to detect the [C II] 158 μm line (Ivison et al. 2010). **With SAFARI, it will become possible to study many more lensed galaxies spectroscopically**, allowing us to probe the physical properties of faint/distant galaxies that are simply beyond our reach without the benefit of lensing amplification.

Clustering and first large scale structures

The source detection estimates presented in previous subsections for spectroscopic surveys assume random Poissonian distributions of galaxies through the various cosmic epochs. However, extragalactic sources are known to be clustered. Significant clustering has been measured in high-redshift (z~ 1-3) *Spitzer* galaxies (Farrah et al. 2006b; Magliocchetti & Brüggen 2007; Magliocchetti et al. 2008; Farrah et al. 2006a), with a strength which increases with redshift, as might be expected. Comparisons with theoretical models have provided a direct estimate of the dark matter mass of such sources, and the derived values ($M \sim 10^{13}$ M$_\odot$) indicate that luminous-IR galaxies at $z \sim 2$ are most likely the progenitors of the giant ellipticals which reside locally in rich clusters. This implies that studies of the infrared population at redshifts z>1-1.5 can provide a unique tool with which to investigate the formation and evolution of super-structures such as proto-clusters, clusters and of the galaxies that belong to them, from even before the peak time of cosmic star formation activity. While the results from *Spitzer* necessarily suffered from limitations due primarily to the lack of measured redshifts, SAFARI in its spectroscopic photometric mode will, for the first time, be able to overcome such problems and provide definite answers to a number of crucial issues:

(i) Direct and unbiased investigation of the evolution of the Large Scale Structure in the Universe from z ~ 3. Thanks to the SAFARI's capabilities, no previous selection on the observed population is needed, as redshifts will be taken for all the objects brighter than the limiting flux which fall in the SAFARI FoV . With our goal 5σ sensitivity, such a task could be easily reached in about 500 hours by "blindly" surveying an area of approximately 0.5 deg^2, which will deliver the redshifts of thousands of sources out to z~3. With such large statistics it will be possible to derive the three-dimensional clustering out to z~3, hence deliver precious cosmological information on the evolution of cosmic structures, that so far could only be achieved up to z~1 through optical massive spectroscopic surveys.

(ii) Studies of galaxy formation and evolution as a function of environment. Since high-redshift sources exhibit strong clustering, galaxies observed by SAFARI in a blind spectroscopic survey will either reside in

overdense or underdense regions. This will give us the unprecedented possibility of investigating the impact of environment on galaxy formation and evolution as a function of redshift up – and possibly beyond – the epoch which marks the bulk of AGN/stellar activity. By doing this, it will be possible to provide answers to a number of questions, such as whether there is any large-scale influence between surrounding environment and galactic AGN/stellar activity and, if so, if seeds for such a phenomenon were already in place by $z \sim 2-3$. This study needs the spectroscopic redshifts of several thousands galaxies to be properly addressed. The spectroscopic diagnostics will be essential to *measure* directly the star formation and AGN luminosities in each cluster component.

(iii) Targeted studies of Proto-clusters. As discussed above, most of high-redshift active galaxies reside in overdense regions or what we call proto-clusters. This was seen by *Spitzer* and in a number of other works which report the discovery of $z \sim 2-3$ proto-cluster candidates in the NIR and for instance via the concentration of Lyman Break galaxies around powerful radio sources. With the imaging capabilities of SAFARI it will be possible for the first time to collect a large sample of high redshift proto-clusters in a relatively short time. When targeting regions centred on "known" high-redshift sources, we expect the number of sources detectable per SAFARI field to be boosted by as much as *a factor 10* above the predictions presented earlier in this section.

Beating spatial confusion

The third, spectral dimension offered by spectroscopic surveys provides us with a way to overcome confusion even in the deepest explored fields. Narrow-band line emission from a source at a given redshift appears only at very specific and discrete wavelengths, and so the high density of sources in an individual beam that causes confusion is drastically reduced relative to all sources emitting in the continuum (Figure 1.17). This enables individual objects, whose continuum may be substantially below the continuum confusion limit, to be detected. Through simulations (Clements et al. 2007; Raymond et al. 2009) we have found that **sources more than 10 times below the traditional (photometric) confusion limit at, for example, 120 μm can be isolated** and detected. In this way, the majority of sources that contribute significantly to the CIRB can be detected and classified spectroscopically, as described above. Targetting galaxy clusters known to be strong gravitational lenses allows one to further reduce the confusion limit, as e.g. demonstrated by recent *Herschel* observations (Egami et al. 2010). Powerful techniques are being developed to extract sources down to the faintest flux levels in confused images from *Herschel* (e.g. Roseboom et al. 2010) – the approach of using higher resolution images at shorter wavelength as positional "priors" can be used in combination with SAFARI's spectral cubes to push to even fainter limits.

1.6.6 Deep photometric imaging surveys with SAFARI

Requirements and predictions

The existence of a large number of distant sources radiating most of their energy in the IR implies that the critical phases of the star-formation and nuclear accretion history **took place in heavily obscured systems**, embedded within large amounts of gas and dust. The substantial reddening affecting these dust-obscured objects makes their characterisation in the optical/UV severely biased and sometimes even impossible. Observations in the FIR/sub-mm to very faint flux densities (few $\times$ 10μJy) are often the only means to detect star-formation and/or AGN activity in most of these heavily obscured sources at large cosmological distances. Indeed, a significant fraction of the star-forming galaxies dominating the SFR density of the Universe at z=1–4, when most of the stellar populations in the most massive galaxies were being assembled (Fontana et al. 2006; Pérez-González et al. 2008; Marchesini et al. 2009), are very faint in the UV/optical (Pérez-González et al. 2005), and their SFRs **can only be measured through mid-/far-IR observations reaching fluxes well below 1 mJy** (see Figure 1.18).

The major observational limitation for imaging observations of galaxies in the far-IR is the confusion limit. Due to large beam sizes and high projected source densities, the very same galaxies we wish to study in the far infrared make the Universe opaque. To overcome, at least partially, this source of blindness – i.e., the

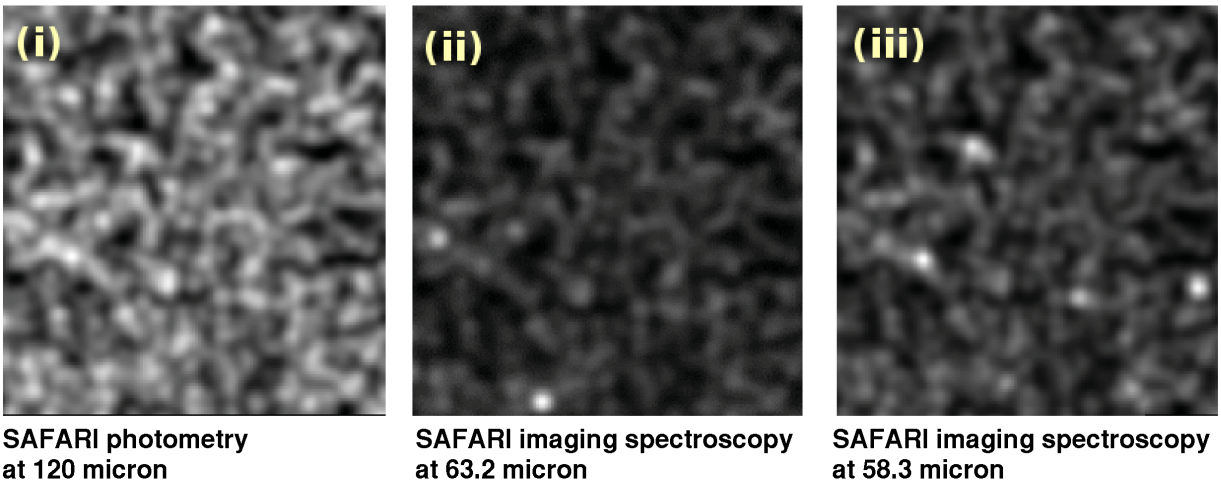

Figure 1.17: Deep, spectroscopic surveys with SAFARI will enable us to break through the confusion limit and characterise individual galaxies, otherwise indistinguishable. Shown in panel (i) is an image of a single SAFARI FoV, in photometric mode at 120 μm, at a spatial resolution of 9″: no discrete sources can be distinguished against the background; shown in the panels (ii) and (iii) are the same FOVs centred at 63.2 and 58.3 μm respectively with a spectral resolution of $R \sim 1000$, at the same angular resolution: several sources can be seen in each narrow band. In other words the spectral data cube need not be confused, even if the collapsed image is. A combination of prior-based source finding and template SED fitting should enable SAFARI to resolve almost the entire CIRB, determining the type and redshifts of galaxies which make it up.

projected overlapping of galaxies – the design of SPICA has been chosen to reach shorter wavelengths with respect to *Herschel* and to have imaging spectroscopy capability in survey mode. *Herschel*, as a comparison to SPICA, is limited by confusion in five of its six broadband filters, i.e., above 100 μm, and has actually resolved ~60% – 75% of the cosmic infrared background (CIRB) directly measured by COBE/DIRBE at 100 and 160 μm respectively (Berta et al. 2010, Berta et al. 2011 A&A submitted).

Similarly to *Herschel*, SPICA will have a 3.2m telescope. In Figure 1.19a we show the detection limit versus wavelength at which a 3.2m aperture becomes limited by confusion between sources and the amount of the observable Universe that will be resolved at each wavelength. It appears clearly that: (1) 70 μm is the optimal wavelength at which to observe the extragalactic background with a 3.2 m telescope; and (2) *Herschel* will never reach the confusion limit at this wavelength, while SPICA will reach it easily. Specifically, SAFARI will be able to resolve the bulk (>90%) of the cosmological background over a wide wavelength interval from $\sim$ 30 to $\sim$ 100 μm, identifying also high-z contributors. In this sense, SAFARI will complement *Spitzer*/MIPS observations at 24 μm, which were able to resolve more than 80% of the CIB (Dole et al. 2006). Most of these galaxies detected in the mid-IR fell below the detection limits of PACS in the far-IR (see Figure 1.18), reflecting into large uncertainties in the derived SFRs for the LIRG galaxy population that dominates the star formation activity of the Universe in the key redshift range between z~1 and z~4. SAFARI surveys will add data for these galaxies, allowing a better characterization of their SEDs and derived properties. **The joint imaging and spectroscopic information will in fact allow SAFARI to go well beyond the confusion limit even at longer wavelengths, since even for sources whose PSF overlaps on the sky, their emission lines are clearly separated in wavelength.**

Science cases

Deep surveys at short wavelengths – Broadband footprints of distant, obscured AGN

The surveys with SAFARI at 40 μm will not be confusion limited (estimated confusion limit < 10 μJy.) A survey at 40 μm down to a limit of a few 10s of μJy would be sensitive to moderate luminosity ($L_{\rm IR} \sim 10^{11}$ L$_\odot$) type-2/obscured AGN out to $z \sim 5$, and particularly in the $3 \leq z \leq 5$ range, where the co-evolution of star-formation and accretion activity is expected to already be in place. It will also be sensitive to Seyfert-like AGN

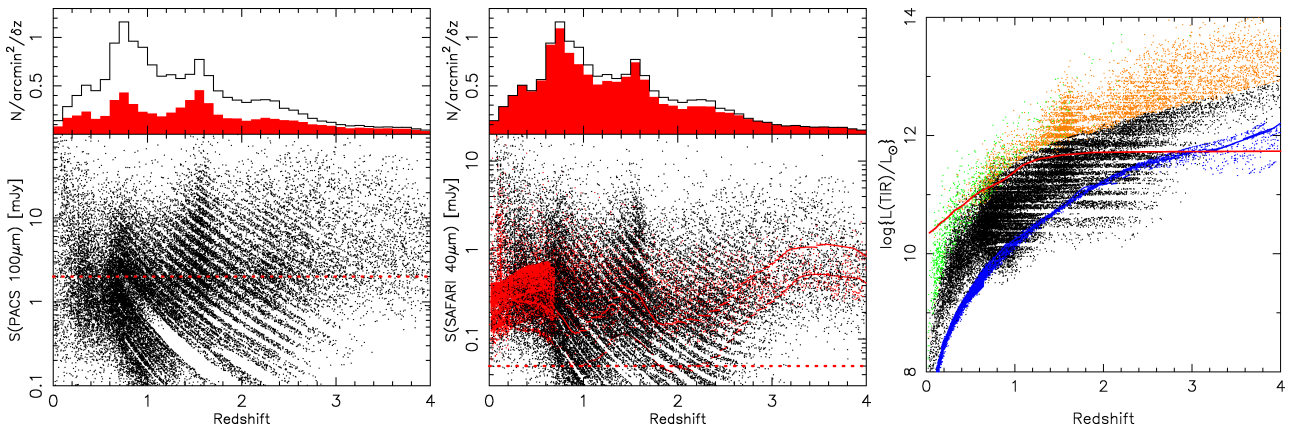

Figure 1.18: Comparison of the galaxy populations detected by Spitzer/MIPS at 24μm, and probed by Herschel/PACS and SAFARI (Pérez-González et al. 2008; Barro et al. 2011). Redshift distributions of the MIPS sample (black histograms) and intersecting galaxy populations (MIPS+PACS, MIPS+SAFARI, filled red histograms) are also shown. ***(a) Left panel****: Predicted fluxes in the PACS band at 100 μm for the galaxies detected at 24μm in the deepest Spitzer Cosmological fields (GOODS, EGS, SpUDS, and Lockman). The PACS 5-σ sensitivity limit is shown with a horizontal red line.* ***(b) Middle panel****: The same for the SAFARI 40 μm band. The red points represent MIPS and PACS undetected galaxies. Assuming upper limits for their MIPS fluxes, they lie well within the sensitivity limits of SAFARI, opening a new window to characterize z>3 sources, an important epoch in the formation of massive galaxies.* ***(c) Right panel****: IR luminosities of the sources detected by MIPS (all of them also detected by SAFARI) and those MIPS sources detected by PACS (color points). Orange points depict sources fainter than the typical optical spectroscopic limit I>25, i.e., sources for which the photometric redshift from IR data would be very useful. The combination of MIPS and SAFARI would allow the robust characterization of LIRGs at z=1–3, a population missed by Herschel. SAFARI will be our only means to systematically probe the LIRG region at z>3 (blue points, showing estimations for sources detected just by SAFARI). The red line traces the redshift evolution of an L_* galaxy.*

at $z\sim1$. The most heavily dust-obscured, Compton-thick sources among them are believed to be responsible for the unresolved peak of the X-ray background at 30 keV (Gilli et al. 2007a; Treister et al. 2009). **These AGN are missed by the deepest current X-rays surveys** (the propotype Compton-thick AGN NGC 1068 would be missed above $z = 0.5$ even in 2 Ms with Chandra), **yet reveal themselves in the mid-IR** thanks to the warm emission from the circum-nuclear dust (i.e. torus) around the central accretion disk source (Netzer et al. 2007; Mor et al. 2009; Pozzi et al. 2010; Mullaney et al. 2010). This can lead to an "MIR excess" in cases where the emission from the AGN heated dust significantly adds to the MIR SED of a galaxy. By selecting mid-IR sources with faint NIR and optical emission, Daddi et al. (2007) and Fiore et al. (2008) suggest that several so called "MIR excess" sources in the *Chandra* Deep Field-South can be obscured AGN at $1 \leq z \leq 3$, on the basis of stacking techniques applied to X-ray wavelengths. In Figure 1.19b we demonstrate how the combination of both the 40μm and 70μm bands can be used with models of circum-nuclear dust emission (i.e. Fritz et al. 2006; Hönig & Kishimoto 2010) and star-forming galaxy templates to determine the part of the luminosity originating from accretion onto a black hole.

Deep surveys at long wavelengths – Probing Dusty Galaxy Evolution to $z\sim4$ and resolving the CIRB

The deepest cosmological survey performed by *Herschel*-PACS as part of the PACS Evolutionary Probe – PEP – Survey at 70μm (the best wavelength for deep cosmological surveys with SAFARI, being the right balance between instrument sensitivity and confusion) covers a very small area (GOODS-S) and is limited in flux density to ~1.1 mJy (3σ; Berta et al. 2011). To this limit, only less than 50% of the CIRB is resolved. According to current models, the 70 μm confusion limit for SPICA-SAFARI is around ~100 μJy. To reach such depths with *Herschel*-PACS would take an enormous and unrealistic amount of time (>10,000 hours at 5σ!), **while with SAFARI this can be achieved in minutes.** Using current assumptions for the intensity of the CIRB at this wavelength, a 70 μm confusion-limited survey (Figure 1.18c) would resolve more than 90% of the CIRB over 80% of the Hubble time ($z \sim 2$), detecting galaxies down to a star formation rate regime at which rest-

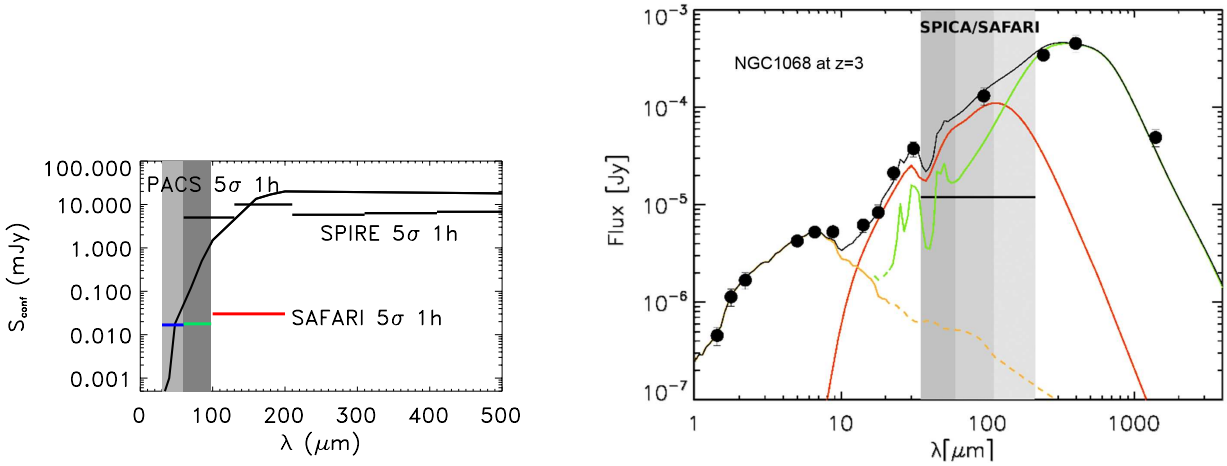

Figure 1.19: ***(a) Left panel****: The confusion limit in the FIR/sub-mm, with the wavelength coverage and sensitivity of selected instruments overlaid. The light and dark grey spectral regions show the 40 and 70 μm cosmological bands, respectively.* ***(b) Right panel****: The broadband SED of NGC1068 (in black) redshifted to z ∼ 3; overlaid are the emission components produced by a torus (red: model by Fritz et al. 2006), a starburst (modeled by the galaxy NGC1482) and a stellar component (orange) based on stellar evolution models. The vertical bars indicate the three bands of SAFARI and show how the combination of 40 μm and 70 μm emission can be used to differentiate between AGN- and starburst-dominated galaxies.*

frame UV observations meet the IR, i.e., 10 $M_\odot$ yr^{-1} (Lagache et al. 2004); note that more luminous galaxies emit the majority of their light in the IR. By observing at 70μm we can avoid the effects of contamination by the strong mid-IR PAH features, and thus make very reliable determinations of the IR flux for sources with $z < 2$, combining the SAFARI data with mid-IR observations at 24 μm (which will enable better k-corrections in the IR). Such a survey would increase significantly the range in IR luminosity and redshift over which galaxies will have been detected: at the more luminous end, LIRGs out to $z \sim 4$ and ULIRGs to beyond, and appreciable numbers of L_* galaxies out to $z \sim 3$. **With SAFARI it will also be possible to detect galaxies as quiescent as our own ($L_{IR} < 10^{10} L_\odot$) out to** $z \sim 1$ where the cosmic SFR peaks (see Figure 1.13b and Figure 1.6.6a). Moreover, it will be possible to go even further (typically to $z \sim 2$) with the help of strong gravitational lensing. Whilst this less IR-luminous population contributes only minimally to the CIRB, these galaxies are extremely abundant, and dominate the extragalactic background light at optical wavelengths. Confusion-limited surveys at 70 μm are unique territory for SAFARI.

A confusion limited survey with SAFARI at 70 μm will be ideal to study the evolution of galaxies and AGN and of the star formation density (SFD) and black hole accretion density (BHAR) with redshift at z>2, where *Spitzer* and *Herschel* were only able to provide hints. In particular, the first Luminosity Function studies performed with the Science Demonstration Phase data of *Herschel* (Gruppioni et al. 2010; Eales et al. 2010b) were limited to $z \simeq 2$ because of sensitivity and/or lack of identification, although some hints about evolution to $z \sim 3$ were derived from PACS data (Gruppioni et al. 2010). With the whole set of cosmological information coming from both PACS and SPIRE from the PEP (Lutz et al. 2011) and HerMES (Oliver et al. 2010) surveys we expect to push deeper into the evolution of dusty galaxies, with much stronger statistics and higher quality catalogues, but we will still be limited to $z \sim$2-3.

In Figure 1.6.6a, we show the SFD and BHAR (multiplied by a factor of 500) that we expect to obtain with IR data from the confusion limited Survey with SAFARI at 70 μm, compared to the predicted SFD and BHAR from the Gruppioni et al. (2011) model, corresponding to an "ideal" far-IR survey covering all the luminosities at all redshifts. For comparison, in Figure **??**b, we show the same simulation with the deepest PEP Survey in the GOODS-S, reaching 1.7mJy at 100 μm (the GOODS-Herschel Survey will reach ∼0.6 mJy, but in only a very small area of 50 $arcmin^2$). As is clear from the figure, PEP is complete in SFD up to $z \sim 1$–1.5, becoming more and more incomplete with increasing redshift (i.e. at z=3 the incompleteness in SFD due to the survey flux limit is about a factor of 3 or more). The BHAR that we could measure with PEP is complete up to $z \sim 1.5$–2,

then decreases less rapidly than the SFD up to z=3 and drops down at higher zs. **With the SAFARI Survey we expect to be able to measure almost all the SFD to z~2 and most of it to z~3–3.5, as well as almost all the BHAR to z~3.** Moreover, as mentioned in the previous Sections, the high resolution spectrometer of SAFARI will be crucial in identifying AGN and separating the SB from the AGN contributions, to measure with great precision the SFD and BHAR in the high redshift Universe.

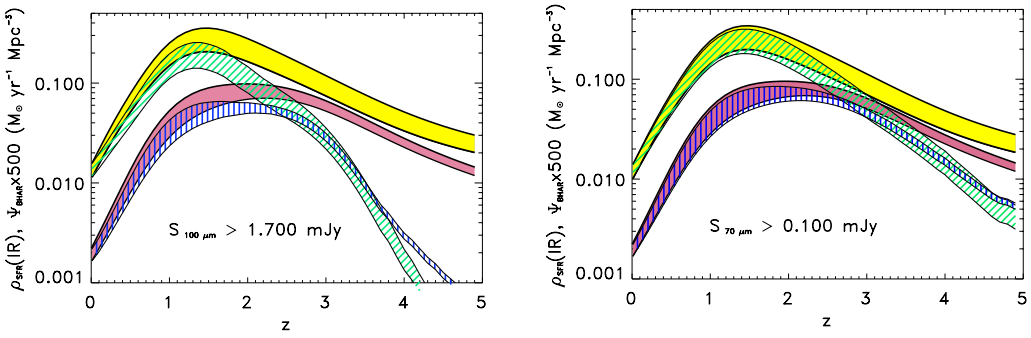

Figure 1.20: ***(a) Left panel:*** *BHAR density, Ψ_{BHAR} (blue vertical-dashed area), and SFD, ρ_{SFR} (green diagonal-dashed area), from IR luminosity as predicted by the Gruppioni et al. (2011) model for the deepest PEP* Herschel *Survey at 100 μm.* ***(b) Right panel:*** *the same estimate for a confusion-limited Survey with SAFARI at 70 μm. In both plots (panels b and c) the Herschel and SAFARI results are compared to the "total" model expectations corresponding to an "ideal" far-IR survey covering all luminosities at all redshifts (yellow area for SFD and pink area for BHAR).*

Photometric redshifts in the MIR/FIR

To date, photometric redshifts of SCUBA and *Spitzer* sources have been determined using optical/NIR data taken with many different surveys. Photometric redshifts have also been estimated for *Herschel* sources using a combination of far-IR and (sub-)mm data (e.g., Pérez-González et al. 2010, , and references therein), showing its usefulness when characterizing (U)LIRGs at high-z which might be tremendously faint in the optical, even undetected (Gonzalez et al. 2009; Negrello et al. 2010; Frayer et al. 2011). This procedure has been demonstrated to help obtain the correct identification of optical/NIR counterparts for far-IR and (sub-)mm sources, which are affected by confusion. **With SPICA we will be able to determine redshifts** using the combination of the NIR, MIR, and FIR. Simulations suggest that with as few as 13 ($R \approx 8$) filters, evenly spaced over the 15 – 70 μm wavelength, it is possible to determine the redshift and type of a very wide range of galaxies, to an accuracy of a few %. By including SAFARI bands we not only extend the redshift range of the technique, but also increase accuracy: with SAFARI bands we sample well the PAH and silicate absorption features, which, in turn, break most of the degeneracy in the MIRACLE-only estimations. Sources for which the match between recovered and true redshift is poor are those lacking distinct PAH/silicate features: in the case of the AGN, these are intrinsically optically bright, and thus good candidates for spectroscopy.

Spectral Energy Distributions: UV vs FIR

Dust plays a dual role in extragalactic studies, simultaneously helping (emission by heated dust) and hindering (obscuration) our understanding of the physical processes driving galaxy evolution. The deep 40 and 70 μm surveys described above will allow us to study the evolution with redshift of the dust attenuation of stellar light in galaxies. Takeuchi et al. (2005) showed that the balance between directly observable (i.e. UV-detected) and obscured (i.e. far-IR-detected) star formation changes from 50/50 at z=0 to 20/80 at z=1. However, it remains unclear how this fraction changes with further increasing redshift. At some point in cosmic history, obscured environments must become less common, since it takes time for dust to be produced and to spread through the ISM of a young galaxy. This question can be addressed with deep IR surveys by directly detecting the dust emission of optically (UV rest-frame) selected samples of galaxies at z>1.

One of the selection techniques available to us to access the high redshift Universe is the Lyman Break method. Lyman Break Galaxies (LBGs) are selected from their ultraviolet (UV) emission, typically found from GALEX observations at 1< z < 2, and ground-based-telescope and HST data at $3 < z < 5$. JWST will very likely provide large samples of LBGs at $z > 6$. However, the UV emission only contributes to part of the LBG luminosity, the rest being emitted in the rest-frame far-IR. **To properly compute the total star-formation rates of these galaxies, and to compare their UV to far-IR luminosity ratio, deep far-IR data are necessary.** *Herschel* and GALEX LBG samples enable us to directly obtain an information on the far-IR emission of the lowest redshift or lensed LBGs, but, even for the deepest extragalactic programmes, the *Herschel* data are still very limited. ALMA will have the sensitivity to detect high redshift LBGs, but large surveys are not feasible with ALMA: not being a survey machine, ALMA will only observe relatively small LBG samples.

Tracing the evolution of Milky Way-type galaxies

Tracing the cosmic evolution of (U)LIRGs is one of the key goals of SAFARI; however, whilst this population makes a very significant contribution to the CIRB, such objects only make up a small fraction of the total number of galaxies. With SAFARI we will have, for the first time, the sensitivity to obtain IR photometric data of the complete $z \sim 1$ population, and so to follow the evolution of the normal, most ubiquitous galaxies out to that redshift. **Our own Milky Way would be easily detectable in the continuum out to $z \sim 1$.** This will help us further address the bimodality in the star-formation efficiency that is related to merger-driven vs cold-flow gas accretion and that is presented in Section 1.6.1.

1.7 SPICA/SAFARI in the ALMA, JWST and E-ELT era

SPICA will be the bridge between three other very large astronomical facilities that are due to become fully operational in the next years - namely ALMA, JWST and E-ELT. The JWST will revolutionise near-IR and mid-IR astronomy through its impressive sensitivity, and ALMA and E-ELT will make a huge impact with their unprecedented sensitivity and high angular resolution in the sub-mm and optical/near-IR respectively. **SPICA/SAFARI will probe the crucial far-IR regime, filling the gap between E-ELT, JWST and ALMA regions at much improved sensitivity and spectroscopy mapping speeds than *Herschel*.**

While ALMA will detect the “cold” interstellar and circumstellar material, E-ELT will detect the “hot” stellar component of the Milky Way and of more distant galaxies. Both ALMA and E-ELT will provide extremely high angular resolution observations of very small fields. These facilities are designed to resolve compact sources (prestellar cores, protostars, protoplanetary disks, stars, etc.) but not to scan large fractions of the sky. Hence, they will not place the observations in the context of the large scale structures where these sources are located (clouds, filaments, stellar clusters, etc.). Most of the energy injected in these extended regions, whether radiative (UV photons and X-rays from nearby stars) or mechanical (shock waves and other dissipative processes) is released as far-IR radiation, either as dust continuum emission or as bright gas cooling lines. SAFARI’s large field-of-view for spectral mapping will be especially well adapted to study the extended gas and dust emission that ALMA, JWST and E-ELT will miss, thus allowing us to capture the “global picture”.

By observing at mid– and far–IR wavelengths, SPICA will cover critical spectral diagnostics (at their rest frame wavelengths) that are complementary to ALMA. While the study of the oxygen chemistry with ALMA, for example, will be limited to observations of CO, HCO^+ and other trace species, SPICA will observe the emission of the major oxygen reservoirs like atomic oxygen, water ice or the thermal emission of water vapour. ALMA will detect the millimetre and sub-mm dust continuum emission, but only SPICA will be able to observe the specific grain and ice spectral features that are needed to determine the dust mineral composition and its formation history along the life-cycle of interstellar matter. ALMA and SPICA will be complementary to address the chemical complexity in the Universe. In particular, SPICA will allow us to observe key organic molecules without permanent electric dipole (*i.e.*, only detectable through vibrational transitions in the mid- and far-IR) and the mid-IR emission of PAHs, neither detectable with ALMA. Even if JWST/MIRI will also cover the mid-IR, SPICA/MCS will provide and order of magnitude better spectral resolution than MIRI, allowing for

much more detailed spectroscopic studies (line profiles and kinematics, resolving ro-vibrational bands, etc.).

Although many "galactic" investigations specifically require far-IR observations – "SAFARI's unique science" (*e.g.* the detection of [O I]63, the brightest gas line in protoplanetary disks; the characterisation of Kuiper and asteroid belts in exoplanetary systems; or the detection of the intrinsic emission of bodies in the outer Solar System), a wealth of synergies between ALMA, JWST and E-ELT exist. In fact, **most open questions in Astronomy will only be answered by observing the entire electromagnetic spectrum, and SPICA will play a key role by observing the mid– and far–infrared window contemporaneously with these facilities**.

In the "extragalactic" domain, ALMA will have a spatial resolution so high that it will not be suited for studying large samples of galaxies in a cosmological context; it will only follow-up targeted galaxies or produce pencil beam surveys. These are, by definition, not ideal for developing an understanding of the anti-hierarchical behaviour of galaxies, since they will suffer from cosmic variance and limited statistics. Submm observations from ground-based facilities are also limited by confusion to a few mJy, hence to the very brightest tip of the galaxy population (i.e., more luminous than a hundred times L_*, the average galaxy luminosity).

Since the discovery of the cosmic infrared background and the important populations of luminous dusty galaxies at high redshift, it has become clear that obscured star formation accounts for a large fraction of the stellar mass assembly budget. Enormous progress in infrared/(sub)mm/radio source count surveys will be made by Herschel, ALMA and EVLA. While ALMA will probe the molecular ISM in these objects and JWST the stellar component, the highly diagnostic mid-IR region is exclusive SAFARI territory. For instance, for an object at $z \sim 3$, JWST will be able to observe the rest-frame spectrum only out to 7 μm. The most luminous PAH features, hot dust continuum and key fine-structure lines will all be accessible only with SAFARI. This opens up the intermediate redshift Universe for scrutiny with the techniques that have been successfully used on low-z galaxies since ISO and *Spitzer*. The line sequence [Ne II]/[Ne III]/[Ne V] will characterise star formation as well as the importance of AGN activity. Many other similar probes are available for SAFARI, but neither ALMA nor JWST provides equivalent diagnostics. Thus the unique role of SAFARI is the characterisation of the sources of the cosmic infrared background. A further complementarity between ALMA and SAFARI is provided by SAFARI's ability to trace the energy budget of the star forming ISM out to $z \sim 2$ using the [O I]63 μm line and [C II]158 μm at lower redshift, while ALMA will access the [C II] line only at $z > 2$.

To enhance our understanding of coeval black hole and galaxy growth, observations of galaxies at the peak of the cosmic star formation and black hole accretion rate are a key requirement. A fundamental diagnostic is provided by the [O IV] line at 25.89 μm. This line can be used to probe AGN activity in dusty galaxies out to z~4, and its width can be used to asses black hole mass (Dasyra et al. 2008). SAFARI will thus play a key role in establishing the inventory of AGN in obscured galaxies at intermediate and high redshifts, and trace the mass-buildup of the nuclear SMBHs. Equivalent diagnostics are not available with either ALMA or JWST.

Both JWST and ALMA will probe galaxies at the epoch of reionisation ($z > 6$). At these redshifts the most luminous CO lines shift out of the observing band, and the [C II] line becomes the key probe (Walter & Carilli 2008). In pristine (zero-metallicity) gas, however, this line is not available. The molecular medium in zero metallicity galaxies cools principally through H_2 rotational and vibrational lines. As shown by Ciardi & Ferrara (2001) and Mizusawa et al. (2004), a number of these lines may be detectable with SAFARI, over a wide range of conditions. Targets will be provided by JWST, which is expected to discover significant numbers of $z > 6$ galaxies, with the prime targets for SAFARI being those that are not detected in CO or [C II] by ALMA. Alternatively such high-z sources may even be found from blind spectroscopic surveys with SAFARI in blank fields or behind strong lensing clusters. In both cases, the detection of the signatures of a metal-free molecular interstellar medium is again unique SAFARI territory.

Finally, the full complementarity of SAFARI with both ALMA and JWST is manifest in their completely different capabilities for sky surveys: the supreme spatial resolution and tiny field-of-view of ALMA and the excellent spatial resolution of JWST make very deep integrations on small fields the optimal observing mode for them. On the other hand, the fast survey speed of SPICA (both MIRACLE and SAFARI in the spectroscopic and imaging modes) will allow us to perform extensive sky surveys over the whole 5 to 200 μm range, hence probing quite a different region of the parameter space.

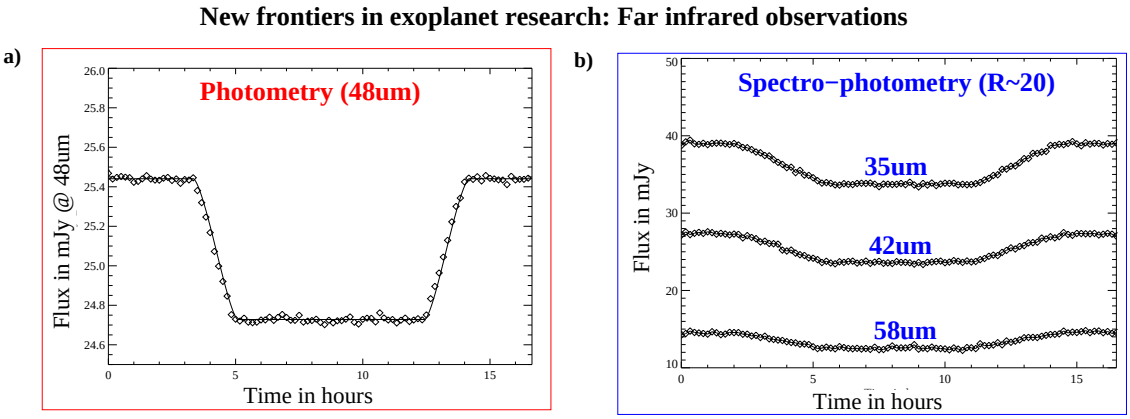

Figure 1.21: ***(a)*** *Synthetic light-curve of a transiting Jupiter-like EP around a cool M0 star at 10 pc observed with SAFARI SW (48 μm) in photometry.* ***(b)*** *Same as (a) but using the spectro-photometric mode (R~20) to detect modulations produced by atmospheric spectral features. Points are averages of 10 min exposures (simulations by S. Pezzuto).*

1.8 Discovery Science with SPICA

The science cases we have presented illustrate the concrete and definitive progress in our understanding of the Universe that SPICA will allow. However, as with all strides in increased sensitivity or the opening of new wavelength bands, new discoveries are certain once SPICA starts observing. To give a flavour of what might be expected in the new discovery space opened by SPICA, we give here some examples of speculative research projects from both the nearby and distant Universe.

A new window in exoplanet research –far infrared observations with SAFARI: In the field of exoplanets (EPs), SAFARI will provide capabilities to complement SPICA studies in the MIR (either coronagraphic or transit studies). With very stable detectors, and efficient, high cadence observations, SAFARI will be used to perform transit photometry and, on some favourable candidates, spectrophotometry for the first time in the FIR domain. Therefore, SPICA could be the only planned mission able to study exoplanets in a completely new wavelength domain (not covered by JWST and too faint for *Herschel*). This situation is often associated with unexpected discoveries. We estimate that the minimum EP sizes that will produce a detectable transit around a Sun-like star at 35 pc are: $\sim 5.8 R_{Earth}$ at 48 μm, $\sim 1.0 R_{Jup}$ at 85 μm and $\sim 2.4 R_{Jup}$ at 160 μm (Pezzuto 2009). In the shortest wavelength photometric band ($\sim$ 48 μm), primary and secondary eclipses of Jupiter-size EPs around F to M stars will be detected in a single transit (a $\sim 2.2 R_{Jup}$ exoplanet will be detectable at a $\gtrsim$100 pc distance). FIR measurements will be specially suited for EPs around cool M stars. Since cooler EPs show much higher contrast in the FIR than in the NIR/MIR (e.g., Jupiter's effective temperature is $\sim$ 110 K), if such EPs are found in the next $\sim$10 years, their transit studies with SAFARI will help to constrain their main properties, which are much more difficult to infer at shorter wavelengths. The SAFARI shorter wavelength range hosts a variety of interesting atmospheric molecular features (e.g., H_2O at 39 μm, HD at 37 μm, NH_3 at 40 and 42 μm, etc.). Strong emission/absorption of these features was first detected by ISO in the atmospheres of Jupiter, Saturn, Titan, Uranus and Neptune (Feuchtgruber et al. 1999). Suitable EP candidates for SAFARI spectro-photometric observations may not be numerous (see simulations on an optimal target in Fig. 1.21) and a considerable amount of observing time will be needed to extract their main atmospheric composition. However, in a few appropriate systems, SAFARI observations may allow us to expand the variety of "characterisable" extrasolar planets. These are crucial steps to enter in a new era of quantitative characterisation of EPs.

First identification of PAHs molecules in Space (the "GrandPAHs"): The ubiquitous MIR emission bands are attributed to the emission of a family of carbonaceous macromolecules: the PAHs. However, because these bands are due to the nearest neighbour vibrations of the C-C or C-H bonds, they are not specific to individual PAH species. Therefore, in spite of their relevance for astrophysics (as tracers of UV radiation fields or

star forming regions in a broader extragalactic context), the identification and characterisation of a given PAH molecule in space has not been possible yet. The hope for such an identification lies in their FIR lower-energy bands (PAH skeleton modes) which are specific fingerprints of individual molecules. The energy that is emitted in these bands is expected to be very weak, typically a few tenths of the energy absorbed in the UV (Joblin et al. 2002; Mulas et al. 2006). For example, it can be shown that if all the MIR emission observed in the ISM was due to a unique PAH such as ovalene, its FIR emission should be detectable even with a low ($\sim$ 10) signal-to-noise ratio (Mulas et al. 2006; Berné et al. 2009). Progress in the field suggests that there are in fact only a few (or at least limited number) of large and compact PAHs in space, that can resist the harsh interstellar conditions. These large PAHs are the so called "Grand-PAHs". The instantaneous broad band coverage of SAFARI will be especially adapted for deep searches of the Grand-PAH FIR bands, which is crucial since their position are not known. The narrow instantaneous bandwidth and limited sensitivity of PACS has turned inadequate to detect such broad and weak features. Therefore, SAFARI can represent our first chance to identify specific PAHs.

Feeding hungry mouths–mass accretion from the IGM: The means by which primordial gas is accreted from the IGM to fuel on-going star formation in galaxies remains an unanswered question in galaxy evolution. Any mechanism for this direct fuelling requires a means by which to cool what will be hot gas. The cooling process is widely believed to be mediated by the injection of metals into the IGM in galactic winds, which themselves cool by inelastic collisions with dust grains at the IGM/wind interaction zone (Dwek & Werner 1981; Montier & Giard 2004). The recent discovery by *Spitzer* of a diffuse IR counterpart to the X-ray emitting intracluster medium of Stefan's Quintet supports this hypothesis, its luminosity exceeding that of the X-ray emission by two orders of magnitude. *Herschel* will search for the far-IR signatures from the hot plasma in dense cluster and group environments; however, exploring this phenomenon in the bulk of the galaxy population will fall to SAFARI, that be able to trace the far-IR emission both photometrically and spectrophometrically, thus enabling not only determinations of the cooling properties of the IGM, but also characterisation of the dust grains.

The diagnostic potential of the high-J CO lines: As already mentioned, the high-J ($J \geq 13$) CO lines provide a method for studying the obscuring medium of type 2 AGN through their associated XDR (Krolik & Begelman 1988; Meijerink & Spaans 2005), for determining the energy budgets of composite starburst/ AGN systems (Meijerink et al. 2007), and for identifying accreting black holes in the early universe (Spaans & Meijerink 2008; Schleicher et al. 2010) This method has already been successfully proven by *Herschel* through the observations of a few nearby, powerful AGNs (van der Werf et al. 2010; Hailey-Dunsheath et al. 2010). The differences between the expected CO spectral line energy distributions in X-ray (XDR) and photon-dominated regions are most significant (3 orders of magnitude) in the SAFARI band. By summing the CO, [C II]158 μm and [O I]63 μm emission one can evaluate the total cooling rate for gas within the locale of the AGN, and, assuming thermal balance, derive the accretion rate. Thus, one can infer the accretion properties of black holes residing in obscured environments even in the absence of X-ray measurements. While *Herschel* is opening the way to these kind of studies, it is limited to the brightest and most nearby targets; the sensitivity of SAFARI will take us to the next stage and give access to a representative sample covering a wide range of mass and accretion luminosities, thus tracing the role and destiny of torus-covered black holes both locally and out to $z \sim 1$.

Estimating the masses of black holes in obscured galaxies at z>1: Rapid growth of black holes often occurs in obscured environments. In such systems, the only lines accessible for us to characterize the AGN activity are often the forbidden lines of ionized gas at low densities. When originating from ions of high ionization potential, these lines trace gas clouds that are photoionized by the AGN. Their luminosities scale with the rate of accretion onto the black hole, and their widths scale with the black hole mass (Dasyra et al. 2008; 2011, ApJ submitted), providing a unique means to deduce information on the masses of black holes in obscured environments. The systematic detection of such lines in cosmological surveys will thus permit the comparison of the already accumulated black hole mass vs the host-galaxy mass in obscured systems as a function of look-back time. It will also enable us to compare the mass functions of obscured vs unobscured black holes to assess what fraction of their growth occurs in obscured environments at different *z*s. SAFARI will cover an entirely new parameter space for such studies, as *Spitzer* only provided the local Universe calibration and JWST will only

enable the detection of the required mid-IR lines out to z∼1, without getting past the peak of the star-formation and black-hole-accretion history of the Universe.

Searching for the first generation of star formation with H_2: How the first stars (population III stars) formed out of primordial gas is one of the most exciting questions in modern astrophysics. It has long been realized that the formation of molecular hydrogen plays a key role in this process, serving as an effective coolant at temperatures below 10^4 K (Schlemmer et al. 2010), and the primary coolant of UV and X-ray irradiated gas in regions of low metallicity ($\leq 10^{-2}$ solar). Kamaya & Silk (2002) and Mizusawa et al. (2004) considered the H_2 rotational emission from primordial molecular cloud kernels to be associated with the formation of the first stars at the earliest epochs of z∼20. To establish the detectability of H_2 from primordial galaxies, we used the predictions of Obreschkow & Rawlings (2009) based on the Millemium simulations. The details of the properties of the galaxies involved in the simulations can be found at $http://s-cubed.physics.ox.ac.uk/s3_S AX/sky$. The simulations suggest that the majority of galaxies at redshifts 8−10 are expected to have M(H_2)∼ 10^9 solar masses. Assuming M(H_2) = 10^9 $M_\odot$, standard cosmology, i.e., Hubble constant H_0=70 km s^{-1}Mpc^{-1}, Ω_M=0.7, Ω_Λ=0.3, and a cosmological distance of d_L≈86 Gpc we calculate the flux of the H_2S(0) line to be 3.6x10^{-18} W m^{-2}. This value is within the SAFARI sensitivity estimates.

Surveying the early stages in the formation of massive galaxies (z>3): One of the most interesting results in extragalactic astronomy in the last decade is the discovery of a numerous population of massive galaxies (M>10^{11} $M_\odot$) at high redshift (Yan et al. 1999; Franx et al. 2003). Some of them are already evolving passively (Daddi et al. 2004), being good candidates for the progenitors of massive nearby ellipticals (Hopkins et al. 2009). Even more puzzlingly, these galaxies present very small sizes, and thus large mass densities (Daddi et al. 2005b; Trujillo et al. 2007; Toft et al. 2007) comparable to the density of a globular cluster (Buitrago et al. 2008). The existence of very compact massive dead galaxies at high-redshift is extremely challenging for models of galaxy formation, based on the hierarchical ΛCDM paradigm (e.g., Baugh et al. 1996; Cole et al. 2000; De Lucia et al. 2006; Croton et al. 2006). The typical redshift of these passively-evolving galaxies is z∼2, and their stellar population ages range around 1–2 Gyr (e.g., Förster Schreiber et al. 2004; Damjanov et al. 2009; Onodera et al. 2010; Whitaker et al. 2010), which imply a formation epoch at z=3–5. These values are in good agreement with the expectations based on the analysis of the stellar populations of nearby ellipticals and bulges (e.g., Thomas et al. 2005) and the evolution of stellar mass functions and specific star formations at z=2–5 (Pérez-González et al. 2008; Mancini et al. 2009). SAFARI will thus allow us to study the first ignition of the star formation in the progenitors of local ellipticals and bulges.

Detecting $z > 4$ IR-luminous galaxies with the 7.7 μm PAH feature and gravitational lensing: By exploiting the strong lensing power of massive galaxy clusters with SAFARI, we may be able to probe the properties of IR-luminous ($L_{\rm IR} > 10^{11} L_\odot$) galaxies in the epoch of cosmic reionisation for the first time in the MIR/FIR (Egami 2009). By utilizing SAFARI's low-resolution (R ∼20) FTS mode, we can search for high-redshift ($z > 4$) galaxies through the detection of the 7.7 μm PAH feature, the most luminous and conspicuous emission feature seen in the rest-frame mid-IR spectra of star-forming galaxies. Note that the SAFARI's field of view ($2' \times 2'$) matches well with the size of a cluster core where the lensing amplification is the strongest. If we assume that: (i) the IR galaxy luminosity function at $z \sim 2$ (Caputi et al. 2007) is representative of that at higher redshifts; (ii) the fractional IR luminosity in the 7.7 μm PAH feature is at least that observed in $z \sim 2$ submillimetre galaxies (Pope et al. 2008); and (iii) a typical cluster has a lensing potential similar to that of Abell 773. Then in a survey of 50 massive clusters with SAFARI in spectrophometry mode (assuming a line flux sensitivity of 10^{-19} Wm^{-2} at R ∼20), we would expect to detect ∼23 IR-luminous galaxies at $7 < z < 10$ using the 7.7 μm PAH feature. A blank-field survey with the same areal coverage would produce ∼ 8 detections in the same redshift range, so the lensing survey will offer a factor of ∼ 3 gain in number. The gain will be even larger if there is an abundance of low-mass/low-luminosity galaxies at such high redshift as, for instance, predicted by hierarchical structure formation theories. In fact, by accessing an epoch at which the space density of IR-luminous galaxies is virtually unknown, SAFARI will provide valuable observational data on the epoch of reionization.

1.9 Concluding remark

We have seen in the preceding sections that pushing forward our knowledge and understanding of the formation of galaxies and planets requires a leap in sensitivity in mid to far infrared spectroscopic and far infrared photometric capabilities. Only by placing a cold (< 6 K) 3.2 m telescope in space with instruments sensitive enough to take advantage of the low photon background, can we achieve the detection limits required to fulfil the ambitions of the ESA Cosmic Vision and gain a true insight into the **conditions for star & planet formation and the emergence of life, how planetary systems, including our own Solar System work and how galaxies originated and what the Universe is made of**. In other words, SPICA will play a central and vital part in ESA's Science Programme in the next decade.

References

Abe, L., Enya, K., Tanaka, S., et al. 2007, Comptes Rendus Physique, 8, 374
Adams, F. C. 2010, ARA&A, 48, 47
Adams, F. C. & Fatuzzo, M. 1996, ApJ, 464, 256
Agnor, C. B. & Ward, W. R. 2002, ApJ, 567, 579
Aikawa, Y., van Zadelhoff, G. J., van Dishoeck, E. F., & Herbst, E. 2002, A&A, 386, 622
Alatalo, K., Blitz, L., Young, L. M., et al. 2011, ArXiv e-prints
Alexander, T., Lutz, D., Sturm, E., et al. 2000, ApJ, 536, 710
Alonso-Herrero, A., Pérez-González, P. G., Alexander, D. M., et al. 2006, ApJ, 640, 167
André, P., Men'shchikov, A., Bontemps, S., et al. 2010, A&A, 518, L102+
Arimatsu, K., Izumiura, H., Ueta, T., Yamamura, I., & Onaka, T. 2011, ApJ, 729, L19+
Armus, L., Bernard-Salas, J., Spoon, H. W. W., et al. 2006, ApJ, 640, 204
Armus, L., Charmandaris, V., Bernard-Salas, J., et al. 2007, ApJ, 656, 148
Austermann, J. E., Dunlop, J. S., Perera, T. A., et al. 2010, MNRAS, 401, 160
Barger, A. J., Cowie, L. L., Sanders, D. B., et al. 1998, Nature, 394, 248
Barman, T. 2007, ApJ, 661, L191
Barro, G., Pérez-González, P. G., Gallego, J., et al. 2011, ApJS, 193, 30
Baugh, C. M., Cole, S., & Frenk, C. S. 1996, MNRAS, 283, 1361
Beaulieu, J. P., Carey, S., Ribas, I., & Tinetti, G. 2008, ApJ, 677, 1343
Berné, O., Joblin, C., Mulas, G., & Tielens, X. 2009, in SPICA Joint European/Japanese Workshop, EDP Sciences Web of Conferences
Berta, S., Magnelli, B., Lutz, D., et al. 2010, A&A, 518, L30+
Bertoldi, F., Altenhoff, W., Weiss, A., Menten, K. M., & Thum, C. 2006, Nature, 439, 563
Bitner, M. A., Richter, M. J., Lacy, J. H., et al. 2008, ApJ, 688, 1326
Blain, A. W., Kneib, J.-P., Ivison, R. J., & Smail, I. 1999, ApJ, 512, L87
Bockelée-Morvan, D., Lis, D. C., Wink, J. E., et al. 2000, A&A, 353, 1101
Bonsor, A. & Wyatt, M. 2010, MNRAS, 409, 1631
Borys, C., Chapman, S., Halpern, M., & Scott, D. 2003, MNRAS, 344, 385
Boss, A. P. 2003, ApJ, 599, 577
Bouché, N., Dekel, A., Genzel, R., et al. 2010, ApJ, 718, 1001
Bournaud, F., Chapon, D., Teyssier, R., et al. 2011, ApJ, 730, 4
Bowey, J. E., Barlow, M. J., Molster, F. J., et al. 2002, MNRAS, 331, L1
Braine, J. & Hughes, D. H. 1999, A&A, 344, 779
Brandl, B. R., Bernard-Salas, J., Spoon, H. W. W., et al. 2006, ApJ, 653, 1129
Brucker, M. J., Grundy, W. M., Stansberry, J. A., et al. 2009, Icarus, 201, 284
Brunt, C. M., Heyer, M. H., & Mac Low, M. 2009, A&A, 504, 883
Bryden, G., Beichman, C. A., Trilling, D. E., et al. 2006, ApJ, 636, 1098
Buitrago, F., Trujillo, I., Conselice, C. J., et al. 2008, ApJ, 687, L61
Caputi, K. I., Dunlop, J. S., McLure, R. J., & Roche, N. D. 2005, MNRAS, 361, 607
Caputi, K. I., Lagache, G., Yan, L., et al. 2007, ApJ, 660, 97
Carpenter, J. M., Bouwman, J., Mamajek, E. E., et al. 2009, ApJS, 181, 197
Carr, J. S. & Najita, J. R. 2008, Science, 319, 1504
Cernicharo, J., Ceccarelli, C., Ménard, F., Pinte, C., & Fuente, A. 2009, ApJ, 703, L123
Cernicharo, J. & Crovisier, J. 2005, Space Science Reviews, 119, 29
Cernicharo, J., Heras, A. M., Tielens, A. G. G. M., et al. 2001, ApJ, 546, L123
Chen, C. H., Sargent, B. A., Bohac, C., et al. 2006, ApJS, 166, 351
Chen, H.-W., Perley, D. A., Pollack, L. K., et al. 2009, ApJ, 691, 152
Ciardi, B. & Ferrara, A. 2001, MNRAS, 324, 648
Clements, D. L., Isaak, K. G., Madden, S. C., & Pearson, C. 2007, A&A, 465, 125
Clements, D. L., Rigby, E., Maddox, S., et al. 2010, A&A, 518, L8+
Colbert, J. W., Malkan, M. A., Clegg, P. E., et al. 1999, ApJ, 511, 721
Cole, S., Lacey, C. G., Baugh, C. M., & Frenk, C. S. 2000, MNRAS, 319, 168
Comastri, A., Setti, G., Zamorani, G., & Hasinger, G. 1995, A&A, 296, 1
Coppin, K., Chapin, E. L., Mortier, A. M. J., et al. 2006, MNRAS, 372, 1621
Cowie, L. L., Songaila, A., Hu, E. M., & Cohen, J. G. 1996, AJ, 112, 839
Croton, D. J., Springel, V., White, S. D. M., et al. 2006, MNRAS, 365, 11
Crovisier, J., Leech, K., Bockelee-Morvan, D., et al. 1997, Science, 275, 1904
Daddi, E., Alexander, D. M., Dickinson, M., et al. 2007, ApJ, 670, 173

Daddi, E., Cimatti, A., Renzini, A., et al. 2004, ApJ, 617, 746
Daddi, E., Dickinson, M., Chary, R., et al. 2005a, ApJ, 631, L13
Daddi, E., Elbaz, D., Walter, F., et al. 2010, ApJ, 714, L118
Daddi, E., Renzini, A., Pirzkal, N., et al. 2005b, ApJ, 626, 680
Dalgarno, A. 2000, in Molecular Hydrogen in Space, ed. F. Combes & G. Pineau Des Forets, 3–+
Damjanov, I., McCarthy, P. J., Abraham, R. G., et al. 2009, ApJ, 695, 101
Dartois, E., Cox, P., Roelfsema, P. R., et al. 1998, A&A, 338, L21
Dasyra, K. M., Ho, L. C., Armus, L., et al. 2008, ApJ, 674, L9
Dasyra, K. M., Tacconi, L. J., Davies, R. I., et al. 2006, ApJ, 651, 835
Dasyra, K. M., Yan, L., Helou, G., et al. 2009, ApJ, 701, 1123
Davies, G. T., Gilbank, D. G., Glazebrook, K., et al. 2009, MNRAS, 395, L76
de Graauw, T., Feuchtgruber, H., Bezard, B., et al. 1997, A&A, 321, L13
De Lucia, G., Springel, V., White, S. D. M., Croton, D., & Kauffmann, G. 2006, MNRAS, 366, 499
Dekel, A., Birnboim, Y., Engel, G., et al. 2009, Nature, 457, 451
Deming, D., Harrington, J., Laughlin, G., et al. 2007, ApJ, 667, L199
Deming, D., Harrington, J., Seager, S., & Richardson, L. J. 2006, ApJ, 644, 560
Demory, B.-O., Gillon, M., Barman, T., et al. 2007, A&A, 475, 1125
Devlin, M. J., Ade, P. A. R., Aretxaga, I., et al. 2009, Nature, 458, 737
Dole, H., Lagache, G., Puget, J.-L., et al. 2006, A&A, 451, 417
Donley, J. L., Rieke, G. H., Pérez-González, P. G., & Barro, G. 2008, ApJ, 687, 111
Donley, J. L., Rieke, G. H., Pérez-González, P. G., Rigby, J. R., & Alonso-Herrero, A. 2007, ApJ, 660, 167
Dullemond, C. P., Dominik, C., & Natta, A. 2001, ApJ, 560, 957
Dutrey, A., Guilloteau, S., & Ho, P. 2007, in Protostars and Planets V, 495–506
Dutton, A. A., van den Bosch, F. C., & Dekel, A. 2010, MNRAS, 405, 1690
Duvert, G., Guilloteau, S., Ménard, F., Simon, M., & Dutrey, A. 2000, A&A, 355, 165
Dwek, E. & Werner, M. W. 1981, ApJ, 248, 138
Eales, S., Dunne, L., Clements, D., et al. 2010a, PASP, 122, 499
Eales, S. A., Raymond, G., Roseboom, I. G., et al. 2010b, A&A, 518, L23+
Egami, E. 2009, in The Next-Generation Infrared Space Mission: SPICA, ed. A. M. Heras, B. M. Swinyard, K. G. Isaak, & J. R. Goicoechea, 4008–+
Egami, E., Rex, M., Rawle, T. D., et al. 2010, A&A, 518, L12+
Egami, E., Rieke, G. H., Fadda, D., & Hines, D. C. 2006, ApJ, 652, L21
Ehrenfreund, P., Boogert, A. C. A., Gerakines, P. A., Tielens, A. G. G. M., & van Dishoeck, E. F. 1997, A&A, 328, 649
Elbaz, D., Daddi, E., Le Borgne, D., et al. 2007, A&A, 468, 33
Elmegreen, B. G. & Lada, C. J. 1977, ApJ, 214, 725
Engelbracht, C. W., Gordon, K. D., Misselt, K., et al. 2006, in Astronomical Society of the Pacific Conference Series, Vol. 357, 215
Evans, N. J., Dunham, M. M., Jørgensen, J. K., et al. 2009a, ApJS, 181, 321
Evans, N. J., Dunham, M. M., Jørgensen, J. K., et al. 2009b, ApJS, 181, 321
Fabian, A. C. 1999, MNRAS, 308, L39
Fadda, D., Jannuzi, B. T., Ford, A., & Storrie-Lombardi, L. J. 2004, AJ, 128, 1
Fadda, D., Yan, L., Lagache, G., et al. 2010, ApJ, 719, 425
Farihi, J., Barstow, M. A., Redfield, S., Dufour, P., & Hambly, N. C. 2010, MNRAS, 404, 2123
Farrah, D., Lonsdale, C. J., Borys, C., et al. 2006a, ApJ, 643, L139
Farrah, D., Lonsdale, C. J., Borys, C., et al. 2006b, ApJ, 641, L17
Farrah, D., Lonsdale, C. J., Weedman, D. W., et al. 2008, ApJ, 677, 957
Fedele, D., van den Ancker, M. E., Henning, T., Jayawardhana, R., & Oliveira, J. M. 2010, A&A, 510, A72+
Ferrarese, L. & Ford, H. 2005, Space Science Reviews, 116, 523
Ferrarese, L. & Merritt, D. 2000, ApJ, 539, L9
Feruglio, C., Maiolino, R., Piconcelli, E., et al. 2010, A&A, 518, L155+
Feuchtgruber, H., Lellouch, E., Encrenaz, T., et al. 1999, in Astronomical Society of the Pacific Conference Series, Vol. 427, 133
Fiore, F., Grazian, A., Santini, P., et al. 2008, ApJ, 672, 94
Fischer, J., Luhman, M. L., Satyapal, S., et al. 1999, Ap&SS, 266, 91
Fischer, J., Sturm, E., González-Alfonso, E., et al. 2010, A&A, 518, L41+
Fontana, A., Salimbeni, S., Grazian, A., et al. 2006, A&A, 459, 745
Förster Schreiber, N. M., Genzel, R., Lutz, D., Kunze, D., & Sternberg, A. 2001, ApJ, 552, 544
Förster Schreiber, N. M., van Dokkum, P. G., Franx, M., et al. 2004, ApJ, 616, 40
Franceschini, A., Rodighiero, G., Vaccari, M., et al. 2010, A&A, 517, A74+
Franx, M., Labbé, I., Rudnick, G., et al. 2003, ApJ, 587, L79
Frayer, D. T., Harris, A. I., Baker, A. J., et al. 2011, ApJ, 726, L22+
Fritz, J., Franceschini, A., & Hatziminaoglou, E. 2006, MNRAS, 366, 767
Fujiwara, H., Honda, M., Kataza, H., et al. 2006, ApJ, 644, L133
Fukagawa, M., Tamura, M., Itoh, Y., et al. 2006, ApJ, 636, L153
Galliano, F., Madden, S. C., Jones, A. P., Wilson, C. D., & Bernard, J.-P. 2005, A&A, 434, 867

Galliano, F., Madden, S. C., Tielens, A. G. G. M., Peeters, E., & Jones, A. P. 2008, ApJ, 679, 310
Gautier, III, T. N., Rieke, G. H., Stansberry, J., et al. 2007, ApJ, 667, 527
Geers, V. C., Augereau, J.-C., Pontoppidan, K. M., et al. 2006, A&A, 459, 545
Genzel, R., Lutz, D., Sturm, E., et al. 1998, ApJ, 498, 579
Genzel, R., Tacconi, L. J., Gracia-Carpio, J., et al. 2010, MNRAS, 407, 2091
Georgantopoulos, I., Dasyra, K. M., Rovilos, E., et al. 2011, ArXiv e-prints
Gilli, R., Comastri, A., & Hasinger, G. 2007a, A&A, 463, 79
Gilli, R., Daddi, E., Chary, R., et al. 2007b, A&A, 475, 83
Gilli, R., Salvati, M., & Hasinger, G. 2001, A&A, 366, 407
Gillon, M., Pont, F., Demory, B.-O., et al. 2007, A&A, 472, L13
Goicoechea, J. R., Rodríguez-Fernández, N. J., & Cernicharo, J. 2004, ApJ, 600, 214
Gomes, R., Levison, H. F., Tsiganis, K., & Morbidelli, A. 2005, Nature, 435, 466
Gonzalez, A. H., Clowe, D., Bradač, M., et al. 2009, ApJ, 691, 525
González-Alfonso, E., Smith, H. A., Ashby, M. L. N., et al. 2008, ApJ, 675, 303
González-Alfonso, E., Smith, H. A., Fischer, J., & Cernicharo, J. 2004, ApJ, 613, 247
Gorti, U. & Hollenbach, D. 2004, ApJ, 613, 424
Gorti, U. & Hollenbach, D. 2008, ApJ, 683, 287
Goto, M., Usuda, T., Dullemond, C. P., et al. 2006, ApJ, 652, 758
Goulding, A. D. & Alexander, D. M. 2009, MNRAS, 398, 1165
Graciá-Carpio, J., Sturm, E., Hailey-Dunsheath, S., et al. 2011, ApJ, 728, L7+
Greaves, J. S. & Wyatt, M. C. 2010, MNRAS, 404, 1944
Greve, T. R., Ivison, R. J., Bertoldi, F., et al. 2004, MNRAS, 354, 779
Grigorieva, A., Thébault, P., Artymowicz, P., & Brandeker, A. 2007, A&A, 475, 755
Gruppioni, C., Pozzi, F., Andreani, P., et al. 2010, A&A, 518, L27+
Güdel, M., Lahuis, F., Briggs, K. R., et al. 2010, A&A, 519, A113+
Habart, E., Natta, A., Testi, L., & Carbillet, M. 2006, A&A, 449, 1067
Hailey-Dunsheath, S., Nikola, T., Oberst, T., et al. 2008, in EAS Publications Series, Vol. 31, 159–162
Hailey-Dunsheath, S., Nikola, T., Stacey, G. J., et al. 2010, ApJ, 714, L162
Haisch, Jr., K. E., Barsony, M., Ressler, M. E., & Greene, T. P. 2006, AJ, 132, 2675
Harrington, J., Luszcz, S., Seager, S., Deming, D., & Richardson, L. J. 2007, Nature, 447, 691
Hasegawa, S. 2000, Institute of Space and Astronautical Science Report, 14, 27
Hasinger, G., Miyaji, T., & Schmidt, M. 2005, A&A, 441, 417
Henning, T. K., ed. 2003, Lecture Notes in Physics, Berlin Springer Verlag, Vol. 609, Astromineralogy, ed. T. K. Henning
Hernán-Caballero, A., Pérez-Fournon, I., Hatziminaoglou, E., et al. 2009, MNRAS, 395, 1695
Hönig, S. F. & Kishimoto, M. 2010, A&A, 523, A27+
Hopkins, P. F., Bundy, K., Murray, N., et al. 2009, MNRAS, 398, 898
Houck, J. R., Soifer, B. T., Weedman, D., et al. 2005, ApJ, 622, L105
Huang, J., Faber, S. M., Daddi, E., et al. 2009, ApJ, 700, 183
Hughes, D. H., Serjeant, S., Dunlop, J., et al. 1998, Nature, 394, 241
Ida, S. & Lin, D. N. C. 2005, ApJ, 626, 1045
Ilgner, M., Henning, T., Markwick, A. J., & Millar, T. J. 2004, A&A, 415, 643
Ingleby, L., Calvet, N., Bergin, E., et al. 2009, ApJ, 703, L137
Israel, F. P. & Maloney, P. R. 2011, ArXiv e-prints
Ivison, R. J., Swinbank, A. M., Swinyard, B., et al. 2010, A&A, 518, L35+
Iwasawa, K. & Comastri, A. 1998, MNRAS, 297, 1219
Jewitt, D. & Luu, J. 1993, Nature, 362, 730
Joblin, C., Toublanc, D., Boissel, P., & Tielens, A. G. G. M. 2002, Molecular Physics, 100, 3595
Kalas, P., Graham, J. R., Chiang, E., et al. 2008, Science, 322, 1345
Kalas, P., Graham, J. R., & Clampin, M. 2005, Nature, 435, 1067
Kamaya, H. & Silk, J. 2002, MNRAS, 332, 251
Kamp, I., Tilling, I., Woitke, P., Thi, W., & Hogerheijde, M. 2010, A&A, 510, A18+
Kamp, I., van Zadelhoff, G., van Dishoeck, E. F., & Stark, R. 2003, A&A, 397, 1129
Kauffmann, G., Heckman, T. M., White, S. D. M., et al. 2003, MNRAS, 341, 33
Kennedy, G. M. & Kenyon, S. J. 2008, ApJ, 673, 502
Kennedy, G. M. & Wyatt, M. C. 2011, MNRAS, 412, 2137
Kenyon, S. J. & Bromley, B. C. 2008, ApJS, 179, 451
Kerschbaum, F., Ladjal, D., Ottensamer, R., et al. 2010, A&A, 518, L140+
Kim, K. H., Watson, D. M., Manoj, P., et al. 2009, ApJ, 700, 1017
Knudsen, K. K., Barnard, V. E., van der Werf, P. P., et al. 2006, MNRAS, 368, 487
Knutson, H. A., Charbonneau, D., Allen, L. E., et al. 2007, Nature, 447, 183
Komossa, S., Burwitz, V., Hasinger, G., & Predehl, P. 2003, Astronomische Nachrichten Supplement, 324, 33
Kornet, K., Bodenheimer, P., & Różyczka, M. 2002, A&A, 396, 977
Krolik, J. H. & Begelman, M. C. 1988, ApJ, 329, 702
Labbé, I., González, V., Bouwens, R. J., et al. 2010, ApJ, 708, L26
Lacy, M., Storrie-Lombardi, L. J., Sajina, A., et al. 2004, ApJS, 154, 166

Lada, C. J. & Lada, E. A. 2003, ARA&A, 41, 57
Lagache, G., Dole, H., Puget, J.-L., et al. 2004, ApJS, 154, 112
Lagrange, A.-M., Gratadour, D., Chauvin, G., et al. 2009, A&A, 493, L21
Lahuis, F., van Dishoeck, E. F., Blake, G. A., et al. 2007, ApJ, 665, 492
Laurent, G. T., Aguirre, J. E., Glenn, J., et al. 2005, ApJ, 623, 742
Le Floc'h, E., Papovich, C., Dole, H., et al. 2005, ApJ, 632, 169
Le Floc'h, E., Pérez-González, P. G., Rieke, G. H., et al. 2004, ApJS, 154, 170
Lecar, M., Podolak, M., Sasselov, D., & Chiang, E. 2006, ApJ, 640, 1115
Lellouch, E., Crovisier, J., Lim, T., et al. 1998, A&A, 339, L9
Lellouch, E., Kiss, C., Santos-Sanz, P., et al. 2010, A&A, 518, L147+
Levrier, F., Gerin, M., Hennebelle, P., et al. 2009, in The Next-Generation Infrared Space Mission: SPICA, ed. A. M. Heras, B. M. Swinyard, K. G. Isaak, & J. R. Goicoechea , 3003–+
Lim, T. L., Stansberry, J., Müller, T. G., et al. 2010, A&A, 518, L148+
Lissauer, J. J. 1993, ARA&A, 31, 129
Lutz, D., Sturm, E., Genzel, R., et al. 2003, A&A, 409, 867
Machalek, P., McCullough, P. R., Burke, C. J., et al. 2008, ApJ, 684, 1427
Madden, S. C., Galliano, F., Jones, A. P., & Sauvage, M. 2006, A&A, 446, 877
Magliocchetti, M. & Brüggen, M. 2007, MNRAS, 379, 260
Magliocchetti, M., Cirasuolo, M., McLure, R. J., et al. 2008, MNRAS, 383, 1131
Magorrian, J., Tremaine, S., Richstone, D., et al. 1998, AJ, 115, 2285
Maiolino, R. 2007, Highlights of Astronomy, 14, 262
Maiolino, R., Nagao, T., Grazian, A., et al. 2008, A&A, 488, 463
Maldoni, M. M., Robinson, G., Smith, R. G., Duley, W. W., & Scott, A. 1999, MNRAS, 309, 325
Malfait, K., Waelkens, C., Bouwman, J., de Koter, A., & Waters, L. B. F. M. 1999, A&A, 345, 181
Mancini, C., Matute, I., Cimatti, A., et al. 2009, A&A, 500, 705
Marchesini, D., van Dokkum, P. G., Förster Schreiber, N. M., et al. 2009, ApJ, 701, 1765
Marconi, A., Risaliti, G., Gilli, R., et al. 2004, MNRAS, 351, 169
Marley, M. S., Fortney, J., Seager, S., & Barman, T. 2007, in Protostars and Planets V, 733–747
Marois, C., Macintosh, B., Barman, T., et al. 2008, Science, 322, 1348
Martin, D. C., Seibert, M., Neill, J. D., et al. 2007, Nature, 448, 780
Matsuura, M., Dwek, E., Meixner, M., et al. 2011, ArXiv e-prints
Mayer, A., Jorissen, A., Kerschbaum, F., et al. 2011, A&A, 531, L4+
McKee, C. F. & Ostriker, E. C. 2007, ARA&A, 45, 565
Meeus, G., Pinte, C., Woitke, P., et al. 2010, A&A, 518, L124+
Meijerink, R. & Spaans, M. 2005, A&A, 436, 397
Meijerink, R., Spaans, M., & Israel, F. P. 2007, A&A, 461, 793
Meléndez, M., Kraemer, S. B., Schmitt, H. R., et al. 2008, ApJ, 689, 95
Menéndez-Delmestre, K., Blain, A. W., Smail, I., et al. 2009, ApJ, 699, 667
Merloni, A., Bongiorno, A., Bolzonella, M., et al. 2010, ApJ, 708, 137
Merloni, A., Rudnick, G., & Di Matteo, T. 2004, MNRAS, 354, L37
Meyer, M. R., Carpenter, J. M., Mamajek, E. E., et al. 2008, ApJ, 673, L181
Miville-Deschênes, M., Martin, P. G., Abergel, A., et al. 2010, A&A, 518, L104+
Mizusawa, H., Nishi, R., & Omukai, K. 2004, PASJ, 56, 487
Mizusawa, H., Omukai, K., & Nishi, R. 2005, PASJ, 57, 951
Molinari, S., Swinyard, B., Bally, J., et al. 2010, PASP, 122, 314
Montier, L. A. & Giard, M. 2004, A&A, 417, 401
Moore, M. H. & Hudson, R. L. 1992, ApJ, 401, 353
Moore, M. H. & Hudson, R. L. 1994, A&AS, 103, 45
Mor, R., Netzer, H., & Elitzur, M. 2009, ApJ, 705, 298
Mordasini, C., Alibert, Y., Benz, W., & Naef, D. 2008, in Astronomical Society of the Pacific Conference Series, Vol. 398, Extreme Solar Systems, ed. D. Fischer, F. A. Rasio, S. E. Thorsett, & A. Wolszczan, 235–+
Moro-Martín, A. 2009, in SPICA Joint European/Japanese Workshop, EDP Sciences Web of Conferences
Moustakas, J. & Kennicutt, Jr., R. C. 2006, ApJS, 164, 81
Muñoz Caro, G. M., Meierhenrich, U. J., Schutte, W. A., et al. 2002, Nature, 416, 403
Mulas, G., Malloci, G., Joblin, C., & Toublanc, D. 2006, A&A, 460, 93
Mullaney, J. R., Alexander, D. M., Huynh, M., Goulding, A. D., & Frayer, D. 2010, MNRAS, 401, 995
Müller, T. G., Lellouch, E., Stansberry, J., et al. 2010, A&A, 518, L146+
Nagao, T., Maiolino, R., Marconi, A., & Matsuhara, H. 2011, A&A, 526, A149+
Nagasawa, M., Thommes, E. W., Kenyon, S. J., Bromley, B. C., & Lin, D. N. C. 2007, in Protostars and Planets V, 639–654
Najita, J. R., Carr, J. S., Glassgold, A. E., & Valenti, J. A. 2007, in Protostars and Planets V, 507–522
Natta, A., Testi, L., & Randich, S. 2006, A&A, 452, 245
Negrello, M., Hopwood, R., De Zotti, G., et al. 2010, Science, 330, 800
Netzer, H., Lutz, D., Schweitzer, M., et al. 2007, ApJ, 666, 806
Neufeld, D. A., Hollenbach, D. J., Kaufman, M. J., et al. 2007, ApJ, 664, 890

Noeske, K. G., Faber, S. M., Weiner, B. J., et al. 2007, ApJ, 660, L47
Öberg, K. I., Qi, C., Fogel, J. K. J., et al. 2011, ApJ, 734, 98
Obreschkow, D. & Rawlings, S. 2009, ApJ, 696, L129
Ogle, P., Antonucci, R., Appleton, P. N., & Whysong, D. 2007, ApJ, 668, 699
Okada, Y., Onaka, T., Miyata, T., et al. 2008, ApJ, 682, 416
Oliver, S. J., Wang, L., Smith, A. J., et al. 2010, A&A, 518, L21+
Omont, A., Forveille, T., Moseley, S. H., et al. 1990, ApJ, 355, L27
Onodera, M., Daddi, E., Gobat, R., et al. 2010, ApJ, 715, L6
Osterbrock, D. E. & Ferland, G. J. 2006, Astrophysics of gaseous nebulae and active galactic nuclei (University Science Books)
Papovich, C., Dole, H., Egami, E., et al. 2004, ApJS, 154, 70
Papovich, C., Moustakas, L. A., Dickinson, M., et al. 2006, ApJ, 640, 92
Peeters, E., Spoon, H. W. W., & Tielens, A. G. G. M. 2004, ApJ, 613, 986
Pereira-Santaella, M., Diamond-Stanic, A. M., Alonso-Herrero, A., & Rieke, G. H. 2010, ApJ, 725, 2270
Perera, T. A., Chapin, E. L., Austermann, J. E., et al. 2008, MNRAS, 391, 1227
Pérez-González, P. G., Egami, E., Rex, M., et al. 2010, A&A, 518, L15+
Pérez-González, P. G., Rieke, G. H., Egami, E., et al. 2005, ApJ, 630, 82
Pérez-González, P. G., Rieke, G. H., Villar, V., et al. 2008, ApJ, 675, 234
Pettini, M., Madau, P., Bolte, M., et al. 2003, ApJ, 594, 695
Pettini, M., Zych, B. J., Murphy, M. T., Lewis, A., & Steidel, C. C. 2008, MNRAS, 391, 1499
Pezzuto, S. 2009, in The Next-Generation Infrared Space Mission: SPICA, ed. A. M. Heras, B. M. Swinyard, K. G. Isaak, & J. R. Goicoechea , 2007–+
Polehampton, E. T., Baluteau, J., Swinyard, B. M., et al. 2007, MNRAS, 377, 1122
Pollack, J. B., Hubickyj, O., Bodenheimer, P., et al. 1996a, Icarus, 124, 62
Pollack, J. B., Hubickyj, O., Bodenheimer, P., et al. 1996b, Icarus, 124, 62
Pontoppidan, K. M., Blake, G. A., van Dishoeck, E. F., et al. 2008, ApJ, 684, 1323
Pontoppidan, K. M., Dullemond, C. P., van Dishoeck, E. F., et al. 2005, ApJ, 622, 463
Pontoppidan, K. M., Salyk, C., Blake, G. A., & Käufl, H. U. 2010, ApJ, 722, L173
Pope, A., Chary, R.-R., Alexander, D. M., et al. 2008, ApJ, 675, 1171
Powell, L. C., Bournaud, F., Chapon, D., et al. 2011, ArXiv e-prints
Pozzi, F., Vignali, C., Comastri, A., et al. 2010, A&A, 517, A11+
Qi, C., Wilner, D. J., Calvet, N., et al. 2006, ApJ, 636, L157
Raymond, G., Isaak, K. G., Clements, D., Rykala, A., & Pearson, C. 2009, in The Next-Generation Infrared Space Mission: SPICA, ed. A. M. Heras, B. M. Swinyard, K. G. Isaak, & J. R. Goicoechea , 4019–+
Reddy, N. A., Steidel, C. C., Pettini, M., et al. 2008, ApJS, 175, 48
Rex, M., Rawle, T. D., Egami, E., et al. 2010, A&A, 518, L13+
Richardson, L. J., Deming, D., Horning, K., Seager, S., & Harrington, J. 2007, Nature, 445, 892
Richardson, L. J., Harrington, J., Seager, S., & Deming, D. 2006, ApJ, 649, 1043
Richstone, D., Ajhar, E. A., Bender, R., et al. 1998, Nature, 395, A14+
Rigby, J. R., Diamond-Stanic, A. M., & Aniano, G. 2009, ApJ, 700, 1878
Rigby, J. R., Marcillac, D., Egami, E., et al. 2008, ApJ, 675, 262
Rigby, J. R., Rieke, G. H., Maiolino, R., et al. 2004, ApJS, 154, 160
Rigopoulou, D., Kunze, D., Lutz, D., Genzel, R., & Moorwood, A. F. M. 2002, A&A, 389, 374
Roberge, A., Feldman, P. D., Weinberger, A. J., Deleuil, M., & Bouret, J. 2006, Nature, 441, 724
Rodighiero, G., Vaccari, M., Franceschini, A., et al. 2010, A&A, 515, A8+
Roseboom, I. G., Oliver, S. J., Kunz, M., et al. 2010, MNRAS, 409, 48
Rosenthal, D., Bertoldi, F., & Drapatz, S. 2000, A&A, 356, 705
Roussel, H., Helou, G., Hollenbach, D. J., et al. 2007, ApJ, 669, 959
Sajina, A., Yan, L., Lutz, D., et al. 2008, ApJ, 683, 659
Salyk, C., Pontoppidan, K. M., Blake, G. A., et al. 2008, ApJ, 676, L49
Santini, P., Fontana, A., Grazian, A., et al. 2009, A&A, 504, 751
Sargent, B. A., Forrest, W. J., Tayrien, C., et al. 2009, ApJS, 182, 477
Saslaw, W. C. & Zipoy, D. 1967, Nature, 216, 976
Sauter, J. & Wolf, S. 2011, A&A, 527, A27+
Schaerer, D. & de Barros, S. 2010, A&A, 515, A73+
Schleicher, D. R. G., Spaans, M., & Glover, S. C. O. 2010, ApJ, 712, L69
Scott, K. S., Austermann, J. E., Perera, T. A., et al. 2008, MNRAS, 385, 2225
Scott, S. E., Fox, M. J., Dunlop, J. S., et al. 2002, MNRAS, 331, 817
Seager, S. & Sasselov, D. D. 2000, ApJ, 537, 916
Selsis, F., Despois, D., & Parisot, J.-P. 2002, A&A, 388, 985
Shankar, F., Weinberg, D. H., & Miralda-Escudé, J. 2009, ApJ, 690, 20
Shetty, R., Glover, S. C., Dullemond, C. P., & Klessen, R. S. 2011, MNRAS, 412, 1686
Shi, Y., Rieke, G. H., Hines, D. C., et al. 2006, ApJ, 653, 127
Shim, H., Colbert, J., Teplitz, H., et al. 2009, ApJ, 696, 785
Siana, B., Smail, I., Swinbank, A. M., et al. 2009, ApJ, 698, 1273

Smail, I., Ivison, R. J., & Blain, A. W. 1997, ApJ, 490, L5+
Smith, J. D. T., Draine, B. T., Dale, D. A., et al. 2007, ApJ, 656, 770
Soifer, B. T., Neugebauer, G., Matthews, K., Egami, E., & Weinberger, A. J. 2002, AJ, 124, 2980
Spaans, M. & Meijerink, R. 2008, ApJ, 678, L5
Spinoglio, L., Andreani, P., & Malkan, M. A. 2003, in Active Galactic Nuclei: From Central Engine to Host Galaxy, Vol. 290, 559
Spinoglio, L. & Malkan, M. A. 1992, ApJ, 399, 504
Spinoglio, L., Malkan, M. A., Smith, H. A., González-Alfonso, E., & Fischer, J. 2005, ApJ, 623, 123
Springel, V., Frenk, C. S., & White, S. D. M. 2006, Nature, 440, 1137
Stansberry, J. A., Grundy, W. M., Margot, J. L., et al. 2006, ApJ, 643, 556
Stark, D. P., Ellis, R. S., Bunker, A., et al. 2009, ApJ, 697, 1493
Stern, D., Eisenhardt, P., Gorjian, V., et al. 2005, ApJ, 631, 163
Sturm, B., Bouwman, J., Henning, T., et al. 2010a, A&A, 518, L129+
Sturm, B., Bouwman, J., Henning, T., et al. 2010b, A&A, 518, L129+
Sturm, E., González-Alfonso, E., Veilleux, S., et al. 2011, ApJ, 733, L16+
Sturm, E., Verma, A., Graciá-Carpio, J., et al. 2010c, A&A, 518, L36+
Su, K. Y. L., Rieke, G. H., Misselt, K. A., et al. 2005, ApJ, 628, 487
Swain, M. R., Bouwman, J., Akeson, R. L., Lawler, S., & Beichman, C. A. 2008a, ApJ, 674, 482
Swain, M. R., Vasisht, G., & Tinetti, G. 2008b, Nature, 452, 329
Swinbank, A. M., Smail, I., Chapman, S. C., et al. 2004, ApJ, 617, 64
Swinbank, A. M., Smail, I., Longmore, S., et al. 2010, Nature, 464, 733
Tacconi, L. J., Genzel, R., Neri, R., et al. 2010, Nature, 463, 781
Takeuchi, T. T., Buat, V., & Burgarella, D. 2005, A&A, 440, L17
Tanaka, H., Himeno, Y., & Ida, S. 2005, ApJ, 625, 414
Teixeira, P. S., Lada, C. J., Wood, K., Robitaille, T. P., & Luhman, K. L. 2009, ApJ, 700, 454
Terada, H., Tokunaga, A. T., Kobayashi, N., et al. 2007, ApJ, 667, 303
Thi, W., Mathews, G., Ménard, F., et al. 2010, A&A, 518, L125+
Thomas, D., Maraston, C., Bender, R., & Mendes de Oliveira, C. 2005, ApJ, 621, 673
Tielens, A. G. G. M., Waters, L. B. F. M., Molster, F. J., & Justtanont, K. 1998, Ap&SS, 255, 415
Tinetti, G. & Beaulieu, J.-P. 2009, in IAU Symposium, Vol. 253, IAU Symposium, 231–237
Tinetti, G., Vidal-Madjar, A., Liang, M.-C., et al. 2007, Nature, 448, 169
Toft, S., van Dokkum, P., Franx, M., et al. 2007, ApJ, 671, 285
Tommasin, S., Spinoglio, L., Malkan, M. A., & Fazio, G. 2010, ApJ, 709, 1257
Tommasin, S., Spinoglio, L., Malkan, M. A., et al. 2008, ApJ, 676, 836
Treister, E., Urry, C. M., & Virani, S. 2009, ApJ, 696, 110
Trujillo, I., Conselice, C. J., Bundy, K., et al. 2007, MNRAS, 382, 109
Ueta, T., Speck, A. K., Stencel, R. E., et al. 2006, ApJ, 648, L39
Ueta, T., Stencel, R. E., Yamamura, I., et al. 2010, A&A, 514, A16+
Vaccari, M., Marchetti, L., Franceschini, A., et al. 2010, A&A, 518, L20+
Valiante, E., Lutz, D., Sturm, E., Genzel, R., & Chapin, E. L. 2009, ApJ, 701, 1814
Valiante, E., Lutz, D., Sturm, E., et al. 2007, ApJ, 660, 1060
van der Werf, P. P., Isaak, K. G., Meijerink, R., et al. 2010, A&A, 518, L42+
van Kempen, T. A., Green, J. D., Evans, N. J., et al. 2010, A&A, 518, L128+
Veilleux, S., Cecil, G., & Bland-Hawthorn, J. 2005, ARA&A, 43, 769
Walter, F. & Carilli, C. 2008, Ap&SS, 313, 313
Warren, S. G. 1984, Appl. Opt., 23, 1206
Waters, L. B. F. M., Molster, F. J., de Jong, T., et al. 1996, A&A, 315, L361
Webb, T. M., Eales, S. A., Lilly, S. J., et al. 2003, ApJ, 587, 41
Weedman, D., Polletta, M., Lonsdale, C. J., et al. 2006, ApJ, 653, 101
Weinmann, S. M., Neistein, E., & Dekel, A. 2011, ArXiv e-prints
Weiß, A., Kovács, A., Coppin, K., et al. 2009, ApJ, 707, 1201
Wetherill, G. W. & Stewart, G. R. 1989, Icarus, 77, 330
Whitaker, K. E., van Dokkum, P. G., Brammer, G., et al. 2010, ApJ, 719, 1715
Willacy, K., Langer, W., Allen, M., & Bryden, G. 2006, ApJ, 644, 1202
Woitke, P., Kamp, I., & Thi, W.-F. 2009a, A&A, 501, 383
Woitke, P., Pinte, C., Tilling, I., et al. 2010a, MNRAS, 405, L26
Woitke, P., Pinte, C., Tilling, I., et al. 2010b, MNRAS, 405, L26
Woitke, P., Thi, W.-F., Kamp, I., & Hogerheijde, M. R. 2009b, A&A, 501, L5
Wolfire, M. G., McKee, C. F., Hollenbach, D., & Tielens, A. G. G. M. 1995, ApJ, 453, 673
Wu, Y., Helou, G., Armus, L., et al. 2010, ApJ, 723, 895
Wyatt, M. C. 2008, ARA&A, 46, 339
Yan, L., McCarthy, P. J., Freudling, W., et al. 1999, ApJ, 519, L47

Acronyms

AD	Applicable Document	**ADR**	Adiabatic Demagnetisation Refrigerators
AGB	Asymptotic Giant Branch	**AGN**	Active Galactic Nucleus/Nuclei
AIV/T	Assembly Integration Verification/Testing	**ALFRP**	Alumina Fibre Reinforced Plastics
ALMA	Atacama Large Millimeter Array	**AO**	Announcement of Opportunity
AOCS	Attitude and Orbit Control System	**AOT**	Astronomical Observation Template
APE	Aperture Pointing Error	**BFL**	Back Focal Length
BHAR	Black Hole Accretion Rate	**BLAST**	Balloon-borne Large-Aperture Sub-millimeter Telescope
BLISS	Background-Limited Infrared-Submillimeter Spectrograph	**BM**	Bus Module
BOL	Beginning Of Life	**BRDF**	Bi-directional Reflectance Distribution Function
CAD	Computer Aided Design	**CCSDS**	Consultative Committee for Space Data Systems
CDF	Concurrent Design Facility	**CDM**	Cold Dark Matter
CEA	Commissariat à l'Énergie Atomique	**CFRP**	Carbon Fiber Reinforced Plastics
CIRB	Cosmic InfraRed Background	**CMB**	Cosmic Microwave Background
COB	Cosmic Optical Background	**CSE**	CircumStellar Envelope
CSO	Caltech Sumbmillimeter Observatory	**CTE**	Coefficient of Thermal Expansion
CXB	Cosmic X-ray Background	**DC**	Digital Converter
DPU	Data Processing Unit	**DS3**	Deep Space Station 3
EADS	European Aeronautic Defence and Space company	**ECSS**	European Cooperation for Space Standardisation
EFL	Effective Focal Length	**EGP**	Exo-Giant Planet
EGSE	Electrical Ground Segment Equipment	**EMI**	Electro-Magnetic Interference
EOL	End Of Life	**EP**	Exo-Planet
ESA	European Space Agency	**ESAC**	European Space Astronomy Centre
ESOC	European Space Operations Centre	**ESSC**	European Spica Science Centre
ESTEC	European Space research & TEchnology Centre	**EVLA**	Expanded Very Large Array
FIR	Far Infrared	**FM**	Flight Model
FOV	Field Of View	**FPC**	Focal Plane finding Camera
FPI	Focal Plane Instrument(s)	**FS**	Flight Spare
iFTS	imaging Fourier Transform Spectrometer	**GALEX**	GALaxy evolution EXplorer
HII-A/B	JAXA launcher vehicle	**HGA**	High Gain Antenna
HKTM	House Keeping Telemetry	**HW**	Hardware
I/F	Interface	**ICC**	Instrument Control Centre
ICS	Interface Control Specification	**IGM**	InterGalactic Medium
IOB	Instrument Optical bench	**ISAS**	Institute of Space and Astronautical Science
ISO	Infrared Space Observatory	**ISS**	International Space Station
IWA	Inner Working Angle	**JAXA**	Japan Aerospace Exploration Agency
JEM	Japanese Experiment Module	**JSET**	Joint Systems Engineering Team
JWST	James Webb Space Telescope	**KBO**	Kuiper Belt Object
KID	Kinetic Inductance Detector	**LEOP**	Launch and Early Orbit Phase
LGA	Low Gain Antenna	**LHB**	Late Heavy Bombardment
M1, M2 . . .	Mirror 1 (primary mirror), Mirror 2 (secondary mirror), . . .	**MGA**	Medium Gain Antenna
MIR	Mid-InfraRed	**MIRACLE**	Mid-InfRAred Camera w/o LEns

MIRHES	Mid-InfraRed High resolution Echelle Spectrometer	**MIRMES**	Mid-InfraRed Medium resolution Echelle Spectrometer
MLA	Multi Lateral Agreement	**MLI**	Multi Layer Insulation
MOC	Mission Operations Centre	**NEP**	Noise Equivalent Power
NIR	Near InfraRed	**NLR**	Narrow Line Region
OWA	Outer Working Angle	**QM**	Qualification Model
QPSK	Quadrature Phase Shift Keying	**PACS**	Photodetector Array Camera and Spectrometer
PAH	Polycyclic Aromatic Hydrocarbons	**PDR**	Photon Dominated Region
PI	Principal Investigator	**PIAA**	Phase Induced Amplitude Apodization
PLM	PayLoad Module	**PSF**	Point Spread Function
PST	Point Source Transmittance	**PTV**	Peak-To-Valley
PUS	Packet utilisation Standard	**RD**	Reference Document
RF	Radio Frequency	**rms**	root mean square
RPE	Random Pointing Error	**Rs**	Symbol Rate
RT	Room Temperature	**RW**	Reaction Wheel
S/C	Spacecraft	**SAFARI**	SpicA FAR-infrared Instrument
SCI	SPICA Coronagraph Instrument	**SCUBA**	Submillimetre Common-User Bolometer Array
SDR	System Design Review	**SE**	Sun-Earth
SED	Spectral Energy Distribution	**SF**	Star Formation
SFR	Star Formation Rate	**SKA**	Square Kilometre Array
SMBH	Super Massive Black Hole	**SMG**	Sub-Millimetre Galaxy
SMILES	Super conducting sub-mm Limb Emission Sounder	**SNe**	Super Novae
SOC	Science Operations Centre	**SPC**	Science Programme Committee
SPICA	SPace Infrared telescope for Cosmology and Astrophysics	**SPIRE**	Spectral and Photometric Imaging REceiver
SRON	Space Research Organisation of the Netherlands	**SRR**	System Requirements Review
SSO	Solar System Object	**STA**	SPICA Telescope Assembly
STSST	SPICA Telescope Science Study Team	**SVM**	Service Module
TAC	Time Allocation Committee	**TAS**	Thales Alenia Space
TBC	To Be Confirmed	**TBD**	To Be Defined
TC	Telecommand	**TDA**	Technology Development Activities
TES	Transition Edge Sensors	**TID**	Total Ionising Dose
TIRCS	Thermal Insulation and Radiative Cooling System	**TIS**	Total Integrated Scatter
TM	Telemetry	**TOB**	Telescope Optical Bench
ToO	Target of Opportunity	**TT&C**	Tracking Telemetry and Command
ULIRG	UltraLuminous InfraRed Galaxy	**UV**	UltraViolet
WFE	Wave Front Error	**XDR**	X-ray Dominated Region